Russian Original Vol. 31, No. 6, December, 1971

Translation published June, 1972

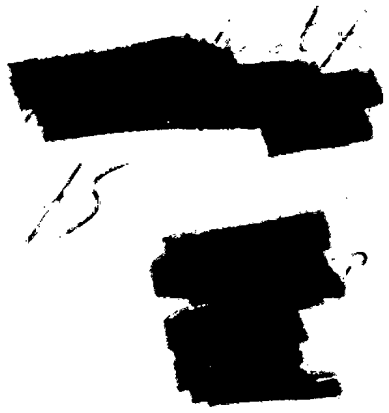

SOVIET ATOMIC ENERGY

АТОМНАЯ ЭНЕРГИЯ
(ATOMNAYA ÉNERGIYA)

TRANSLATED FROM RUSSIAN

CONSULTANTS BUREAU, NEW YORK

SOVIET ATOMIC ENERGY

Soviet Atomic Energy is a cover-to-cover translation of *Atomnaya Énergiya*, a publication of the Academy of Sciences of the USSR.

An arrangement with Mezhdunarodnaya Kniga, the Soviet book export agency, makes available both advance copies of the Russian journal and original glossy photographs and artwork. This serves to decrease the necessary time lag between publication of the original and publication of the translation and helps to improve the quality of the latter. The translation began with the first issue of the Russian journal.

Consultants Bureau journals appear about six months after the publication of the original Russian issue. For bibliographic accuracy, the English issue published by Consultants Bureau carries the same number and date as the original Russian from which it was translated. For example, a Russian issue published in December will appear in a Consultants Bureau English translation about the following June, but the translation issue will carry the December date. When ordering any volume or particular issue of a Consultants Bureau journal, please specify the date and, where applicable, the volume and issue numbers of the original Russian. The material you will receive will be a translation of that Russian volume or issue.

Subscription
$67.50 per volume (6 issues)
2 volumes per year
(Add $5 for orders outside the United States and Canada.)

Single Issue: $30
Single Article: $15

CONSULTANTS BUREAU, NEW YORK AND LONDON

227 West 17th Street
New York, New York 10011

Davis House
8 Scrubs Lane
Harlesden, NW10 6SE
England

Published monthly. Second-class postage paid at Jamaica, New York 11431.

SOVIET ATOMIC ENERGY

A translation of *Atomnaya Énergiya*
Translation published June, 1971

Volume 31, Number 6 December, 1971

CONTENTS

CONTENTS

(continued)

CONTENTS

(continued)

Engl./Russ.

The Russian press date (podpisano k pechati) of this issue was 11/15/1971. Publication therefore did not occur prior to this date, but must be assumed to have taken place reasonably soon thereafter.

Declassified and Approved For Release 2013/02/26 : CIA-RDP10-02196R000300090004-9

ON DETERMINING THE MAXIMUM PERMISSIBLE POWER OF POWER REACTORS, ALLOWING FOR THE THERMOTECHNICAL RELIABILITY OF THE ACTIVE ZONE

V. V. Batov, L. V. Konstantinov,
Yu. I. Koryakin, V. Ya. Novikov,
I. K. Pavlov, and V. V. Postnikov

UDC 621.039.51

There is a well-known general tendency at the present time for power reactors to become more and more powerful; this is because both the capital expediture laid out on atomic power stations and also the steady component of the net cost of the energy produced are inversely proportional to the power. However, increasing (boosting) the power of the reactors with a coolant in the form of water or a water–steam mixture usually involves either a worsening of the heat-removal conditions (boiling crisis) or an increase in the local thermal fluxes (critical flux) and a worsening of the thermotechnical reliability of the operation of the active zone.

As the reactor power increases, so, on the one hand, does the development of energy per unit time, while the specific capital expenditure on the atomic power station and the constant component of the net cost of power diminish; on the other hand, the losses associated with the failure of the fuel channels (cassettes) and the stoppage of the reactor in order to replace these with new ones increase. There is accordingly a certain optimum operating condition for the active zone, and it is with methods of determining this optimum condition that we shall be concerned in this paper.

The determination of the maximum permissible (optimum from the technical–economic point of view) power of the active zone is of great importance in elucidating the requirements to be imposed on the monitoring of the technological parameters. Thus, it is obvious that the structural characteristics of vessel reactors must ensure a high reliability of operation of the active zone, since damage to the fuel elements in these reactors causes serious stoppages and delays in production (relative to that of channel-type reactors). In the case of channel reactors, a more intensive use of the fuel is perfectly acceptable on account of the smaller difference between the nominal and limiting permissible powers of the fuel elements, which also facilitates better control of the technological parameters of each channel in these reactors.

Determination of the Optimum Reactor Power

In order to find the optimum power with due allowance for the thermotechnical reliability of operation of the active zone, we may use the method of reduced expenses [1]; the use of this method for solving various optimization problems in nuclear power was considered earlier [2].

The reduced expenses associated with the production of electrical power are determined in the following manner:

$$E = \frac{C_f}{\bar{B}\eta} + p\frac{K^*_{f.1} + K_{res}}{N\varphi\eta} + \frac{\sum K_i\, a_i + R}{N\varphi\eta}. \qquad (1)$$

Here C_f is the cost of the fuel; $\bar{B}$ is the average depth of burnup; η is the net efficiency of the atomic power station; $K^*_{f.1}$ is the cost of the reactor fuel load when working in the "crisis" mode; K_{res} is the residual cost of the atomic power station (without fuel); φ is the use factor associated with the steady power of the

Translated from Atomnaya Énergiya, Vol. 31, No. 6, pp. 563-566, December, 1971. Original article submitted March 24, 1971.

atomic power station; K* is the cost of an element or component of the equipment composing the atomic power station; a is the amortization factor of the element of equipment; R represents the running expenses of the atomic power station; N is the thermal power of the reactor; p is a norm factor representing the capital outlay engaged in power production; i is the number of the element or component of equipment in question.

Equation (1) may be used to calculate the reduced annual expenses of the atomic power station when working without fuel regeneration ("ejection" mode of operation). For comparing atomic power stations operating at different powers, we may use the formula

$$\tilde{E} = E\frac{N_m}{N}, \tag{2}$$

where N_m is the nominal power of the station.

The dependence of the cost of the fuel load on the number of channels becoming defective may be expressed thus:

$$K^*_{f.l} = K_{f.l}(1+\xi), \tag{3}$$

where $\xi = \nu/n$; $K_{f.l}$ is the cost of the fuel loading of the atomic power station, working in the nominal mode; ν is the number of channels becoming defective per year; n is the total number of channels in the reactor.

According to the methodical principles of operation [1], a convenient indication of the best mode of operation is given by the minimum value of the reduced expenses $\tilde{E}$. If we equate the derivative $\partial\tilde{E}/\partial N$ to zero, we obtain an equation for determining the optimum reactor power:

$$\frac{A}{\bar{B}^2}N^2\frac{\partial\bar{B}}{\partial N} + N\left[\frac{A}{\bar{B}} + \frac{(L+M\xi)}{\varphi^2}\cdot\frac{\partial\varphi}{\partial N}\right] + \frac{2(L+M\xi)}{\varphi} = \frac{MN}{\varphi}\cdot\frac{\partial\xi}{\partial N}. \tag{4}$$

In Eq. (4) we have introduced the following notation:

$$A = \frac{N_m C_f}{\eta}\ \frac{\text{MW}\cdot\text{million roubles}}{\text{mU}};$$

$$L = \frac{N_m\left[p\left(K_{f.l} + K_{res}\right) + \sum K_i a_i + R\right]}{\eta}\ \frac{\text{MW}\cdot\text{million roubles}}{\text{year}};$$

$$M = \frac{pN_m K_{f.l}}{\eta}\ \frac{\text{MW}\cdot\text{million roubles}}{\text{year}}.$$

We may consider that the depth of burnup, averaged over the reactor, is independent of the number of channels becoming defective, i.e.,

$$\partial\bar{B}/\partial N = 0. \tag{5}$$

Then the computing formula for determining the optimum power takes the form

$$N\left[\frac{A}{\bar{B}} + \frac{(L+M\xi)}{\varphi^2}\cdot\frac{\partial\varphi}{\partial N}\right] + \frac{2(L+M\xi)}{\varphi} = \frac{MN}{\varphi}\cdot\frac{\partial\xi}{\partial N}. \tag{6}$$

The use factor of the thermal power of the atomic power station equals

$$\varphi = 1 - \frac{t_s + \Delta t\nu}{8760}, \tag{7}$$

where t_s is the idle time of the power station due to repair work for the normal mode of use in h; ν is the number of fuel channels becoming defective; Δt is the time required for replacing a defective channel.

We note that, for the foregoing method, only the existence of a relationship $\nu = f(N)$ is essential; the exact form of this relationship will depend on the extent to which the theory corresponds to reality. Here we shall assume that, as the power increases, the reason for the channels becoming defective is simply the worsening of the conditions of heat removal (crisis of the second kind).

Dependence of the Number of Channels Becoming Defective on the Power

In channel-type reactors using boiling water as coolant, any excess over the critical power of the evaporating channel will transform the latter into a mode of poor heat removal, corresponding to a crisis of the

second kind, and this may cause the channel to become defective. The critical power of the evaporating channels depends on the flow of water through the channel G, the pressure P, and the temperature of the water at the channel inlet t_{in}.

This relationship is usually found from test-bed experiments. The thermotechnical reliability of the evaporating channel with respect to a crisis of the second kind is determined by the "reserve," or difference between the actual and critical power $X(t) = N_{cr} - N$, where N is the power of the evaporating channel measured in the course of service.

The error committed in maintaining a specified reserve for an individual evaporating channel is determined by the capacities of the regulation system, the operating regulations, the qualifications of the operator, the errors committed in determining N, G, P, and t_{in}, the error committed in determining N_{cr} on the test-bed, and so on. A study of the time dependence of the quantity X(t) carried out over 1.5 years service of the reactors in the Beloyarsk Atomic Power Station for several evaporating channels with high-precision test instruments showed that X(t) might be regarded as a stationary random process, while the random deviations of X(t) from the mean were distributed in accordance with a normal law, having a mean square deviation σ_X [3]. The value of ν, the mean number of failures of the evaporating channels per year in the poor heat-removal mode, may be calculated in accordance with the theory of chance [4]:

$$\nu = A \sum_{i=1}^{n_{ec}} \exp\left[-\frac{1}{2}\left(\frac{N-N_i}{\sigma_x}\right)^2\right], \tag{8}$$

where A is a constant depending on the error of measuring the characteristics of the reactor, determined experimentally from the X(t) relationships already determined [3]; n_{ec} is the total number of evaporating channels in the active zone of the reactor.

On the basis of these data, we may easily calculate the average number of evaporation channels finding themselves in a state of poor heat removal at any given instant

$$S = \sum_{i=1}^{n_{ec}} p_i, \tag{9}$$

where p_i is the probability that the i-th evaporation channel is in a state of poor heat removal; we may also calculate the probability that the reactor will be operating in the crisis-free mode

$$R = \prod_{i=1}^{n_{ec}} (1 - p_i) \tag{10}$$

and the technological reliability of the reactor [3].

The value of ν depends substantially on the power, and in the majority of practical cases is excellently described by the empirical formula

$$\nu = e^{-\alpha+\beta N}. \tag{11}$$

In calculating the optimum power, it was assumed that all the evaporating channels passing into a state of poor heat removal (even if only on one occasion) became inoperative.

Calculation of the Reduced Expenses Allowing for Regeneration of the Exhausted Fuel

The cost of the fuel, with due allowance for the regeneration of exhausted fuel, is by definition equal to

$$C_f^{reg} = C_f + \Delta C_f \tag{12}$$

where C_f is the cost of the fresh fuel and

$$\Delta C_f = C_{ho} + C_{tr} + C_{chem} - C_U - C_{Pu}. \tag{13}$$

Here C_{ho} is the cost of holding (storing) the exhausted fuel in the atomic power station; C_{tr} is the cost of transporting it to the place of regeneration; C_{chem} is the cost of regeneration; C_U is the cost of the residual uranium; C_{Pu} is the cost of the accumulated plutonium.

If the channels become defective by virtue of the heat-transfer crisis, Eq. (13) may be written in the form

$$\Delta C_f^{cr} = C_{ho} + C_{tr} + C_{chem} - \tilde{C}_U - C_{Pu}, \tag{14}$$

where $\tilde{C}_U$ is the cost of the uranium obtained after regeneration with an enrichment factor half-way between the initial ($\varkappa_{init}$) and final ($\varkappa_{fin}$) values.

Let

$$\Delta\tilde{C}_U = C_U - \tilde{C}_U. \tag{15}$$

Then the value of the fuel component of the reduced losses may be written in the form

$$E_f = \frac{C_f}{\bar{B}\eta} + \frac{\Delta C_f + \Delta\tilde{C}_U}{\bar{B}\eta} + p\frac{K_{f.1.}(1+\xi)}{N\varphi\eta}. \tag{16}$$

The final expression for determining the optimum power will be analogous to Eq. (6)

$$N\left[\frac{\tilde{A}}{\bar{B}} + \frac{(L+M\xi)}{\varphi^2}\cdot\frac{\partial\varphi}{\partial N}\right] + \frac{2(L+M\xi)}{\varphi} = \frac{MN}{\varphi}\cdot\frac{\partial\xi}{\partial N}, \tag{17}$$

where

$$\tilde{A} = \frac{N_m C_f^{reg}}{\eta}\ \frac{\text{MW}\cdot\text{million roubles}}{\text{mU}}$$

Calculation of the Optimum Power

Let us slightly simplify Eq. (17). Since

$$\frac{M\xi N}{\varphi^2}\cdot\frac{\partial\varphi}{\partial N} \ll \frac{LN}{\varphi^2}\cdot\frac{\partial\varphi}{\partial N}, \tag{18}$$

we have

$$\frac{LN}{\varphi^2}\cdot\frac{\partial\varphi}{\partial N} + \frac{\tilde{A}}{\bar{B}}N + \frac{2L}{\varphi} = \frac{MN}{\varphi}\cdot\frac{\partial\xi}{\partial N}. \tag{19}$$

Considering that

$$\frac{L}{\varphi^2}\cdot\frac{\Delta t\beta}{8760} = a;\quad \frac{2L}{\varphi} = b;\quad \frac{Mn\beta}{\varphi} = c;\quad \frac{\tilde{A}}{\bar{B}} = d,\quad \frac{\partial\varphi}{\partial N} = -\frac{\Delta t\beta\nu}{8760};\quad \frac{\partial\xi}{\partial N} = \beta\nu,$$

we have

$$e^{-\alpha+\beta N} = \frac{d}{a+c} + \frac{b/c+a}{N}. \tag{20}$$

Equation (20) is transcendental, and may be solved by numerical methods. For the optimum power, we calculate the corresponding optimum values of ν_{opt} and S_{opt}. Calculations carried out for several evaporating channels of the reactors in the Beloyarsk Atomic Power Station showed that the relation between the quantities S and ν depended little on the measuring errors, the form of the N_{cr} relationship, and the nonuniformity of the radial distribution of energy evolution. The quantities ν_{opt} and S_{opt} are extremely stable, and vary over very narrow ranges as the other factors vary; allowance may be made for the latter by operating the reactor without exceeding certain specified values of ν and S.

The most economically effective reactor working conditions are given by $S = S_{opt}$ and $\nu = \nu_{opt}$.

LITERATURE CITED

1. "Standard method of determining the economic effectiveness of capital outlays," Ékonomicheskaya Gazeta, No. 39 (1969).
2. V. V. Batov and Yu. I. Koryakin, Economics of Nuclear Power [in Russian], Atomizdat, Moscow (1969).
3. L. V. Konstantinov et al., At. Énerg., 29, 208 (1970).
4. A. A. Sveshnikov, Applied Methods of Random-Function Theory [in Russian], Nauka, Moscow (1968).

TESTING THE HERMETICITY (AIR TIGHTNESS) OF FUEL ELEMENTS IN THE BR-5 REACTOR

I. A. Efimov, L. I. Mamaev, and V. S. Filonov

UDC 621.039.562

Work on testing the hermetic state of the fuel elements in the BR-5 fast-neutron reactor (sodium coolant) started in 1959. In 1965 a regular test system was introduced into the activity for monitoring the hermetic state of the fuel elements; this consisted of a device for continuously recording the delayed neutrons from the coolant, apparatus for continuously recording the β-activity of the gas in the gas spaces of the first circuit, and also a scintillation spectrometer for periodically testing the composition of gas and sodium samples taken from the first circuit.

The delayed neutrons from the coolant are recorded by means of six independent neutron sensors based on counters with a corona discharge placed in a polyproylene moderator. The small size of the sensors, their temperature stability, and their efficiency in γ-fields up to 0.3 R/sec enabled these sensors to be set directly in the thermal insulation of the first-circuit conduit without any special arrangements for cooling or shielding them. The high sensitivity to delayed neutrons yielded an intensity of at least 100 pulses /sec at the output, the contribution arising from photoneutrons being no greater than 7% under these conditions. Five years of experience with this apparatus showed that the change in readings with time never exceeded 15% over several months of continuous use. The average count rate of all the sensors is recorded continuously on an automatic recorder. The operation of the detectors in an unserviced room made it essential to have a sixfold reserve of these and also of the recording apparatus, despite the high reliability of the sensors; in 15,000 h of work, one or two of the six sensors became defective.

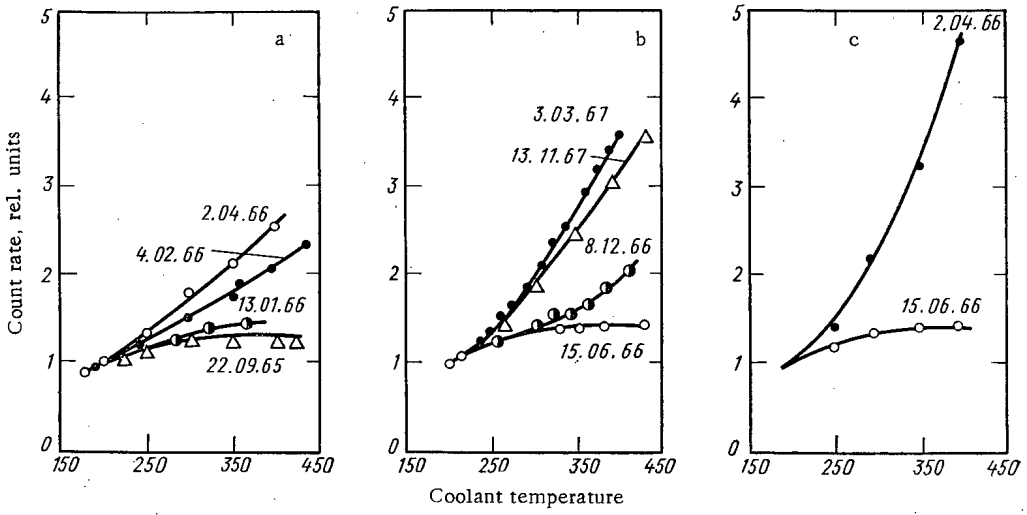

Fig. 1. Effect of coolant temperature on the readings of the apparatus used for testing the hermetic state of fuel elements: a) from delayed neutrons, fuel PuO_2; b) from delayed neutrons, fuel UC; c) from the β-activity of the gas in the gas spaces of the circuits, fuel PuO_2. All the results were obtained with the reactor working at 500 kW and were normalized to unity for a coolant temperature of 200°C. The results 22.09.65 and 15.06.66 were obtained when there were no leaking fuel elements in the reactor.

Translated from Atomnaya Énergiya, Vol. 31, No. 6, pp. 567-571, December, 1971. Original article submitted November 12, 1970.

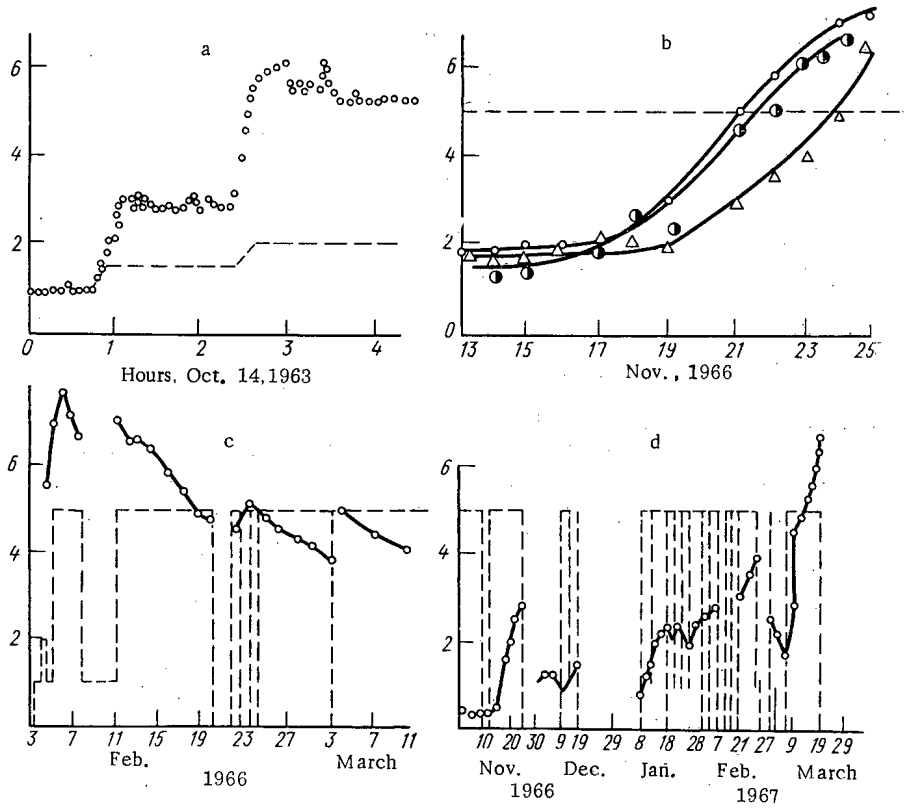

Fig. 2. Change in the activity of the fission products: a) for a leaking PuO_2 fuel element; b) for a leaking UC fuel element; c) active zone contains leaking PuO_2 elements; d) active zone contains leaking UC elements; ○) delayed neutrons; ◑) Xe^{135}; △) Xe^{133}; ———) power level, MW.

TABLE 1. Average Leakages of Fission Products from One Leaking Fuel Element for a Can Temperature of 550°C and Nominal Rector Power

Parameter	Fuel	
	PuO_2	UC
Fission rate in one element, fissions/sec	$5,6 \cdot 10^{13}$	$2,4 \cdot 10^{14}$
Leakage level, fission/sec *	$5,2 \cdot 10^{11}$	$(4,4—11) \cdot 10^{12}$
Proportion of leaking isotopes, % *	0,5	0,9—2,3
Gaseous fission product leakage constant, 1/sec	$3 \cdot 10^{-7}$	$(4,5—58) \cdot 10^{-9}$

* Data obtained from delayed neutrons

As detectors in the apparatus for recording the β-activity of the gaseous fission products in the gas spaces of the circuit, six β-counters are used; these are placed along a stainless steel tube 4 mm in diameter and 0.7 mm thick through which the gas is pumped from the gas spaces. Three counters of the six are screened with an additional layer of steel 1.2 mm thick, so that the screened counters record practically only the γ-activity of the sample. The β-activity of the gas was estimated from the difference between the readings of the screened and unscreened counters; in the worst case the ratio of the count rates for these counters exceeded 1.5. When the time required for the gas to reach the sensor was over 20 min, the greater part of the recorded β-activity was due to the presence of Rb^{88} with traces of Cs^{138}, constituting decay products of Kr^{88} and Xe^{138}. When the time was under 5 min the greater part of the activity recorded by the counters came from Ne^{23}, this being an activation product of sodium. In the first versions, electrodeposition of the rubidium and cesium ions was employed in the sample tube. Later it was found that stimulated deposition could be eliminated, thus simplifying the construction of the whole system. Even in this case, however, some tens of hours after initiating the circulation there was a fall in the rate of flow owing to the blocking of the filter with sodium vapor. Later it was found that the tubes through which the gas returned to the gas space of the circuit also became blocked. Under these conditions the continuous use of the gas-sampling system was accepted as being quite impossible. Using occasional sampling of the gas, the value of the resultant data was much less than that of the scintillation-spectrometer measurements.

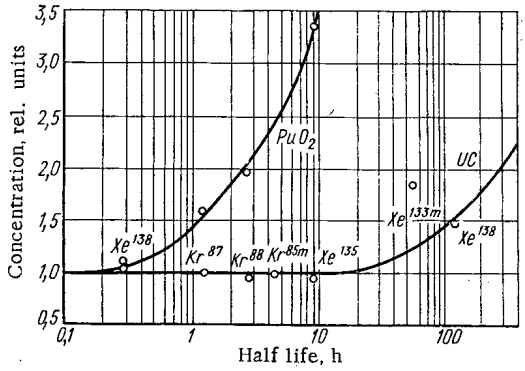

Fig. 3

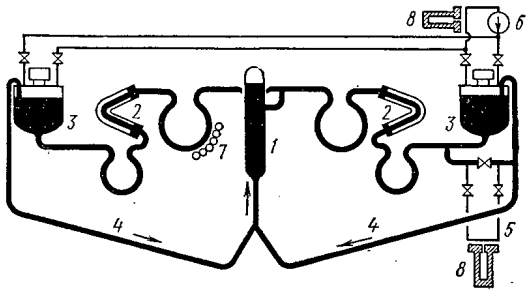

Fig. 4

Fig. 3. Equilibrium concentration of gaseous fission products in the gas spaces of the first circuit as a function of the half-life period (reactor power 5 MW, coolant temperature at the reactor inlet 430°C).

Fig. 4. Arrangement of the sensors for testing the tightness of the fuel elements: 1) reactor; 2) heat exchangers; 3) pumps; 4) sodium-containing tube; 5) sodium-sampling system; 6) gas-sampling system; 7) delayed-neutron sensors; 8) scintillation-spectrometer sensors.

The scintillation spectrometer with an AI-256 analyzer has several sensors containing NaI(Tl) crystals 40 × 40 mm in size placed in the gas-sampling lines and in the bypass section of the sodium circuit. After holding the sodium for a time the activity of the long-lived fission products in the sodium and in the walls of the tubular conduit may be measured. If the sodium is decanted from this section, the activity of the fission products in the conduit walls may be determined on its own.

If there are no leaking fuel elements in the active zone of the reactor, the readings of the test apparatus are directly proportional to the reactor power, whatever the testing method. The accumulation of long-lived isotopes in the circuit follows the ordinary accumulation laws. The activity of the isotopes, including those emitting delayed neutrons, increased roughly by a factor of 1.4 on changing the temperature of the coolant from 200 to 430°C (Fig. 1).

At the instant at which a fuel element containing PuO_2 fuel starts leaking, there is a sharp increase in the count rate of the neutron sensors, with a subsequent spasmodic change for a period of several hours, apparently associated with the cracking of the can. At the end of the spasmodic period the amplitude of the jumps becomes smaller, and the averaged readings continue falling for many weeks (Fig. 2). The leakage of gaseous fission products approximately corresponds to the picture presented, with the sole difference that all the surges in activity have a greater amplitude.

When fuel elements containing UC fuel of hyperstoichiometric composition start leaking, there is a monotonic rise in the activity of the fission products in the circuit, continuing for many days. The activity of the gaseous fission products follows the neutron activity of the coolant, independently of the half-life period, except that it is delayed by a time interval equivalent to the latter.

The stopping of the reactor, followed by an increase in its power, leads to a surge of activity from leaking fuel elements if the fuel consists of PuO_2, but to a fall in the level of activity if the fuel is UC. Finally, there is a difference in the equilibrium isotopic composition of the fission products in the circuit; in the case of PuO_2 the isotope concentration depends very strongly on the half-life period, whereas this effect is far less marked in the case of a leaking UC fuel element (Fig. 3). Judging by the level of neutron activity in the coolant when a single fuel element starts leaking, the leakage of the fission products arises from approximately 1% of all the fuel in the fuel element (Table 1).

The increased activity of the long-lived gaseous fission products in the circuit may be explained as being due to an independent leak, i.e., a leak not associated with fission processes, for example, the diffusion or migration of pores. Accepting this explanation, we may use Fig. 3 to estimate the leakage constant of the gaseous fission products from a single leaking fuel element (Table 1).

The levels of contamination of the circuit with long-lived fission products measured by means of the scintillation spectrometer indicate that the γ-activity of the circuit after the decay of the Na^{24} is mainly

TABLE 2. Levels of Contamination of the Reactor Part of the Circuit by the Fuel

Date of measurement	Level of leakage, fissions/sec	Temperature coefficient	Amount of U^{235} in the reactor part of the circuit, g
June 26 1965	$4,6 \cdot 10^{11}$	1,40	0,1 (Pu)
May 7 1966	$5 \cdot 10^{11}$	1,40	0,1 (Pu)
June 7 1968	$1,1 \cdot 10^{13}$	1,44	6,7
Sept. 23 1968	$3,2 \cdot 10^{13}$	2,15	12,7
Feb. 5 1969	$2,1 \cdot 10^{14}$	2,95	25
May 14 1969	$1,6 \cdot 10^{14}$	2,53	38
Dec. 22 1969	$2,1 \cdot 10^{13}$	1,84	10,7

determined by the Ba^{140} isotope. Comparison of the activity of this isotope (allowing for the period of accumulation) with the readings of the apparatus recording the delayed neutrons indicates a fairly strict correlation between these. This offers a means of predicting the level of γ-activity of the circuit when the reactor is stopped for servicing and repair.

The leaking of the fuel elements leads to an increase in the dependence of the readings obtained from the leak-monitoring apparatus on the coolant temperature (Fig. 1). For a large number of leaking fuel elements, if the effect of the contamination of the reactor part of the circuit by the fuel may be neglected, a change in the coolant temperature from 200 to 430°C increases the readings of the monitoring apparatus based on delayed neutrons by a factor of three. However, if the effect of contamination may not be neglected, the temperature coefficient takes an intermediate value between 3 and 1.4. The temperature coefficient for the neutron activity of the coolant is measured on an average once in two months in the BR-5 reactor. These data are used to estimate the levels of contamination of the reactor part of the circuit presented in Table 2.

In individual cases, the presence of leaking fuel elements in the active zone of the reactor led to a nonlinear dependence of the readings of the apparatus recording the delayed neutrons on the reactor power. The amount by which the readings exceeded the linear relation was equivalent to a factor of two, the nonlinearity increasing on approaching the nominal power of the reactor. In the presence of nonlinearity the level of contamination of the circuit with fuel and fission products increases. Evidently the development of nonlinearity is due to the severe cracking of one of the fuel elements, leading to the penetration of coolant into the central regions of the fuel element; it indicates a state of emergency in the latter.

In seven years of continuous monitoring of the BR-5 reactor, only once did an emergency fuel-element leakage (with PuO_2 fuel) occur (November 1, 1964). Various signs indicated that more than ten fuel elements started leaking in 1 min. The rapidly-worsening dosimetric conditions made it essential to reduce the power to 10% nominal within 6 h, and after another 2 h to shut the reactor down altogether. On recharging the packs, no melted fuel elements were found, although every fifth pack contained a leaking element. The recharging itself involved no difficulties.

In the same seven years' observations, no gas leak from the fuel-element cans which might have been a consequence of technological failure was found. The increase in the activity of the inert gases corresponded to a change in the neutron activity of the coolant. All this suggests seeking the reason for the leakage of the fuel elements not in the slow corrosion of their cans but in their rupture by excess internal pressure due to the swelling of the fuel or an undue rise in inert gas pressure under the can. This circumstance was by no means the least in influencing the decision finally to abandon the continuous recording of the β-activity of the inert gases.

For the last three years the hermetic state of the fuel elements have been monitored by the apparatus recording the delayed neutrons and the scintillation spectrometer. This apparatus enables us:

To determine the instants at which fuel elements start leaking, to estimate the level of tightness loss, and to prevent severe contamination of the circuit in possible emergency situations associated with this loss of tightness; at any instant to verify (by measuring the temperature coefficient) whether any leaking fuel elements exist in the zone, to estimate the level of contamination of the reactor part of the circuit by fuel and long-lived fission products, and also to reveal the existence of dangerous leakages of fuel elements in the active zone.

These data are already sufficient to characterize the state of the fuel elements in the active zone and to indicate the possibility of further use of the reactor. However, the potentialities of the apparatus are much wider: the data may be used to estimate the effect of various modes of reactor operation on the efficiency of the fuel elements, to study the mechanism underlying the passage of fission products from the elements into the sodium and from the sodium into the gas spaces, and also to study the behavior of fission products in the circuit and thus help in purifying the circuit from these. The reliability of the resultant data is additionally verified by piecemeal measurements. The arrangement of the sensors is indicated in Fig. 4.

Experience in using the leak-detecting apparatus in the BR-5 reactor indicates the possibility of securing a considerable economic effect by placing this kind of apparatus in power reactors with a sodium coolant. If we neglect the possibility of preventing rapid emergencies involving the melting of the fuel, the main effect will be the gain in the atomic-power-station loading coefficient, arising as a result of the optimization of the reactor working conditions. On the one hand, the apparatus enables us to prevent the premature discharging of the packs, and on the other it prevents work from continuing with badly leaking fuel elements, which would otherwise severely contaminate the circuit with fuel and fission products and increase the time spent in repair to the equipment of the first circuit.

The effectiveness of the use of the leak-detecting apparatus for the fuel elements is well illustrated by comparing two periods of operation of the BR-5 reactor: 1959-1964 and 1965-1970. In the first stage of reactor operation, in which (up to 1962) there was no leak-detecting apparatus, the reactor only spent 14% of its working time in the nominal mode. Over the last six years the reactor has produced power for twice the time, and the percentage of operation in the nominal modes has increased to 70%. Moreover, despite the fact that in both periods of reactor operation the same high (over 60 kg/ton) fuel burnup was achieved, in the second period the radioactive contaminations of the circuit with fission products were considerably lower, because of the timely removal of defective fuel elements from the active zone.

The authors wish to thank N. N. Aristarkhov, G. K. Ermakov, D. I. Zhestkove, V. P. Kravchenko, and others who took part in the development, testing, and use of the apparatus.

PRINCIPLES UNDERLYING THE ESTABLISHMENT OF NORMS FOR THE EJECTION OF RADIOACTIVE PRODUCTS FROM THE PIPES OF INDUSTRIAL ATOMIC AND POWER INSTALLATIONS (METEOROLOGICAL ASPECTS)

N. E. Artemova and E. N. Teverovskii

UDC 551.510.72

The propagation of impurities ejected from working industrial undertakings through the atmosphere takes place in accordance with the special aspects of turbulent transfer characteristics of the site in question, the power of the installation, and the properties of the impurities themselves. The concentration of harmful substances close to the ground and the density of their fallout in the locality also depend on the thermodynamic state of the atmosphere, the wind speed and direction, the height, volume, and velocity of ejection, the period of operation of the source, precipitation and washing processes, and the capacity of the impurity so transported to undergo radioactive decay. Thus the dissipation of radioactive products ejected into the atmosphere constitutes a process involving the interaction of a large number of mechanisms, leading to the establishment of a certain relationship between the amount of impurity ejected through the pipe and its concentration in the air and the underlying surface at various points in the space surrounding the source of ejection. This relationship may, to a fair degree of accuracy, be characterized by a dilution coefficient P (dimensions of L^3/T, where L is the unit of length measurement and T is the time) in the relation between the intensity of ejection Q (dimensions T^{-1}) of the impurity and its concentration in the air (dimensions L^{-3}):

$$Q = Pc. \tag{1}$$

For continuous ejection with a constant intensity Q, the coefficient P determines the volume required for the impurity ejected from the source in unit time to become dissipated to an extent corresponding to the ground concentration (observed or calculated). The coefficient P depends on the period used for averaging the complex of meteorological conditions, and varies smoothly on moving away from the source in the direction of the prevailing wind (Fig. 1). The minimum value of P corresponds to the greatest ground concentration, i.e., to the point at which the access of impurity in the two-meter layer of air nearest to the ground as a result of vertical diffusion and advection reaches a maximum.

The results of a prolonged study of the laws governing the propagation of various types of substances ejected from the pipes of industrial undertakings enable us to formulate some general principles regarding the calculation of the limiting permissible ejection, allowing for the dilution of the impurity in the atmosphere and the norms of radiation safety applicable to the specific conditions of place and time.

In accordance with the recommendations of the International Commission on Radiation Safety [3] and the International Agency on Atomic Energy [4], the radiation-safety norms NRB-69 [1, 2] are based on the assumption that a linear relationship exists between the doses of irradiation and the biological effect, i.e., it is assumed that there is no threshold of action of the ionizing radiations. In accordance with this assumption, certain average annual limiting permitted somatic doses of external and internal irradiation (differing for the workers inside the undertaking and the population living in its neighborhood) have been established with a view to regulating the access of radioactive isotopes into the human body with air, water, and food, and the amount of isotopes in the air at ground level.

The problem of setting a norm for the ejected material amounts to establishing a limiting permitted ejection of particular isotopes (or the sum of these) for every industrial undertaking, such as to satisfy the

Translated from Atomnaya Énergiya, Vol. 31, No. 6, pp. 573-576, December, 1971. Original article submitted November 16, 1970.

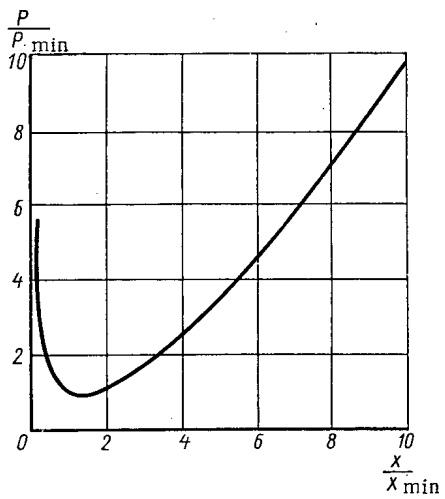

Fig. 1

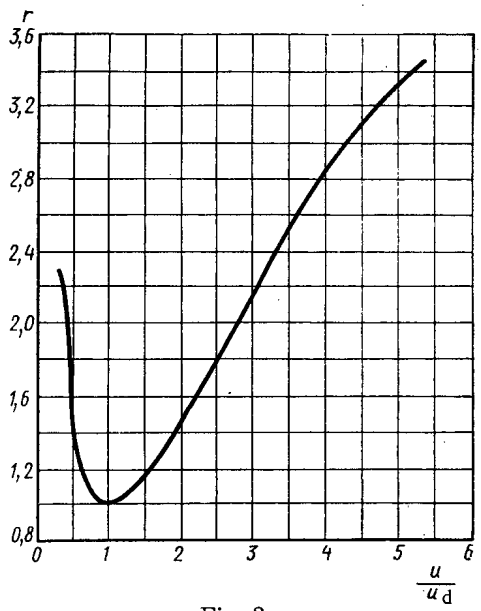

Fig. 2

Fig. 1. Dilution coefficient P as a function of the change in the distance x from the source of ejection.

Fig. 2. Dependence of the parameter r on the ratio u/u_d.

norms of external and internal irradiation for those working in the undertaking or living near it under the conditions prevailing in the particular geographic region. For this purpose a relation of type (1) is employed, linking the limiting permitted ejection to the mean annual permissible concentration and the mean annual dilution coefficient $\overline{P}$, taken with due regard to the character of the source and the meteorological conditions of the particular region.

The mean annual permissible concentration of radioactive products in the air is determined from the mean annual permissible access of isotopes into the human body by inhalation and through the food chain, and also from the limiting permissible external irradiation. The values of the mean annual permissible concentration are given in the norm NRB-69 [2]. The mean annual value of the coefficient $\overline{P}$ may be found experimentally or by calculation; in establishing norms for the amounts ejected, it is essential to consider the minimum values of the dilution coefficients, corresponding to the points characterized by the maximum amount of impurity in the air.

In this paper we shall present a general scheme for estimating the minimum mean annual dilution coefficient for a radioactive impurity continuously emerging from a pipe into the lower layers of the atmosphere; we shall discuss ways of allowing for the characteristics of the real pattern of dilution.

Dilution of a Trace of Long-Lived Impurity Ejected by a Continuously-Acting Raised Source into the Atmosphere

The coefficient P may be determined for a trace of long-lived impurity in accordance with Eq. (1) and existing methods of calculating ground concentrations, each of which uses some particular period of averaging the meteorological parameters under consideration and the ground concentration respectively. The establishment of impurity-ejection norms on the basis of the mean annual permissible access of radioactive isotopes into the human body unambiguously decides that the period of averaging the permissible concentration and dilution coefficient should be "mean annual."

The complexity of the majority of existing analytical formulas for calculating ground concentrations with long averaging periods sometimes compels us (when such calculations have to be made) to use existing methods of calculating short-period concentrations in combination with certain empirical laws, which characterize the relationships between various averaging periods or the functional form of certain climatological quantities. Thus, in order to estimate the minimum dilution coefficient, it is convenient to use the formula recommended earlier [5], which is quite widely employed for calculating the maximum value of the short-term (20 min) concentration, express this in terms of the dilution coefficient, and supplement with a parameter allowing for the relation between the short-term and mean annual concentration, together with a

TABLE 1. Calculation of the Mean Annual Minimum Dilution Coefficient $\bar{P}_{min}$

Climatic zone	Parameter	$\frac{n}{n_0}$ 1:2	1:3	1:4
Central European territory of the USSR	0,12	$350H^2$	—	—
North, north-west European territory of the USSR, Mid-Volga, Ural, Ukraine	0,16	$260H^2$	—	—
Lower Volga, North Caucasus, north Siberia	0,20	$210H^2$	—	—
Kazakhstan, Central Asia, Central Siberia (Omsk, Novosibirsk, Kemerov region)	0,20	—	$140H^2$	
North-east Siberia (Chukotka, Kamchatka), Central Siberia (Krasnoyarsk border, Yakutsk Autonomous SSR)	0,20	—	—	$106H^2$

parameter characterizing the special aspects of the mean annual wind variation:

$$\bar{P}_{min} = \frac{H^2 \sqrt[3]{V\Delta T}}{A\alpha \frac{n}{n_0}}. \quad (2)$$

Here H is the geometrical height of the pipe in m; V is the volume of gas–air mixture ejected from the pipe in m^3/sec; ΔT is the temperature difference between the ejected gases and the surrounding medium in deg; A is a parameter allowing for the special aspects of turbulent mixing under the conditions of fully developed convective exchange applying in various parts of the Soviet Union in $deg^{1/3} \cdot sec^{2/3}$; n/n_0 is an index representing the elongation of the mean annual wind directional diagram for the particular region, constituting the ratio of the actual mean annual reproducibility of the prevailing wind direction to the reproducibility of the winds for the case in which all directions are equally probable (i.e., for the so-called circular wind variation characteristic); α is the coefficient of time averaging, which is equal to the ratio of the dilution coefficients with different averaging periods P_1/P_2, and is in general [6-8] proportional to $(t_1/t_2)^{1/2}$; where t_1 and t_2 are the corresponding periods for averaging the dilution coefficients. This relationship – which is also confirmed by our own experimental data relating to long averaging periods (up to a year) – is due to the difference in the degree of stability of the average wind for different averaging periods, or in other words the dispersion of the direaction of the average wind. For a circular wind variation:

$$\alpha = \frac{P_{s\text{-}t}}{P_{ann}} = \frac{1}{13};$$

The parameter n/n_0 characterizing the actual reproducibility of the prevailing wind direction enables us to allow for the true dispersion of the distribution of the most dangerous wind direction.

The point corresponding to the minimum dilution lies at x_{min} = 15-20 H from the source. Concentrations of radioactive impurity differing by no more than 30% from the maximum occur at a distance of 10-40 H from the source [5].

The values of $\bar{P}_{min}$ calculated from Eq. (2) correspond to the dissipation of the impurity for the so-called "dangerous" wind velocity u_d, for which the change in the height of ejection due to the thermal and dynamic lifting of the jet is most effectively compensated by the change in longitudinal dissipation associated with advection. The value of u_d may be determined, as earlier [5], from the ejection parameters

$$u_d \cong 0.65 \sqrt[3]{\frac{V\Delta T}{H}}. \quad (3)$$

For atomic power stations, with typical parameters $V = 10^5$ m^3/h and $\Delta T = 10°$ (in summer), the dangerous wind velocity for an ejection height of H = 100 m is ~1 m/sec. Table 1 gives the calculated values of the mean annual $\bar{P}_{min}$ for a trace of long-lived radioactive impurity ejected continuously into the atmosphere at a height H (V and ΔT are taken as being the same as in the calculation of u_d). The dilution coefficients are given for various parts of the Soviet Union in accordance with our standarddivision into regions by reference to the reproducibility of the prevailing winds and turbulent exchange characteristics.

Corrections to the Dilution Coefficient $\bar{P}_{min}$ Allowing for Certain Aspects of the Propagation of Radioactive Impurity

Allowance for Radioactive Decay. When rapidly-decaying isotopes are ejected, the amount of impurity in the air diminishes on moving away from the source in the direction of the wind, not only on account of the turbulent dissipation, but also on account of radioactive decay. As a result of this, the dilution coefficient

for the short-lived radioactive products ejected continuously into the atmosphere in the course of a year is determined in the following way:

$$\bar{P}^{*}_{\min} = \bar{P}_{\min} e^{\frac{20H\lambda}{u}}, \quad (4)$$

where λ is the decay constant; u is the mean annual wind velocity at the height of the cowl (10 m).

Allowance for the Real Wind Velocity. If the mean annual wind velocity u differs from the dangerous wind velocity u_d, the mean annual dilution coefficient $\bar{P}^{u}_{\min}$ may be approximately determined [5] from the relation

$$\bar{P}^{u}_{\min} = r\bar{P}_{\min} \quad (5)$$

where r is a certain dimensionless parameter. The dependence of the parameter r on the ratio u/u_d is given in Fig. 2.

In atomic industrial undertakings ejecting at a height of 100 m (u_d = 1 m/sec), for mean annual wind velocities of the order of 2-5 m/sec the dilution increases by a factor of 1.5-3 as compared with the dilution for the dangerous wind velocity. The zone of minimum dilution [5] moves a little closer to the source

$$x^{u}_{\min} = 0.8x_{\min} \quad (6)$$

Allowance for the Climatological Probability of the Establishment of Conditions of Fully-Developed Convective Exchange. The values calculated from Eq. (2) for the minimum dilution coefficient correspond to the intensive vertical transfer of the impurity into the lower two-meter layer of air under conditions of the fully-developed convective exchange characteristic corresponding to a summer day. The duration of such conditions for the majority of regions in the Soviet Union, except for Central Asia and Kazakhstan, averages ~10% in a year (for Central Asia and Kazakhstan the values are 25 and 15% respectively [9]).

In the majority of regions of the Soviet Union, the yearly average state of the thermal stratification of the atmosphere is closest to a neutral or equilibrium state, in which the maximum concentration for high sources is 20-30% smaller than under conditions of developed convection. Hence the coefficients of minimum dilution calculated in accordance with Eq. (2) or the tabulated data contain a certain reserve coefficient, which may be taken into account if we possess information regarding the reproducibility of various categories of stability in the region under consideration.

Allowance for Fallout and the Washing of Impurity from the Jet. The fallout of radioactive products onto the Earth's surface from the jet arises mainly from turbulent precipitation and the capture of radioactive particles by elements of the falling precipitates (in view of the comparatively small dimensions of the radioactive aerosols). On averaging over long periods of time, including days both with and without precipitation (rain and snow), the flow of radioactive dust directed downward is characterized by a certain total rate of precipitation v_g equal (according to our own results and published data [10]) to ~1 cm/sec.

The effect of turbulent precipitation and the washing-out of the impurity by the precipitates, leading to a reduction in the amount of impurity in the jet, may be taken into account by introducing a certain correction factor into the dilution coefficient [11]:

$$\bar{P}^{f.o}_{\min} = \bar{P}_{\min} e^{\frac{v_g x}{ul}},$$

where x is the distance from the source of ejection in m; u is the mean annual wind velocity in m/sec; l is the linear scale of the jet, roughly equal to its mean diameter in m.

The special features of the dilution of radioactive impurity in the atmosphere considered in this paper are associated with the propagation of the impurity in the layer of air close to the ground. The recommended methods of determining the dilution coefficient may be used in calculations of the limiting permissible ejection of those radioactive substances for which norms have been established in relation to the mean annual permissible influx into the human body by inhalation and the mean annual permissible concentration in the atmospheric air.

LITERATURE CITED

1. I. K. Dibobes et al., At. Énerg., 28, 463 (1970).
2. Norms of Radiation Hazard (NRB-69) [in Russian], Atomizat, Moscow (1970).
3. Radiation Shielding (Recommendations of the International Committee of Radiation Shielding, 1962), Publication 6 [Russian translation], Atomizdat, Moscow (1963).
4. Fundamental Norms of Danger in Radiation Shielding (1967), Series of Safety Publications [Russian translation], No. 9, MAGATÉ, Vienna (1968).
5. Guide on the Calculation of the Atmospheric Dissipation of Harmful Substances in the Effluent of Industrial Undertakings (SN-369-67) [in Russian], Gidrometeoizdat, Leningrad (1967).
6. Yu. S. Osipov, Izv. Akad. Nauk SSSR, Ser. Fiz. Atmos. i Okeana, 5, 533 (1969).
7. F. Wipperman, Internat. J. Air and Water Pollution, 5, No. 1/6, 1 (1961).
8. R. Sachdev and S. Nadgir, J. Appl. Meteorology, 8, No. 4, 527 (1969).
9. F. F. Avitaya (editor), Climatic Atlas of the USSR [in Russian], Vol. 1, Gidrometeoizdat, Moscow (1960).
10. K. P. Makhon'ko, Settling of Radioactive Dust and Its Removal from the Atmosphere by Precipitation [in Russian], Atomizdat, Moscow (1968).
11. L. Konig and S. Zehme, Atompraxis, 11, No. 4/5, 191 (1965).

ON THE PURITY OF THE RADIATION ENVIRONMENT NEAR THE REACTOR IRT-2000

I. T. Mishev and M. A. Radicheva

UDC 621.039.58

The control of radioactive contamination in the environs of nuclear reactors is being accomplished in many countries. As a result of accumulated experience it can be asserted that under normal operating conditions reactors do not represent a radiation hazard to the surrounding population. This does not mean, however, that it is advisable to cease observations of possible radioactive contamination.

Low-power experimental reactors have existed for about 30 years, but only during the past 10 years have reactors been utilized as powerful sources of energy. The operation of reactors at high power levels leads not only to an increased potential radiation hazard in emergency situations, but also in general to a higher emission of radioactive substances to the environment.

Control around reactors also allows data to be obtained on the purity of the radiation environment within the territory of a particular country. Irregular or periodic measurements of radioactive contamination of their entire territory are conducted by many governments in connection with the continuing nuclear tests in the atmosphere [1-3].

The reactor IRT-2000 in Sofia commenced operation in September 1961. From the day of its startup until December 31, 1968, $5 \cdot 10^6$ kWh of thermal energy were generated. During this time samples were periodically taken according to a previously prepared program for the determination of the level of radioactive contamination of soils, plants, water in uncovered reservoirs, etc. The observations over seven years in the zone of 1 km radius around the reactor reveal no increase above background in radioactive contamination resulting from reactor operation [4, 5]. A unique occurrence involving the appearance of a measurable concentration of Ca^{45} in the waste water was caused by a violation of existing instructions by

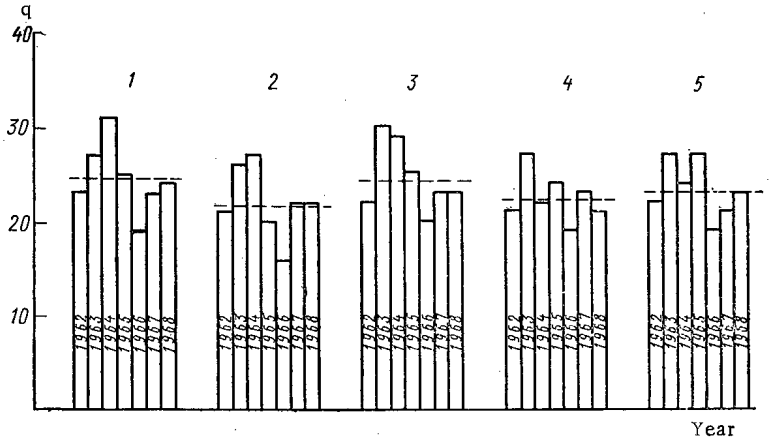

Fig. 1. Specific β-activity q (pCi/g) of soil in the vicinity of the reactor.

Institute of Physics, Bulgarian Academy of Sciences, Sofia. Translated from Atomnaya Énergiya, Vol. 31, No. 6, pp. 577-580, December, 1971. Original article submitted March 9, 1971.

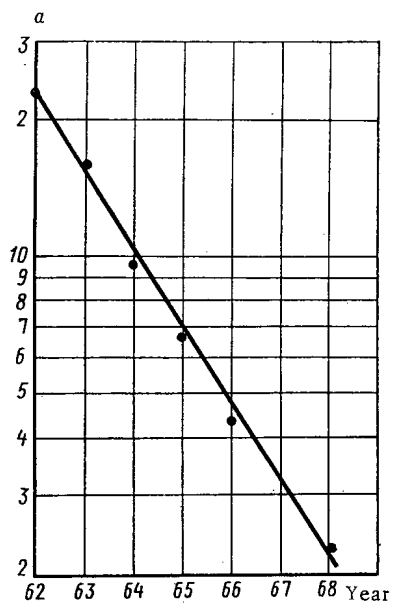

Fig. 2

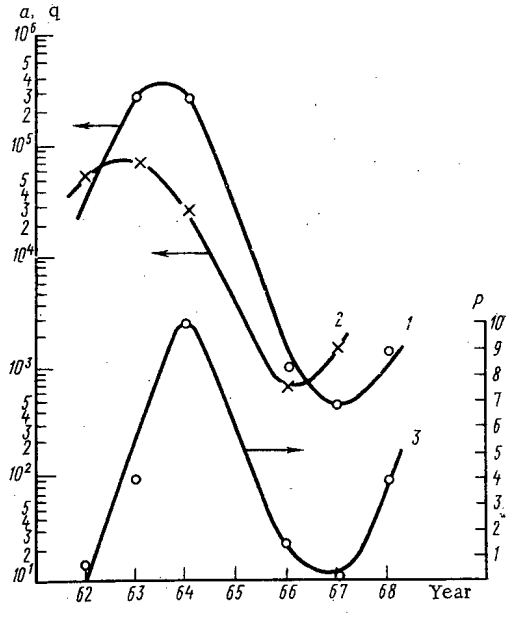

Fig. 3

Fig. 2. Specific β-activity a of water from the secondary coil of the reactor (pCi/liter).

Fig. 3. Specific β-activity a of snow water (pCi/liter) from Mount Vitosha (curve 1), specific β-activity q of the dry residue, (pCi/g) of the water sample (curve 2), and the weight P (g/liter) of the dry residue obtained after filtration of the water (curve 3).

one of the operating groups of the radiochemistry laboratory [5]. The concentration of Ca^{45} remained below the appropriate permissible limit for this isotope.

The space distribution of the concentration of Ar^{41}, emitted through the reactor turbine, was also studied [6], and it was established that this concentration was significantly below the permissible limit for the appropriate category of population.

It is useful to consider the results of the conducted investigations from several viewpoints.

Specific β-Activity of the Surface Layer of the Soil. For the determination of the radioactive contamination of soil, samples were taken each month of the soil cover to a depth of 5 cm, which after appropriate processing were subjected to radiochemical analysis [4]. The observations were systematically arranged into five groups according to direction from the reactor. From the results of the measurements, presented in Fig. 1, it is evident that during the monitoring period the specific β-activity of the surface layer of soil was constant to within the accuracy of the method (20%) and amounted to 22-24 pCi/g of soil (according to the determination of sample activity using a potassium standard). The maximum deviations of the annual averages from the average values for the entire observing period did not exceed the indicated value of the error. One can conclude from this that over a period of seven years an increase in the specific soil activity was not observed and that the operation of the reactor was not accompanied by radioactive contamination of the surface soil layer attributable to such operation. Such a conclusion is confirmed by additional observations. Measurements of the specific β-activity of soil at locations 100 km distant from the reactor yielded similar annual average values, 27 pCi/g ± 20%.

Total β-Activity of the Dry Residue of Water from Uncovered Reservoirs and Snowdrifts. In the immediate vicinity of the reactor there is some uncovered water, a tank of cooling water of the secondary circulation coil. Its level is kept almost constant by an intake of water from the city water supply system. Each month samples were taken from the tank for determination of the specific β-activity of the dry residue. The annual mean results, shown in Fig. 2, indicate a decreasing trend in the activity of the dry residue, resulting from the fact that nuclear tests in the atmosphere essentially ceased during this period. The specific β-activity of water from the Sofia water supply system, measured in April 1968 for comparison purposes, was 0.71 ± 0.11 pCi/liter.

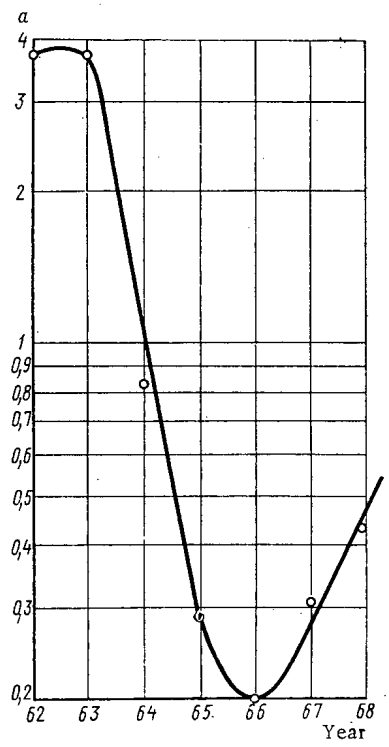

Fig. 4

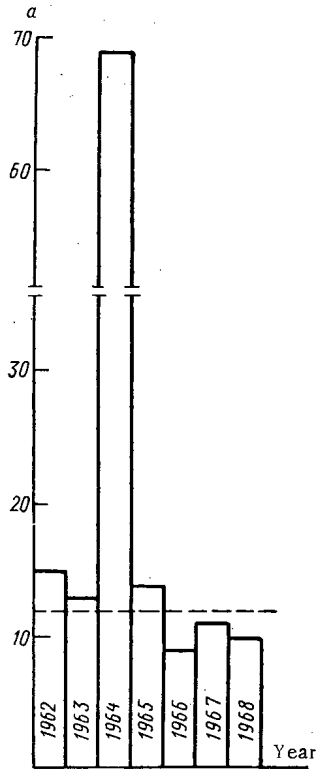

Fig. 5

Fig. 4. Concentration of β-active aerosols a (pCi/m^3).

Fig. 5. Specific β-activity a (pCi/liter) of the liquid effluent of the reactor.

In this connection it is of interest to note that samples from a snowbank on Mount Vitosha, one which remains in existence for the entire year, showed a very high specific β-activity of the dry residue. Samples were taken in July, August, and September. The β-activity of the residue on the filter from 1 liter of water from the melted snow was determined. It is interesting to compare the results of the measurements, shown in Fig. 3, with the values of the concentration of β-active aerosols at a distance of 1.2 km to the west of the reactor (Fig. 4).* It is apparent that for all analyzed cases the total β-activities of the dry residues of samples from the snowbank on Mount Vitosha (Fig. 3, curve 2) were one to five orders of magnitude higher than the specific activities of the dry residues of water samples from the secondary circulating loop of the reactor (Fig. 2).

The weight of dry residue per unit volume of water is not correlated with the specific activity. For example, in 1963 the weight of dry residue was 4 g/liter and the specific activity was $(61 \pm 0.9) \cdot 10^3$ pCi/g, while in 1964 the weight was greater (10 g/liter) and the specific activity significantly less, $(28 \pm 0.6) \cdot 10^3$ pCi/g.

The nearly identical time variations of a and q in Figs. 3 and 4 demonstrate the fact that the radioactivity on the aerosols and in the snow on Mount Vitosha have the same origin, namely, nuclear tests in the atmosphere.

Total β-Activity of the Dry Residue of the Liquid Effluent. The analysis of monthly samples of the liquid effluent of the reactor yields the data given in Fig. 5. It is evident that, with the exception of 1964 when more significant contamination was detected, the total β-activity of the dry residue of the samples was practically constant, amounting to 10-14 pCi/liter. This result was obtained in spite of the fact that the production of isotopes in the radiochemistry laboratory, which is the main source of contamination in the liquid effluent, increased from less than 10 Ci in 1963 to 50 Ci in 1968.

*These were measured by the staff of the Institute of Hydrology and Meteorology of the Bulgarian Academy of Sciences; an SR^{90} source was used as the standard.

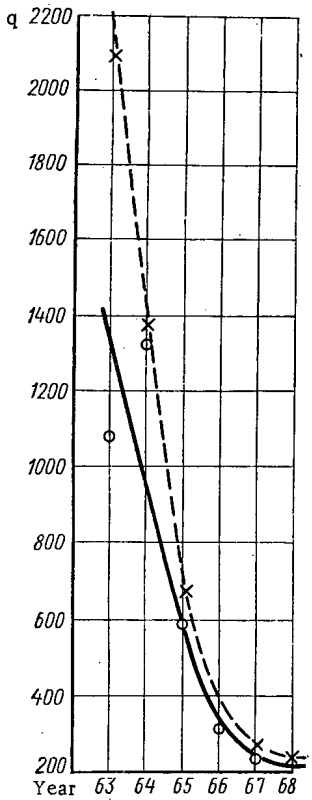

Fig. 6. Specific β-activity q (pCi/g) of pine needles from the vicinity of the reactor.

Specific β-Activity of Several Plants. Vegetation samples have been taken from several regions near the reactor. Branches and needles of a pine tree found in one of these regions were collected each month and subjected after appropriate preparation [4] to radiometric analysis. Since a decreasing trend in mean annual specific activities was found for all vegetation samples, in Fig. 6 are given only the data for samples from the above-mentioned pine tree. It is evident that a continuous decline in specific activity takes place for both unprocessed and washed needles. At the end of the period of investigation there was observed an almost complete absence of external contamination on the needles, which is consistent with the significant decrease in the concentration of radioactive aerosols in the near-ground layer of air.

For comparison purposes, radiometric analysis of samples of pine needles from Mount Vitosha were carried out. The variation in their specific β-activity had the same form, a continuous decrease.

The data given in this paper concerning the systematic decrease in the activity of various samples indicates the fact that, despite a continuous increase in energy generation, the long-term normal operation of the IRT-2000 is not accompanied by any change in the radiation environment at nearby locations.

LITERATURE CITED

1. J. Solanas, A. Darder, and P. Bertou, Health Phys., 12, 43 (1966).
2. M. A. Radicheva and I. T. Mishev, Bull. Inst. Phys. Bulg. Acad. Sci., 15, 5 (1966).
3. N. Yamagata and K. Jwashima, Health Phys., 13, 1145 (1967).
4. I. T. Mishev, M. A. Radicheva, and T. M. Troshev, At. Energ., 16, 344 (1964).
5. I. T. Mishev and M. A. Radicheva, Bull. Inst. Phys. Bulg. Acad. Sci., 14, 57 (1966).
6. I. T. Mishev and M. G. Khristova, At. Énerg., 24, 530 (1968).

MOLECULAR – KINETIC MODEL OF THE FORMATION OF RADIOACTIVE PARTICLES IN UNDERGROUND NUCLEAR EXPLOSIONS

G. A. Krasilov and A. A. Ter-Saakov

UDC 621.039.7.1

It is well known that the local fallout from underground nuclear explosions carried out in the Nevada firing range (USA) and in coral islands in the Pacific Ocean consists mainly of particles betweeen a few microns and a few millimeters in size. The composition of these particles is determined by the nature of the underlying soil at the site of the explosion [1, 2]. In the underground nuclear explosions in the Nevada range, it was found [3] that ~80% of the radioactive substances formed settled on the Earth's surface within a few hundreds of kilometers from the epicenter of the explosion. Some 80% of the total activity was associated with fallout particles 30 μ or over in size [4]. We may therefore take it as proven that radioactive particles of the underlying soil make up the main part of the radioactive particles arising from underground nuclear explosions.

In this paper we shall consider a nonstationary molecular–kinetic model of the formation of radioactive particles in underground nuclear explosions. The model is based on the principle that interaction takes place in a nonequilibrium manner between the radioactive products of the nuclear explosion and the soil particles, at least in the initial stages of particle formation.

In an underground nuclear explosion a great variety of soil particles broken up by the explosion are attracted into the fireball; these are partly melted and partly evaporated [5, 6]. The soil particles are heated by intensive heat exchange with the fireball, the surface temperature of the particles reaching the melting point of the soil material almost instantaneously. From this instant of time the particle may be regarded as completely melted in view of the fact that the velocity of the phase transformation is far greater than the velocity of mass transfer. Since the radioactive products of a nuclear explosion occur in the fireball in the vapor state, any study of the mechanism underlying the distribution of the radioactive isotopes in the soil particles reduces to one of considering the nonstationary interaction between vapor and liquid.

Our investigation concerns the underlying soil particles melted in the fireball of a nuclear explosion. Condensed particles, particles formed by the merging of finer particles, and particles adsorbing radioactive isotopes on their solid surfaces are not taken into account. In future we shall assume that the particles under consideration have a spherical shape.

Let us suppose that at the initial instant of time the fireball is homothermic [5], while the radioactive products of the explosion are uniformly distributed over its volume. The number of soil particles in the fireball is constant, and their size and number remain unaffected during activation. There is no chemical interaction between the soil particles and the molecules of the radioactive isotopes.

The decay and mutual transformations of the radioactive isotopes in the mass chain have the effect that the number of nuclei of any particular isotope changes continuously. Let us introduce the function $\varphi(t)$, the relative (with respect to the number of nuclei directly formed in the explosion) number of nuclei of the radioactive isotope under consideration at the instant t. Since we have assumed that the character of the interaction between the molecules of the isotope under consideration and the soil particles is independent of the presence of other isotopes in the fireball of the nuclear explosion, all subsequent discussions relate to a single isotope.

Translated from Atomnaya Énergiya, Vol. 31, No. 6, pp. 581-584, December, 1971. Original article submitted June 19, 1969; revision submitted May 6, 1971.

According to the Langmuir principles [7, 8] a considerable number of condensation centers exists on the surface of a soil particle. Every molecule of the radioactive isotope finding itself in the immediate vicinity of a condensation center is accelerated by the forces of molecular attraction. On achieving a collision, the molecule interacts with one of the molecules on the surface and gives it some of its own kinetic energy. The remaining energy is insufficient to allow the isotope molecule to overcome the forces of attraction and leave the surface. The condensed molecule of the radioactive isotope will reside at a specific level of the potential pit or well which constitutes the energy equivalent of the condensation center. Since the activation energy of the condensation process is zero, the average value of the depth of the level is numerically equal to the latent heat of vaporization. This enables us to calculate the number of molecules condensing on unit surface in unit time. This equals the number of collisions made by the isotope molecules on unit surface per unit time:

$$q_{cond} = \sqrt{\frac{kT_0(t)}{2\pi m}} \cdot \frac{N(t)}{V(t)}, \tag{1}$$

where V(t) and $T_0(t)$ are the volume and temperature of the fireball; N(t) is the number of molecules of the radioactive isotope in the vapor phase of the fireball; m is the mass of the isotope molecule; and k is Boltzmann's constant.

From the energy point of view, the most probable location of the condensed molecule corresponds to its potential-energy minimum. Executing vibrations about its equilibrium position, the isotope molecule interacts with the surrounding molecules of the soil particle, the amplitude and energy of these vibrations depending on the temperature of the particle. If the lifetime of this molecule on the surface of the particle is sufficiently long, it will come into thermal equilibrium with the molecules of the particle material. Strictly speaking, this will be a quasithermodynamic equilibrium, since the outer levels will not remain constant during the time interval under consideration. This type of approach enables us to determine the proportion of molecules of the radioactive isotope which acquire an energy equal to or greater than ε (the latent heat of vaporization) in the course of the interaction, i.e., to determine the relative number of molecules capable of leaving the surface of the particle and returning to the vapor phase of the fireball. This proportion may be written in the form [7]

$$f\left(\frac{\varepsilon}{kT}\right) = \exp\left(-\frac{\varepsilon}{kT}\right) \sum_{i=0}^{s-1} \frac{\left(\frac{\varepsilon}{kT}\right)^i}{i!}, \tag{2}$$

where T is the temperature of the particle surface; and s is the number of independent oscillators by which the isotope molecule may be represented. In the present case s = 3, since the motion of the molecule on the surface may be regarded as the motion of an ideal-gas molecule in two dimensions and as a classical harmonic vibration in the third dimension.

It should be noted that for molecules of volatile and gaseous radioactive isotopes the average lifetime on the surface of the particle is very short; in other words, there is hardly any potential pit to trap these. However, since in this case the probability of the evaporation of an isotope molecule is almost unity, we may formally write down an analogous expression for the function f(E/kT), replacing the temperature of the particle surface by the temperature of the vapor phase in the fireball.

Then the number of molecules of the radioactive isotope leaving unit surface of the soil particle in unit time

$$q_{evap} = \bar{\nu} f\left(\frac{\varepsilon}{kT}\right) n(R, t),$$

where $\bar{\nu}$ is the mean frequency of the thermal vibrations of the molecules; n(R, t) is the concentration of the radio-isotope molecules on the surface of a soil particle of radius R.

The number of isotope molecules in the volume of a soil particle of radius R may be expressed in the form

$$a(R, t) = \int_0^R 4\pi r^2 c(r, t)\, dr, \tag{3}$$

where c(r, t) is the volume concentration of isotope molecules.

If we suppose that δ is the effective thickness of the surface layer of a soil particle, then the surface concentration of isotope molecules for a soil particle of radius R may be represented by the expression

$$n(R, t) = \frac{1}{4\pi R^2} \int_{R-\delta}^{R} 4\pi r^2 c(r, t)\, dr \simeq \delta c(R, t).$$

According to Ya. I. Frenkel' [8], the effective thickness of the surface layer is

$$\delta = \sqrt{\frac{2\pi kT}{\overline{\frac{\partial^2 u}{\partial x^2}}\Big|_{x=x_0}}},$$

where $\overline{u(x)}$ is the average value of the potential energy of the molecules; $x = x_0$ is the equilibrium position. Since $\bar{\nu} = (1/2\pi)\sqrt{\frac{1}{m} \cdot \overline{\frac{\partial^2 u}{\partial x^2}}\Big|_{x=x_0}}$, we have $\delta = (1/\bar{\nu})\sqrt{\frac{kT}{2\pi m}}$.

Hence the rate of evaporation, i.e., the number of isotope molecules leaving unit surface of a soil particle of radius R in unit time, is

$$q_{evap} = \sqrt{\frac{kT(t)}{2\pi m}} f\left(\frac{\varepsilon}{kT}\right) c(R, t). \tag{4}$$

This expression is valid until the temperature of the solid particle reaches its boiling point. After this, the rate of evaporation is determined by the intensity of heat inflow to the particle, i.e., almost entirely by the temperature difference between the vapor phase of the fireball and the soil particle. This case is not considered in the present treatment.

It is easy to see that, in the case of thermodynamic equilibrium in a system of two phases, the equality of Eqs. (1) and (4) leads to a mathematical formulation of the Henry law $p_\infty/c_\infty = kTf(\varepsilon/kT)$, where p_∞ is the equilibrium partial pressure of the isotope molecules in the fireball, c_∞ is the equilibrium concentration of the isotope molecules in the volume of the soil particles.

The equation for the change in the activity, i.e., the number of molecules of the radioactive isotope in a soil particle of radius R, takes the form

$$\frac{\partial a}{\partial t} = 4\pi R^2 \sqrt{\frac{kT_0(t)}{2\pi m}} \cdot \frac{N(t)}{V(t)} - 4\pi R^2 \sqrt{\frac{kT(t)}{2\pi m}} f\left(\frac{\varepsilon}{kT}\right) c(R, t) - \lambda(t)\, a(R, t). \tag{5}$$

Here $\lambda(t)$ is a certain effective characteristic allowing for the dynamics of the mutual transformations of the radioactive isotopes within the mass chain. In the case in which the chain is represented by one isotope, λ is the decay constant. The quantity $\lambda(t)$ is related to $\varphi(t)$ by the equation

$$\varphi(t) = \exp\left[-\int \lambda(t)\, dt\right].$$

Let us suppose that the soil particles are distributed in size with a normalized probability density p(R). Then the law of conservation of the number of radioisotope molecules in the fireball may be expressed in the form

$$n_0 \int_0^\infty a(R, t)\, p(R)\, dR + N(t) = N_0 \varphi(t), \tag{6}$$

where n_0 is the total number of soil particles drawn into the fireball; N is the number of molecules of the radioactive isotope formed directly in the explosion.

For simplicity of subsequent calculations, we assume a constant volume and temperature of the fireball and also a constant temperature of the soil particles in the course of activation.

The penetration of isotope molecules into the main volume of the soil particles is largely determined by the molecular concentration gradient. The flow of isotope molecules through the surface of a sphere of radius R may be written in the form

$$\Delta A = 4\pi R^2 D \frac{\partial c}{\partial r} \Delta t,$$

where D is the diffusion coefficient. If we put the temperature of the soil particle constant, we may also regard the diffusion coefficient as constant.

The equation describing the distribution of the isotope molecules with respect to the radius of the particle in time may, in the present case, be expressed in the form

$$\frac{\partial u}{\partial t} = D\frac{\partial^2 u}{\partial r^2} - \lambda(t)\,u(r, t),$$

where u(r, t) = rc(r, t).

The initial and boundary conditions of the problem are:

for t = 0 c(r, 0) = 0 and hence u(r, 0) = 0;

for r = 0 c(0, t) is a bounded function, and hence u(0, t) = 0;

for r = R

$$\frac{\partial c}{\partial r}\Big|_{r=R} = \frac{1}{VD}\sqrt{\frac{kT_0}{2\pi m}}\,N(t) - \frac{1}{D}\sqrt{\frac{kT}{2\pi m}}\,f\left(\frac{\varepsilon}{kT}\right)c(R, t)$$

or

$$\frac{\partial u}{\partial r}\Big|_{r=R} - \frac{u(R, t)}{R} + \frac{u(R, t)}{R_0} = \frac{R}{VD}\sqrt{\frac{kT_0}{2\pi m}}\,N(t),$$

where

$$R_0 = \frac{D}{f\left(\frac{\varepsilon}{kT}\right)}\sqrt{\frac{2\pi m}{kT}}.$$

It is easy to see that this boundary condition represents the diffusion flow through the surface of the soil particle of radius R.

The activation of the soil particles will be accompanied by a purification of the vapor phase of the fireball from the radioactive products of the nuclear explosion. It is hardly possible to calculate the exact value of the function N(t) from Eqs. (5) and (6) with due allowance for (3); hence we shall confine ourselves to a certain approximation, which nevertheless coincides with the exact value of the function N(t) at t = 0 and $t \to \infty$:

$$N(t) \approx N_0\varphi(t)\exp\left(-\frac{\beta t}{t+\frac{\beta}{\alpha}}\right),$$

where α and β are certain constants having a specific physical meaning.

In order to solve the problem we use the Fourier method. Then the expression for the activity of the soil particle of radius R will take the form

$$a(R, t) = \frac{8\pi\alpha R^3}{SR_0}N_0\varphi(t)\sum_{n=1}^{\infty}\frac{\int_0^t \exp\left[(\gamma_n R)^2\frac{D(\tau-t)}{R^2} - \frac{\beta\tau}{\tau+\frac{\beta}{\alpha}}\right]d\tau}{(\gamma_n R)^2 + \frac{R}{R_0}\left(\frac{R}{R_0}-1\right)}, \qquad (7)$$

where the eigenvalues of the problem $\gamma_n R$ are the roots of the equation

$$\gamma_n R\,\mathrm{ctg}\,\gamma_n R = 1 - \frac{R}{R_0}.$$

The constant α, which may be defined as the initial rate of purification of the vapor phase of the fireball from radioactive products, is calculated from Eqs. (5) and (6) on the condition that the flow of evaporation may be neglected in comparison with the flow of condensation. Then

$$\alpha = \frac{S}{V}\sqrt{\frac{kT_0}{2\pi m}}.$$

The constant β, characterizing the degree of purification of the vapor phase of the fireball, is determined by substituting expression (7) into Eq. (6) as $t \to \infty$.

Then

$$\beta = \ln\left(1 + \frac{M}{\rho V f}\sqrt{\frac{T_0}{T}}\right),$$

where S and M are the total surface area and the mass of the soil particles drawn into and melted in the fireball of the nuclear explosion; ρ is the density of the material composing the soil particles.

Consideration of Eq. (7) shows that the activity of the soil particle largely depends on its size. This relationship may be described by a power function of the form R^n, where the value of the index n varies between 2 and 3 over a wide range of particle sizes, the value increasing with diminishing diameter.

It follows from Eq. (4) that the rate of evaporation of the radioisotope molecules from the surface of the soil particle largely depends on the form of the function $f(\varepsilon/kT)$. For molecules of refractory elements or oxides (nitrides) of the elements, the values of the function $f(\varepsilon/kT)$ are extremely small up to temperatures equal to the boiling point of the material composing the soil particles. These molecules have on average a long life on the particle surface, while their evaporation rate is low compared with their rate of condensation. For molecules of volatile and gaseous radioactive substances, on the other hand, the lifetime is quite short, and the probability of evaporation is great even on approaching temperatures equal to the solidification point of the soil particles. For these molecules the flow of evaporation is practically equal to the flow of condensation. Hence the character of the interaction between the radioactive isotopes of elements with different thermodynamic properties and the soil particles varies considerably. The total amount of the longest-living representative of the chain in the soil particle is determined not only by its own condensation but also by the condensation of its short-lived ancestors.

The relationships which we have just obtained certainly give no more than an approximation to the real process of the interaction between the radioactive products of a nuclear explosion and soil particles; nevertheless, we feel that the foregoing approach may add a little to the model of thermodynamic equilibrium considered earlier [6, 10].

LITERATURE CITED

1. C. Adams, N. Farlow, and W. Schell, Geochimica et Cosmochimica Acta, 18, 42 (1960).
2. G. Crocker, J. O'Connor, and E. Freiling, Health Phys., 12, 1099 (1966).
3. W. Kellogg, R. Rapp, and S. Greenfield, in Meteorology and Atomic Energy [Russian translation], IL, Moscow (1959), p. 243.
4. J. Holland, Federation Proceedings, 22, No. 6, Part 1 (1963).
5. In: Effects of Nuclear Weapons [in Russian], Voenizdat, Moscow (1965).
6. Report TID-7632, Washington (1962), p. 25.
7. E. A. Melvyn-Hughes, Physical Chemistry [Russian translation], IL, Moscow (1962).
8. K. F. Gertsfel'd, Kinetic Theory of Matter [in Russian], ONTI, Moscow–Leningrad (1935).
9. Ya. I. Frenkel', Kinetic Theory of Liquids [in Russian], Izd. AN SSSR, Moscow–Leningrad (1959).
10. Yu. A. Izrael', Dokl. Akad. Nauk SSSR, 161, 343 (1965).

INVESTIGATION OF EXPERIMENTAL MULTIELEMENT THERMIONIC-EMISSION ASSEMBLIES

V. I. Berzhatyi, N. A. Griboedov,
V. P. Gritsaenko, Yu. I. Danilov,
A. S. Karnaukhov, V. B. Klimentov,
Yu. N. Krasik, V. P. Kirienko,
O. I. Lyubimtsev, V. A. Maevskii,
M. V. Mel'nikov, V. K. Morozov,
N. N. Petrov, A. I. Piskarev,
I. I. Raikov, V. V. Sinyavskii,
and A. I. Yakunin

UDC 621.362:621.039.577

The most important part of a thermionic-emission power generator is its electricity generating channel. In the development of this new power source conditions resembling those under which the device will actually operate can be created only with the aid of a nuclear reactor. The investigation of experimental assemblies in a research reactor is thus an important stage in the design of thermionic-emission power generators.

The construction of two experimental thermionic conversion assemblies (ES-6-1 and ES-6-2) of a relatively high power density (up to 10 W/cm^2), the technique of the investigation of their electricity generating channels in a reactor, and the most important results of this investigation are reported below. No long-term performance tests were attempted.

Construction of Experimental Assembly. The assembly consists of a capsule and head (Fig. 1). The capsule includes the following units and systems: the thermionic-emission generating channel to be tested; an independent compact pump system for evacuating the interelectrode gap of the generating channel which consists of an ion pump connected through a valve to the common fission products evacuating system of the general loop assembly; a vacuum circuit and a cesium vapor supply; a system of electric heaters and devices for measuring and monitoring the operation of the generating channel and other units of the assembly.

All these units and systems are located in an airtight low-pressure chamber formed by the capsule jacket.

The electricity generating channel consists of six series-connected generating elements. Cylindrical emitters made of an alloy of tungsten with 27% rhenium are filled with W + UO_2 metal–ceramic pellets (enriched to 90% U^{235}).

The anode package of the generating channel consists of niobium collectors, aluminum oxide insulation, and a niobium support tube. The collectors are separated by aluminum oxide spacers. The bottom collector is electrically connected to the support tube which, in turn, is connected to the collector current conductor; the top emitter is connected to an insulated conductor. To prevent short-circuits between the emitter and collector, each power element is fitted with a cylindrical beryllium oxide spacer 0.7 mm in diameter. The interelectrode gap is 0.25 mm.

The vacuum circuit consists of a stainless steel pipe that connects the interelectrode gaps and the cesium thermostat with the ion pump. Cesium vapors are supplied from the cesium thermostat mounted in a common housing with the thermostat valve. When this valve is open the interelectrode gaps and the thermostat become connected to the ion pump.

Translated from Atomnaya Énergiya, Vol. 31, No. 6, pp. 585-588, December, 1971. Original article submitted November 2, 1970; revision submitted April 23, 1971.

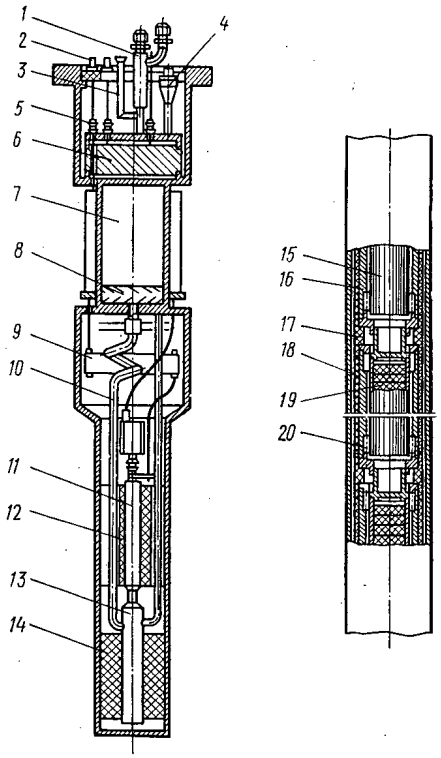

Fig. 1

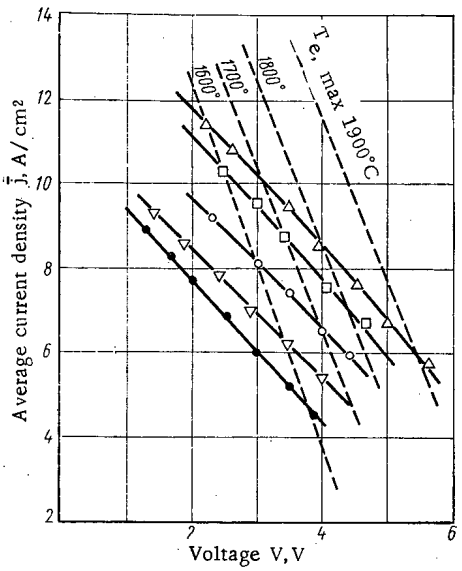

Fig. 2

Fig. 1. Construction of experimental assembly: 1) valve; 2) electric connector; 3) vacuum gauge; 4) connecting plug; 5) lead-in; 6) biological shield; 7) ion pump; 8) cesium trap; 9) shunt; 10) exhaust tube; 11) generating channel; 12) collector heater; 13) cesium thermostat; 14) cesium thermostat heater; 15) emitter; 16) collector; 17) spacing ring; 18) insulation; 19) fuel pellet; 20) spacer.

Fig. 2. Experimental current–voltage characteristics of the ES-6-1 assembly together with a net of calculated isotherms (calculated isotherms take into account the nonuniform heat release distribution along the assembly). Heat flux density on the emitter q_F in W/cm²: ●) 28; ▽) 31; ○) 34.5; □) 49; △) 53. T_{Cs} in °C: ●) 330; ▽) 350; ○) 370; □) 350; △) 380.

Heat from the generating elements collector is carried off to the reactor cooling water through the anode insulators, the support tube, a graphite sleeve, the low-pressure chamber (0.3-0.5 mm), and the capsule jacket. The collector temperature is regulated by varying helium pressure in the low-pressure chamber from 10^{-2} to 1200 mm Hg, and by increasing or decreasing the collector heater power.

The system for measuring and monitoring the generating channel parameters provides readings on temperature, heat release, potential distribution in the channel and in the current conductors, the pump pressure, and also makes it possible to plot current–voltage characteristics. The temperature of the experiment assembly units is measured by Chromel–Alumel thermocouples. The specific heat release is monitored with the aid of a set of differential thermocouples mounted in graphite sleeves. The thermocouples are calibrated in a special test stand.

The head of the assembly holds the biological shield, vacuum and gas pipes, and the thermocouple and other electrical conductors. These main lines connect the capsule with the corresponding system of a general-purpose loop assembly.

Reactor Tests. The ES-6-1 and ES-6-2 assemblies were tested in the general-purpose loop assembly of a water-cooled water-moderated reactor. The test assembly made it possible to record the performance of the power element, the control the collector heat removal, and to maintain the necessary temperature conditions. Provisions were made for removing fission products and desorbed gases from the electricity

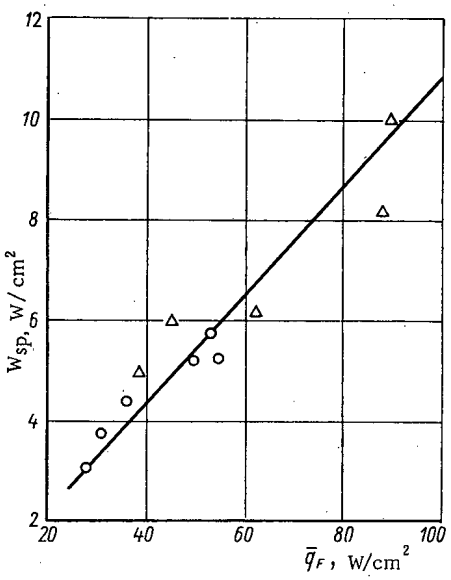

Fig. 3

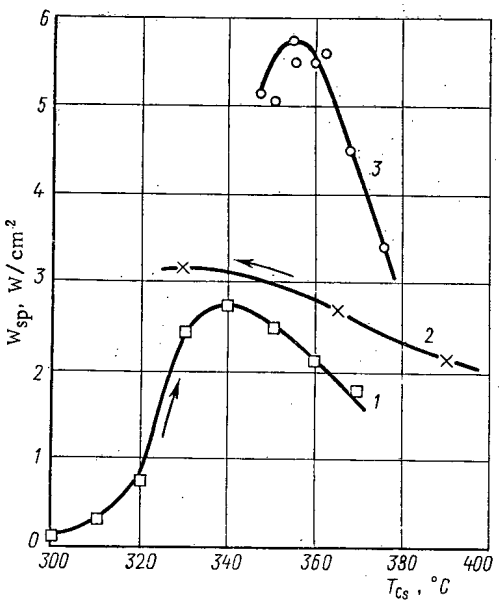

Fig. 4

Fig. 3. Specific generated power $\overline{W}_{sp}$ of the ES-6-1 (⊙) and ES-6-2 (Δ) assemblies as a function of the average heat flux density on the emitter $\bar{q}_F$.

Fig. 4. Effect of cesium vapor pressure: 1) first rise of cesium thermostat temperature (q_F = 30 W/cm^2); 2) drop of cesium thermostat temperature (q_F = 30 W/cm^2); 3) effect of cesium thermostat temperature in steady-state operating mode (q_F = 53 W/cm^2).

generating channels into the common ventilation system of the reactor after a suitable delay and radiation testing.

Immediately after the experimental assembly was placed into the reactor reflector, the generating channel gaps and the low-pressure chamber were evacuated by the pump. As soon as the pressure in the channel gap fell to $5 \cdot 10^{-5}$ mm Hg, the reactor was put into operation at an intermediate power at which the electrodes of the generating channel were degassed. The maximum emitter temperature under zero power takeoff operating conditions was 2000°C. After degassing the cesium ampoule was opened by remote control, and the reactor power was made equal to the rated power density of the element of 5-10 W/cm^2.

The first ES-6-1 assembly operated for 75 h and failed after a leak developed in the channel casing so that helium from the low-pressure chamber leaked into the interelectrode gap of the power channel. The average electric power density on the emitter surface of the ES-6-1 assembly was 6 W/cm^2.

The ES-6-2 assembly was operated at a power density of 10 W/cm^2 for 220 h after which the reactor was shutdown. Before the planned shutdown a small leak was found between the internal space of the generating channel and the low-pressure chamber of the capsule. The parameters of the assembly remained steady throughout the tests; the electrical power of the channel fluctuated not more than 5-7%.

Results. The principal purpose of the tests was to check the operation of all systems of the main loop assembly and to find the efficiency of the six-element thermionic emission converters under reactor conditions with an average power density of 5-10 W/cm^2. Accordingly, we made no attempt of a detailed examination of the assembly performance. Nevertheless, the obtained results revealed certain specific features of the tested assemblies and made it possible to draw some conclusions.

One or more static current–voltage characteristics were plotted at each reactor power level with a constant heat power applied to the emitter. Characteristics of the ES-6-1 assembly taken at five different reactor powers are shown in Fig. 2. Similar characteristics were obtained for the ES-6-2 assembly. All characteristics are linear in the operating range and correspond to the arc operating mode of the converters. The dependence of the average power density on the surface of six emitters measured at the optimum points of the characteristics on the average heat flux on the emitter is shown in Fig. 3.

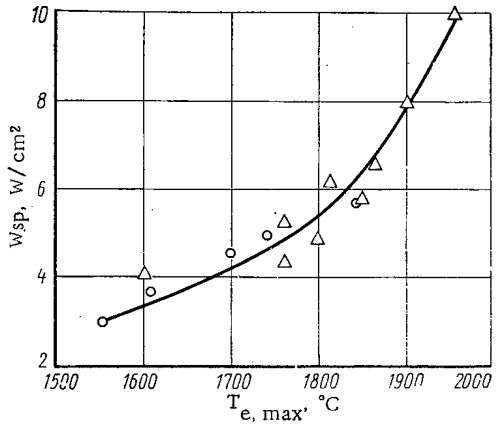

Fig. 5. Electrical power of ES-6-1 (○) and ES-6-2 (△) assemblies as a function of maximum emitter temperature.

The experimental characteristics obtained at constant heat power as well as the isothermal characteristics of laboratory thermionic converters are extremely sensitive to cesium vapor pressure. For power densities of 5-6 W/cm^2 the optimum cesium pressure corresponds to a cesium thermostat temperature T_{Cs} = 355-360°C (~8 mm Hg) as shown in Fig. 4 curve 3. The electric parameters of the assembly exhibit a certain time lag after thermostat temperature changes. Curves 1 and 2 in Fig. 4 illustrate the dependence $W_{sp}(T_{Cs})$ for stepwise rises and drops of T_{Cs} respectively.

The statistical characteristics obtained in reactor studies for discrete changes of the load resistance are constant heat power characteristics. Thus, the thermal field of the emitter $T_e(z)$ will be different for each point of such a characteristic. Considering that the emitters of the investigated elements are not isothermal, safe operation of the device requires that the maximum emitter temperature $T_{e,max}$ be known.

The emitter temperature was found by two indirect methods: by the heat balance method and by comparing the theoretical and experimental current–voltage characteristics. In the first method $T_{e,max}$ is found by solving the heat balance equation for the emitter taking into account the heat carried off by the electron current and by heat conduction through cesium vapors, as well as the nonuniform current density distribution along the emitter. It should be noted that this method gives the value of $T_{e,max}$ with a quite large error (10-15%) as a result of inaccuracies in the determination of heat fluxes, the degree of electrode blackness, and of the current density nonuniformity.

In the second method the value of $T_{e,max}$ is found by comparing theoretical and experimental current–voltage characteristics. The characteristics obtained for q = const are plotted on graphs on which theoretical isothermal current–voltage characteristics have already been plotted. The experimental characteristics of the ES-6-1 assembly with superimposed theoretical isotherms $T_{e,max}$ = const are shown in Fig. 2.

The current–voltage characteristics of an element were calculated on a digital computer allowing for the nonisothermicity and nonisopotentiality of the emitter as well as other heat and electrical losses. The assembly characteristics were obtained by adding the element characteristics taking into account the energy field distribution along the assembly. An important advantage of this method is the fact that the determination of $T_{e,max}$ is practically independent of the accuracy of determination of the heat release and of the degree of blackness which are usually known quite inaccurately.

The dependence of the electric power of the assemblies on $T_{e,max}$ is shown in Fig. 5. A power density of 5-10 W/cm^2 is obtained at $T_{e,max}$ = 1750-1950°C. At the same time, the nonisothermicity of individual elements $T_{e,max} - T_{e,min}$ amounts to 150-250°C, while the difference in $T_{e,max}$ of the central and peripheral elements due to nonuniform heat release along the assembly is about 100°C.

In tests made at power densities between 5 and 10 W/cm^2, the efficiency was 10-14%. It should be noted that the error in efficiency due to inaccurate calibration and placement of the heat flux sensor can be as high as 10-20%.

STUDY OF PARTICLE BEAMS WITH ENERGIES UP TO 70 GeV USING A SPARK SPECTROMETER

I. A. Aleksandrov, V. N. Bolotov,
M. N. Devisheva, M. I. Devishev,
V. V. Isakov, and A. V. Samoilov

UDC 539.1.074

The accuracy and quality of the experiments carried out in modern accelerators are largely determined by the characteristics of the magnetooptical channels forming the secondary-particle beams. A comparison of theory with direct experimental results is therefore important from several points of view. Firstly, such a comparison offers the possibility of estimating the accuracy of the calculations and the validity of the approximations made. A knowledge of the accuracy of the computing procedure is essential in designing future channels and determines the range within which the optimum characteristics of these is to be sought. Secondly, the aquisition of such information enables us to verify the method of adjusting the channel by an independent means. Thirdly, we are thus enabled to verify the stability of the channel characteristics during its experimental and service operation.

The principal characteristics of a particle beam formed in a magnetooptical channel are: the absolute average momentum of the particles transported by the channel; the momentum composition of the beam in various operating modes of the channel; the phase parameters of the beam (dimensions and divergence) in a number of cross sections of the channel.

The presence of a magnetic spark spectrometer in the channel provides information regarding the momentum–space–angular distribution of the particles in the beam. The advantages of the spark spectrometer for studying the channel are associated with its high spatial resolution and high accuracy in determining the momentum of particles up to 100 GeV. As a result of the use of the spark spectrometer we are able to study background conditions in the channel for a variety of operating conditions.

In this paper we shall present an estimate of the accuracy of calculations relating to one of the channels of the Institute of High-Energy Physics accelerator [1] by comparing these with the results of spark-spectrometer measurements. Statistics were collected during calibration measurements associated with an experiment search for particles with a fractional charge [2]. During these measurements the channel was set to a momentum of 60 or 65 GeV/sec with a mean particle escape angle from the target $(\bar{\theta})$ of 11 and 0.14 mrad respectively.

Magnetic Spark Spectrometer

Description of the Apparatus. The magnetic spark spectrometer [2] consists of four wide-gap spark chambers with an SP-12A1 magnet situated between them [3]. The spark chambers have a gap of 200 mm and a working area of 400×400 mm^2, and are filled with neon. When the system of scintillation counters and the system of logical electronics operates, a high-voltage pulse with an amplitude of 160 kV and a growth time of 10 nsec is applied to the chambers. The chambers are photographed in both projections by means of a pair of photorecorders, thus increasing the reliability of the recording of various events. In order to determine the distortions and introduce corresponding corrections, special stretched filaments are photographed during each exposure. The films are processed in semiautomatic machines operating in conjunction with a Minsk-2 computer [4].

Determination of the Momentum of the Particles in the Magnetic Spark Spectrometer and Possible Errors. The momentum of the particles in the spectrometer is found from the equation

Translated from Atomnaya Énergiya, Vol. 31, No. 6, pp. 589-594, December, 1971. Original article submitted June 2, 1970.

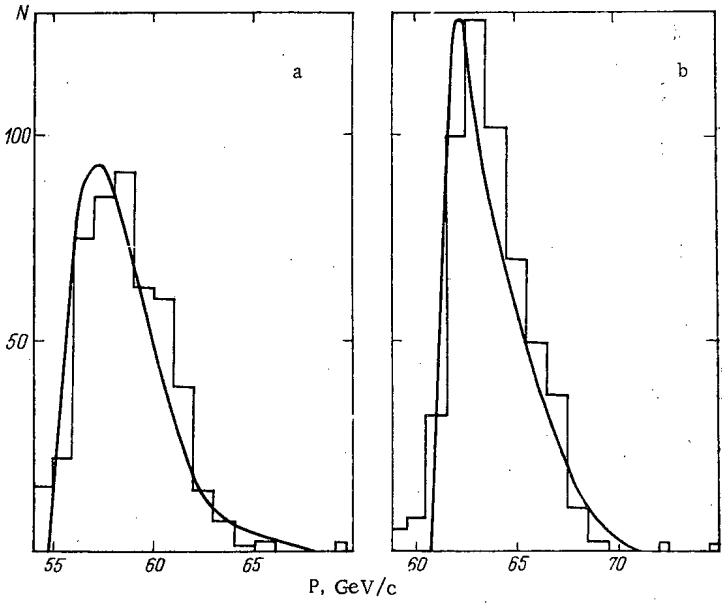

Fig. 1. Momentum distribution of the particles in the channel for δ_{mc} = 70 mm: a) P_0 = 60 GeV/c; b) P_0 = GeV/c.

$$P = \frac{0.3BL}{\varphi},$$

where φ is the angle of deflection of the particle in the magnetic field in radians; BL is the deflecting force of the magnet in T · m. The angle of deflection in the magnetic field is determined from the difference between the entrance and exit angles (θ_{in} and θ_{out}) of the particle in the spectrometer; these may be measured from the coordinates of the tract x in two chambers separated by a known distance l_{ik} (ik are indices denoting the number of the chamber), or from the direction of the track θ in any one of the chambers. Then θ_{in} equals θ_1 and θ_2; θ_{out} equals θ_3 or θ_4. In both cases $\varphi = \theta_{out} - \theta_{in}$.

The systematic error in determining the absolute value of the momentum P depends on the accuracy of estimating the product BL; for the SP-12A1 magnet this is approximately 1% [3]. The main sources of apparatus errors are associated with the accuracy of measuring the angle φ and are determined by the following factors.

1. By the accuracy of tracing the spark along the particle trajectory. According to existing data [5], the angular accuracy of tracing a spark along a track in a chamber (with a 20 cm gap) is $\sigma(\theta_s) \leq 0.8$ mrad and the spatial error $\sigma(x_s) \leq 0.5$ mm.

2. By the accuracy of establishing geodesic reference marks in the space $\sigma(x_{geod}) \leq 0.2$ mm.

3. By the accuracy of allowing for optical distortions associated with aberrations in the system and with the method of reproducing the particle trajectory in space from the photographs. According to our own estimates $\sigma(x_{opt}) \leq 0.1$ mm.

4. By the measuring error, which is defined as $\sigma(\theta_{anal}) = \sqrt{\Sigma(\Delta\theta)^2}$, where $\Delta\theta$ is the difference between the angles obtained for the same event in two analyses. This error depends on the method of determining the angle and equals 0.043 ± 0.006 mrad for the first method of determination and 0.92 ± 0.2 mrad for the second.

5. By the scattering of particles in the material of the scintillation counters and the electrodes of the chamber (for P ≈ 60 GeV/c, $\bar{\varphi}_{scat}$ = 0.15 mrad).

The total error in determining the angular deviation of the particle in the magnetic field from the coordinates of the tracks in four chambers was expected to be equal to

$$\sigma_{\varphi\Sigma} = (\sigma_4^2 + \bar{\varphi}_{scat}^2)^{1/2} \approx 0.32 \text{ mrad},$$

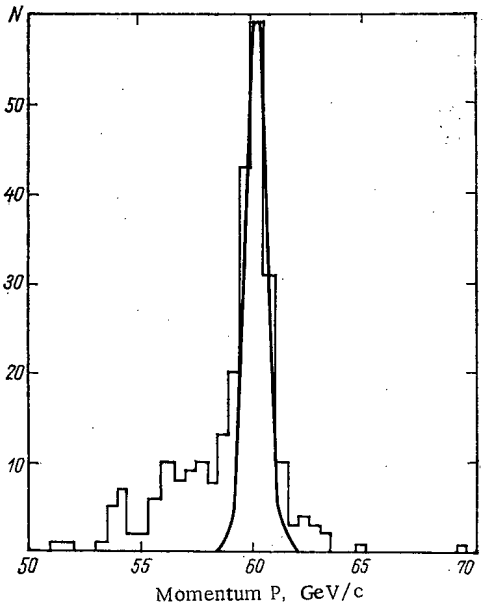

Fig. 2

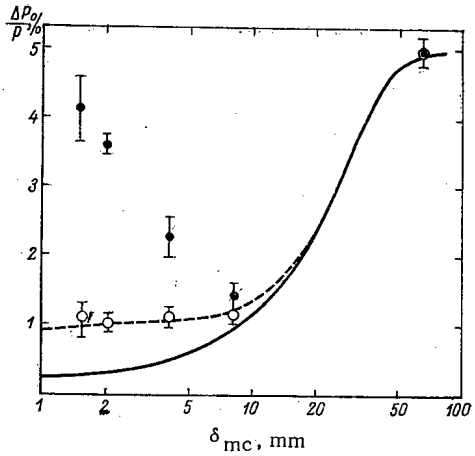

Fig. 3

Fig. 2. Momentum distribution of the particles for P_0 = 60 GeV/c, δ_{mc} = ±2 mm.

Fig. 3. Momentum resolution of the channel at half the height of the distribution in relation to the collimator width: ——) calculation with due allowance for the spectrum [7].

where

$$\sigma_4 = [l_{ik}^2(\sigma^2 x_s + \sigma^2 x_{geod} + \sigma^2 x_{opt} + \sigma^2 x_{anal})]^{1/2} \approx 0.28 \text{ mrad},$$

and that in determining the angle from the direction of the tracks in two chambers $\sigma_\varphi \approx$ mrad. For an experimental determination of the accuracy of the spark spectrometer, a special exposure was made with the magnetic field switched off. The halfwidth of the distribution of the measured values of φ was σ_φ = 0.18 ± 0.3 mrad. Allowing for the scattering in the material, we find the error due to the remaining factors as σ_φ = 0.12 mrad, which corresponds to an error of ΔP/P = ±0.5% when measuring momentum in the range P = 60-65 GeV/c ($\bar{\varphi}$ = 21.6 mrad). This is the limiting accuracy with which the spectrometer in question may be operated; it is only obtained when there is no material between the chambers. In any practical form of the experiment, the dispersion in the angles of deviation σ_φ is principally attributable to the scattering of the particles, and when measuring momenta of P ~ 60-70 GeV/c equals ΔP/P = ±0.85%.

We also analyzed the accuracy of the spectrometer for the second case, in which the angle was determined from the directions of the tracks in two chambers. The results showed that the total errors committed in determining the angle by using information from the two chambers amounted to σ_φ = (1.5 ± 0.25) mrad. This corresponds to an error of ΔP/P = ±5% when determining particle momentum of P = 60-70 GeV/c.

Angular and Spatial Accuracy of Tracing the Spark along the Particle Trajectory. The accuracy of tracing a spark along a track is one of the most important characteristics of spark chambers. The angular accuracy of the tracing may be found by comparing the entrance angles determined a) from the slope of the track in any one chamber (θ_i) and b) from the coordinates of the tracks in two chambers (θ_{in}). By calculating the dispersion of the difference between these angles $\sigma(\theta_i - \theta_{in}) = [\sigma^2(\theta_s) + \sigma^2(\theta_{anal}) + \sigma^2(\theta_{in})]^{1/2}$ and knowing the error involved in the analysis, as well as the accuracy of the reproduction of the angle from measurements in two chambers, we obtained $\sigma(\theta_s)$ = (0.68 ± 0.12) mrad. The spatial accuracy of locating the spark channel relative to the particle trajectory equaled $\sigma(x_s)$ = (0.13 ± 0.5) mm. The values of the angular and spatial tracing accuracy obtained under physical-experiment conditions agree with the results obtained by methodical analysis [5, 6].

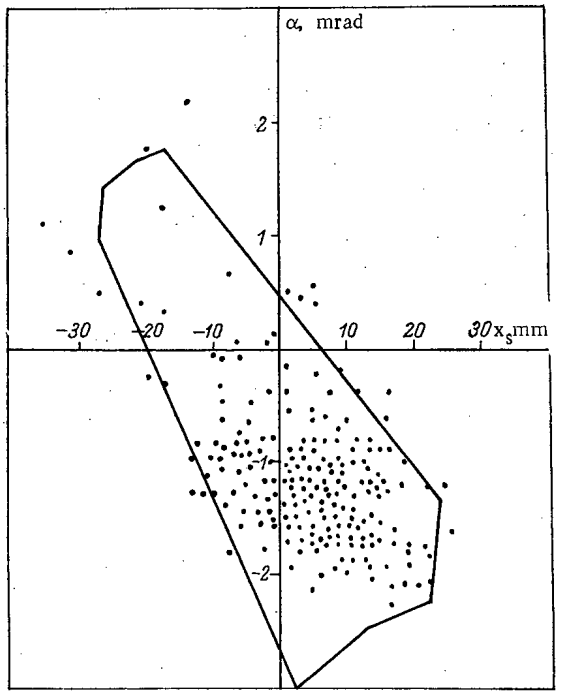

Fig. 4

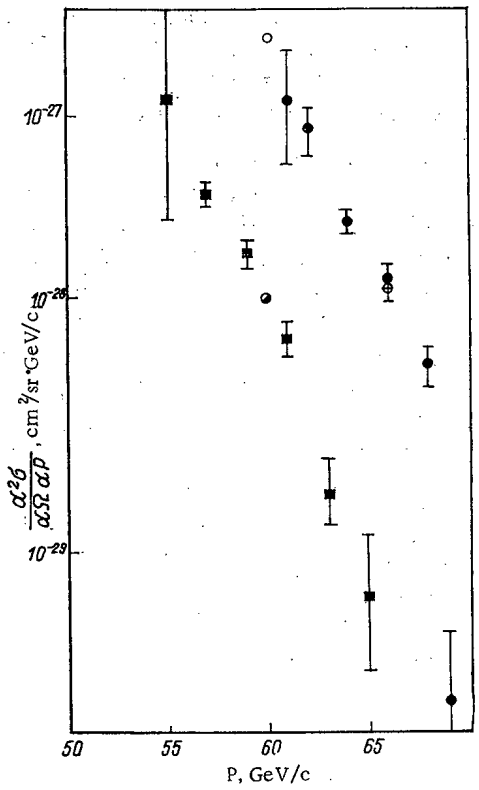

Fig. 5

Fig. 4. Phase characteristics of the beam at the entrance into the distribution in relation to the collimator width: $P_0 = 60$ GeV/c, $\delta_{mc} = \pm 70$ mm.

Fig. 5. Cross section for the formation of negative particles by protons in aluminum nuclei. Present results: ●) $\theta = 0.14$ mrad; ■) $\theta = 11$ mrad. Results of earlier paper [8]: ○) $\theta = 0$ mrad; ◐) $\theta = 8$ mrad.

Comparison between the Calculated and Experimental Channel Characteristics

In the present investigation we regarded the most probable momentum P_N as being that corresponding to the maximum in the spectrum of the particles in the channel $(dN/dP)_{max}$. In order to obtain the calculated spectra (continuous curves in Figs. 1 and 2) we used the Trilling formula [7]. The experimental value of P_N was compared with the calculated value for various apertures δ_{mc} of the momentum collimator. The quantities $P_{N_{exp}}$ and $P_{N_{calc}}$ agree to an accuracy of 1.5%, despite the fact that for $\delta_{mc} = \pm 70$ mm the momentum P_N differs considerably from the equilibrium momentum P_0 specifying the axis of the channel, and also from the momentum $P_{\Omega_{max}}$ corresponding to the maximum capture angle. For example, if $P_0 = 65$ GeV/c, calculation gives $P_{\Omega_{max}} = 63$ GeV/c and $P_N = 62.2$ GeV/c for the working mode. This indicates that the accuracy achieved in calculating $P_{\Omega_{max}}$ is no worse than 1.5%.

Momentum Composition of the Beam and Momentum Resolution of the Channel. A special feature of the channel [1] is the fact that its optical system is able to transmit particles over a fairly wide range of momenta. For complete opening of the collimator in the case $P_0 = 60$ GeV/c, the calculated momentum range is $\Delta P = 4.6$ GeV/c, and for $P_0 = 65$ GeV/c it is $\Delta P = 3.4$ GeV/c (see Fig. 1). The difference between the momentum ranges in the modes $P_0 = 60$ GeV/c (~7.80%) and $P_0 = 65$ GeV/c (~5.2%) is associated with the fact that in the first case the beam was initially made slightly converging instead of parallel, thus raising the transmission factor for the hard part of the spectrum and expanding the momentum range. The experimental spectra are indicated in the same figures in the form of histograms. The momentum ranges of the experimental and calculated spectra agree. In order to establish the complete validity of the calculation, we studied the momentum distributions of the particles in the channel on varying the width of the collimator σ_{mc} from ±1.5 to ±70 mm. The results are presented in Fig. 3 in the form of a relationsip between

the momentum resolution of the channel and the width of the momentum collimator. The light circles represent the experimental values of the momentum resolution at half the height; the broken lines represent the expected calculated values, with due allowance for scattering. The agreement between the calculated and experimental values is no worse than 1%.

It should nevertheless be noted that, for narrow collimators, the particle spectrum is severely distorted, and the background conditions are worsened; a "collimator effect" due to the scattering of the particles in the material of the collimator walls appears. The maximum difference in momentum between the "background" particles and P_0 is 10-12%; their distribution is shifted in the direction of the softer part of the spectrum. In Fig. 3 the black circles indicate the standard deviation, with due allowance for all the recorded particles, in relation to the collimator width. We see that, starting from $\delta_{mc} = 10$ mm, the value of $\Delta P/P$ increases rapidly with narrowing collimator slits. If no special measures are taken (redetermination of the phase volume of the beam or repreated momentum analysis), the "collimator effect" (the actual value of which depends on the structure of the particular channel) will in fact worsen the momentum resolution. This must be taken into account for cases in which a high momentum resolution is demanded by the experimental conditions.

Phase Parameters of the Beam. In addition to making indirect estimates, it is interesting to compare the calculated phase parameters of the beam with direct measurements (Fig. 4). The calculation (continuous line) was carried out for the adjusted working mode of the channel. The statistics were collected for a momentum-collimator width $\delta_{mc} = \pm 70$ mm and $P_0 = 60$ GeV/c. For comparison with calculation we took particles from the momentum range $\Delta P_0 = \pm 1$ GeV/c. The points in Fig. 4 represent the experimental phase coordinates of the particles in the horizontal plane. We see that only an insignificant porportion of the points falls outside the calculated region. On the whole the calculated phase characteristics describe the beam quite correctly.

Differential Cross Sections for the Formation of Negative Particles by Protons in Aluminum Nuclei

The existence of a magnetic spark spectrometer in the channel provided useful information regarding the cross section for the generation of negative particles in the inner target of the accelerator by protons. Knowing the experimental spectrum of the beam and the calculated dependence of the solid capture angle on the momentum of a proton $\Omega(P)$, we may determine the quantity

$$\frac{d^2N}{dPd\Omega} \simeq \frac{d^2\Omega}{dPa\Omega}.$$

Measurements were carried out for two angles of generation of the secondary particles $\bar{\theta}$ equal to 0.14 and 11 mrad. The energy of the protons interacting with the aluminum nuclei was 70 GeV. In order to convert to the differential cross section we matched our own data to earlier results [8] at the point with a momentum of 60 GeV/c (in this part of the spectrum the measurements were made in parallel and in the same channel). The absolute values of the cross sections in the earlier paper [8] were measured with an error of ±30%. The errors illustrated in Fig. 5 include both the statistical error and the error associated with inaccuracy in matching the calculated $\Omega(P)$ relationship to the experimental distribution.

It follows from a comparison of the calculated and experimental beam characteristics that the accuracy of calculating the phase parameters of the beam is fairly high, while the technical construction of the channel enables this accuracy to be realized under practical conditions

The energy dependence of the differential cross sections for the formation of negative particles measured with the spark spectrometer agrees closely with the results of the earlier paper [8], which were based on a completely different method.

The authors wish to thank Yu. D. Prokoshkin, who initiated the present investigation, and V. I. Kotov for great interest in the work; they also wish to thank Yu. S. Khodyrev and S. P. Denisov for useful discussions.

LITERATURE CITED

1. I. A. Aleksandrov, I. I. Grachev, et al., Preprint IFVE 69-66 [in Russian], Serpukhov (1969).
2. Yu. M. Antipov et al., Preprint IFVE 69-49 [in Russian], Serpukhov (1969).

3. A. V. Alekseev et al., Preprint IFVE 68-62 [in Russian], Serpukhov (1968).
4. V. V. Ammosov et al., Preprint IFVE 69-53 [in Russian], Serpukhov (1969).
5. V. N. Bolotov et al., Pribory i Tekh. Éksperim., 2, 57 (1964).
6. L. Keller, K. Schuter, and T. White, Nucl. Instrum. and Methods 41, 309 (1966).
7. G. Trilling, UCRL-16,000, 200, ADS, Vol. 1 (1965), p. 13.
8. Yu. B. Bushnin et al., Yadernaya Fiz., 10, 585 (1969).

RESONANCE PARAMETERS OF FISSILE NUCLEI

S. I. Sukhoruchkin

UDC 539.125.5.162.3

This paper evaluates results obtained for the principal fissile (U^{235} and Pu^{239}) and heavy isotopes (Th^{232}, U^{238}, and Pu^{240}). Such an evaluation is necessary, first, because new measurements (in the period 1966-1970) were called for in the construction requirements for reactors operating with fast and intermediate neutrons, and, second, because a final conclusion about the actual accuracy of the various reactor constants can only be reached by analyzing the different data. Considerable attention was devoted to a comparison of experimental results at the Helsinki conference also [1, 2]. The evaluations showed that the required accuracy of data has not yet been achieved in the majority of experiments, and a significant number of questions have merely been formulated.

A list of required nuclear data in the first category, i.e., highest in importance and urgency, is presented in [1-4]. One should note among these requirements for the resonance-energy region the 5% accuracy in the determination of the Th^{232} cross section, the 3% accuracy for the U^{238} cross section, the 3-5% accuracy for the cross sections of U^{233}, U^{235}, and Pu^{239}, and the 10% accuracy in the determination of the resonance parameters of U^{235}, Pu^{239}, and other isotopes. More rigorous requirements also exist [4]. Data on the measurement of the constant α was interpreted in [5, 6]. The neutron resonance-energy region should be discussed in greater detail because extrapolation of results from the resonance region to the kilovolt neutron energy region of practical importance is often made.

Resonance Parameters and Cross Sections for Th^{232}, U^{238}, and Pu^{240}. Data from even–even isotopes is most convenient for analysis because the nucleus which is formed by neutron capture, i.e., an odd-N, even-Z nucleus, has a rather low level density and a single spin state for all resonances (at low energies). A comparison of the experimental data for Th^{232} [2] showed that two different measurements of the total cross section of this isotope in the energy region up to 1 keV, each made with outstanding resolution, gave practically identical integral values of the reduced neutron widths (80 and 83 mV). For the subsequent ranges of 1-2 and 2-3 keV, however, 92 and 89 mV were obtained at Saclay [7], and 63 and 65 mV at the Columbia synchrocyclotron (USA) [8], i.e., there was a 30% difference. A systematic decrease beyond the limit of error (as the resonance energy increases) is observed in the ratio of the Γ_n^0 values for the neutron resonances in Th^{232} measured in [7, 8]. The spread in values of Γ_n^0 obtained in other measurements [9-11] is often considerably greater than the error also [2]. It is possible that the systematic difference in the results of [7, 8] arose from different methods of analysis [12]. Relatively good agreement exists between the data of [7] and [13] with respect to neutron level widths in the 20-200 eV range (the ratio of the measured strength functions is 0.99).

The average radiation widths $\bar{\Gamma}_\gamma$ for Th^{232} in the 50-350 eV range are in sufficiently good agreement and are 20.9 mV [13], 21.1 mV [9], and 21.6 mV [7], and $\bar{\Gamma}_\gamma = 20.5 \pm 3$ mV [13] over the entire range 20-2000 eV. An anomalously low value of Γ_γ for one of the levels ($E_0 = 712.9$ eV), 13.1 ± 4 mV [13] and 8 ± 8 mV [7], was obtained and may indicate the reality of strong fluctuations in Γ_γ [9, 13]. Thus the basic discrepancy in the Th^{232} data is still the divergent results for Γ_n^0 (and for the strength functions) in the region above 2 keV. It is very important to allow for contributions from p levels in that region. While the p levels can be distinguished up to 500 eV by their relatively small neutron widths, as can be seen in Fig. 1, such a separation is impractical in the region above 2-3 keV. In connection with the separation of levels into s and p resonances, we point out that a similarity of the reduced s and p neutron width distributions to a distribution with degree of freedom $\nu = 2$ (instead of the Porter–Thomas distribution with $\nu = 1$) has been noted [13]. However, this effect requires verification because the majority of data from other nuclei is consistent with a theoretical distribution for $\nu = 1$.

Translated from Atomnaya Énergiya, Vol. 31, No. 6, pp. 595-609, December, 1971. Original article submitted December 14, 1970; revision submitted May 27, 1971.

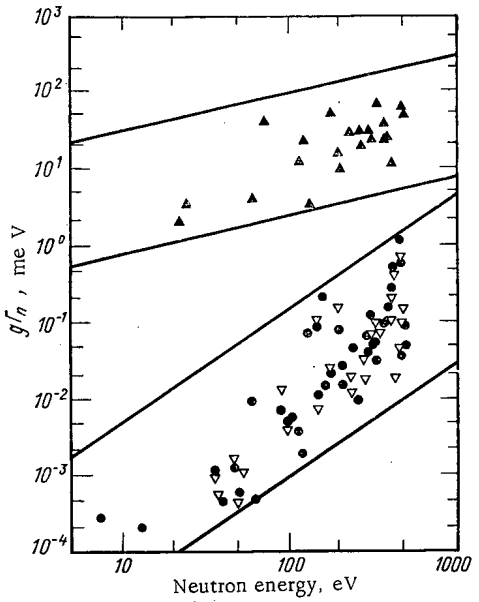

Fig. 1. Grouping of neutron widths for Th^{232} levels together with the expected energy dependence of these widths for s- and p-wave resonances: ●) [7]; Δ) [8]; ▽) [13].

TABLE 1. Total Width of First Neutron Resonance and Average Radiation Width of Pu^{240} Resonances According to Various Authors

Γ mV	$\bar{\Gamma}_\gamma$, mV	Γ_n, mV	Reference and year
42±5	39	3,1±0,4	[36], 1955
40±3	38	2,06±0,10	[37], 1958
34,5±3	32	2,4±0,05	[38], 1959
30,6±4,0	28	2,30±0,2	[39], 1959
30,8±2,0	29	2,15±0,10	[35], 1970
31,0±3,0	29	2,18±0,10	[35], 1970
—	23,2	—	[33], 1968
—	29,5±1.5	—	[34], 1971

Values of the mean neutron widths in another nucleus – U^{238} – also varied considerably up until recently (this is clear from Fig. 1); the ratio of $\bar{\Gamma}_n$ from [13] to $\bar{\Gamma}_n$ from [14] is 0.83 with the variation in neutron widths increasing to 40% at high energies [2].

However, additional measurements of the U^{238} total cross section gave better agreement of strength function values: $(1.13 \pm 0.13) \cdot 10^{-4}$ [15] and $(1.02 \pm 0.10) \cdot 10^{-4}$ [16]. Earlier work gave the values $(0.70 \pm 0.15) \cdot 10^{-4}$ [17], $(0.90 \pm 0.10) \cdot 10^{-4}$ [8], $(1.09 \pm 0.15) \cdot 10^{-4}$, and $(1.00 \pm 0.15) \cdot 10^{-4}$ [18]. The last two values and both new ones [15, 16] are in agreement. They obviously should be taken as recommended values.

From data obtained at three laboratories where measurements were made on radiative capture in U^{238} [19, 17, 20], the experimentally determined quantity $\Sigma\Gamma_n\Gamma_\gamma/\Gamma$ is respectively 290, 266, and 262 mV [2] for the first twenty resonances with the last and lowest value from Los Alamos [20] corresponding to a mean radiation width $\bar{\Gamma}_\gamma = 19.1$ mV. At the same time, a structure in Γ_γ was observed in this paper which did not recur in the more recent measurements [19, 21]. It is clear from Fig. 2 that the extremum values (high and low) in [20] were not confirmed, i.e., the proposed structure in Γ_γ does not exist below 1 keV. One ought, therefore, use the very low average value $\bar{\Gamma}_\gamma = 19.1 \pm 1.6$ mV from [20] with caution (according to the data in [19, 17, 21], the average values are respectively 24.64 ± 0.85, 23.74 ± 1.09, and 24 mV). Recent measurements by the Columbia group [16] gave the value $\Gamma_\gamma = 22.8 \pm 0.6$ mV (in the region below 1 keV), which differs only insignificantly from the old value given by this same group, $\Gamma_\gamma = 24.6 \pm 0.8$ mV [22].

While one can speak of agreement among the average values of the radiation widths ($\bar{\Gamma}_\gamma$) in the resonance region, it is impossible to say the same thing about direct measurements of the capture cross section in the region of a few kiloelectron volts. Thus the results of measurements of the Oak Ridge linear accelerator [23] are in rather poor agreement with data in [24, 25] although close to the values obtained from resonance parameters (the set in the Brookhaven library of evaluated data [23]). The unsatisfactory state of the data in the 2-20 keV region, where the difference reaches 20% at $E_n \approx 6$ keV, is indicated also in [26] where it is noted that this difference cannot be cleared up by corrections for self-screening, for example. Estimates of the capture cross section made by various authors [27-30] also vary by amounts up to 15% in the 3-25 keV region (difference between [29] and [30]).

There are also significant differences in the data for the isotope Pu^{240}. Thus the average values $\bar{\Gamma}_n^0$ differ by 30% in [31] and [32]. Here, as in the case of Th^{232} and U^{238}, the inclusion of experimental data for neutron scattering gives a systematically lower value of the average neutron width than does data from a transmission experiment [2].

One can judge from the data of two different experiments [33, 34] how much the average radiation widths $\bar{\Gamma}_\gamma$ for Pu^{240} differ from one another; the values are 23.2 and 29.5 ± 1.5 mV, respectively.

Table 1 shows how much the data for the total width Γ differ, and hence the data for the radiation width $\Gamma_\gamma = \Gamma - \Gamma_n$ also, for the very first resonance in Pu^{240} at $E_0 = 1$ eV [35].

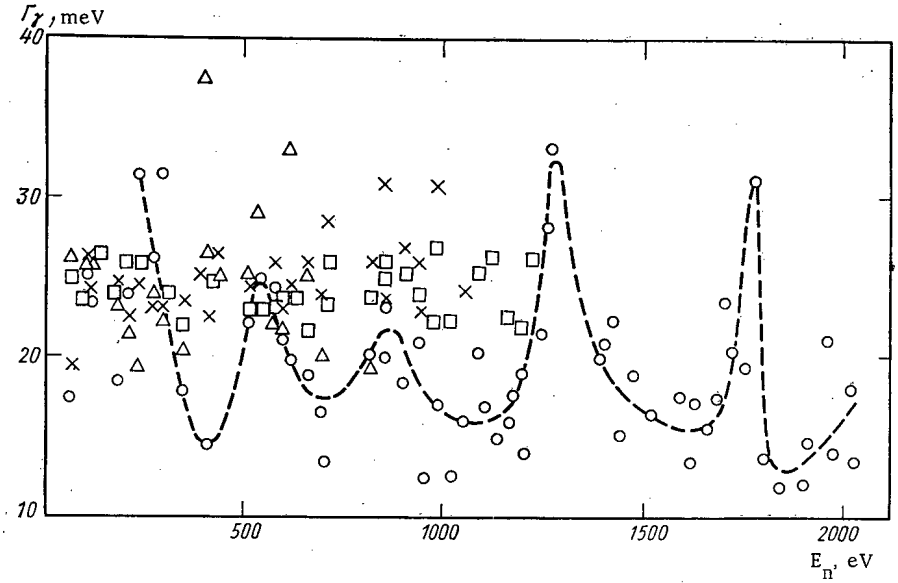

Fig. 2. Radiation widths Γ_γ of U^{238} neutron resonances from data in: ○) [20]; △) [17]; ×) [19]; □) [21].

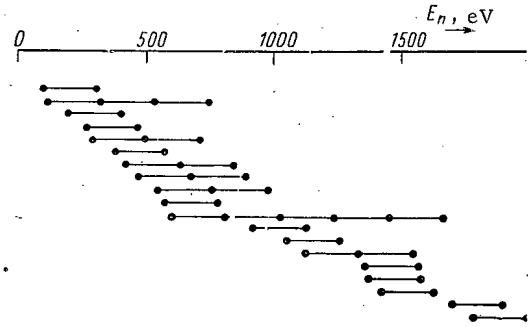

Fig. 3. Location of pairs of neutron levels in Pu^{240} separated by a 213 ± 1 eV spacing [50] (data from [31]).

A comparison of these values shows that only in 1971 did there appear a real hope for having self-consistent independent data for the first resonance (E_0 = 20-500 eV [34]); however, it is still necessary to analyze thoroughly the validity of the remarks (in the discussion of [35]) that the values of the resonance parameters from that paper (for the first resonance) do not completely describe the thermal cross section of Pu^{240} and a hypothetical "negative level" must be introduced.

One can conclude from an analysis of the data for Γ_n and Γ_γ that the required accuracies in measurements of most quantities have not yet been achieved for the even-even nuclei. In the case of U^{238}, integral experiments undertaken to eliminate significant uncertainty in the data for the amount of neutron capture in this nucleus may be some help in refining the results for the resonance parameters (Γ_γ and others).

It has already been noted [5] that data on subthreshold fission in the neutron resonance region (particularly data for Pu^{240} and Np^{237}) conclusively demonstrated the reality of an "intermediate structure" in the fission cross section which is related to the model of nuclear fission by a barrier of complex shape [40, 41]. New data on fission widths in U^{234} [1, 4 2] are in good agreement with the predicted shape of the subthreshold fission cross section envelope. In addition, indications of an intermediate structure were obtained in recent data for the nuclei Pu^{238}, Pu^{242}, and Pu^{244} [43, 44]. At the same time, in nuclei heavier than plutonium, where the effect from a second barrier should vanish according to the calculations of V. Strutinsky [45], an intermediate structure was actually not observed (in the fission of the heavy isotopes Cm^{246} and Cm^{248} [46]), i.e., the Γ_f distribution is described by a statistical model. Because of the appearance of new data for californium fission [47], this effect will evidently be tested for it also. Recent measurements of the spins of those Np^{237} resonances [48] for which an anomalously large Γ_f was found earlier are another check on the intermediate-structure model. All four spins turned out to be identical (J = 2) and in agreement with the model. The intermediate structure in subthreshold fission of nuclei like Np^{237}, U^{234}, and Pu^{240} thus gives a very convincing example of deviation from a statistical distribution. At the present time, a search is going on for deviations from statistical behavior not only in Γ_f, but also in the distribution of other resonance parameters (as an example, we point out the "structure" in the distribution of level spacing in Th^{232} [5, 49]).

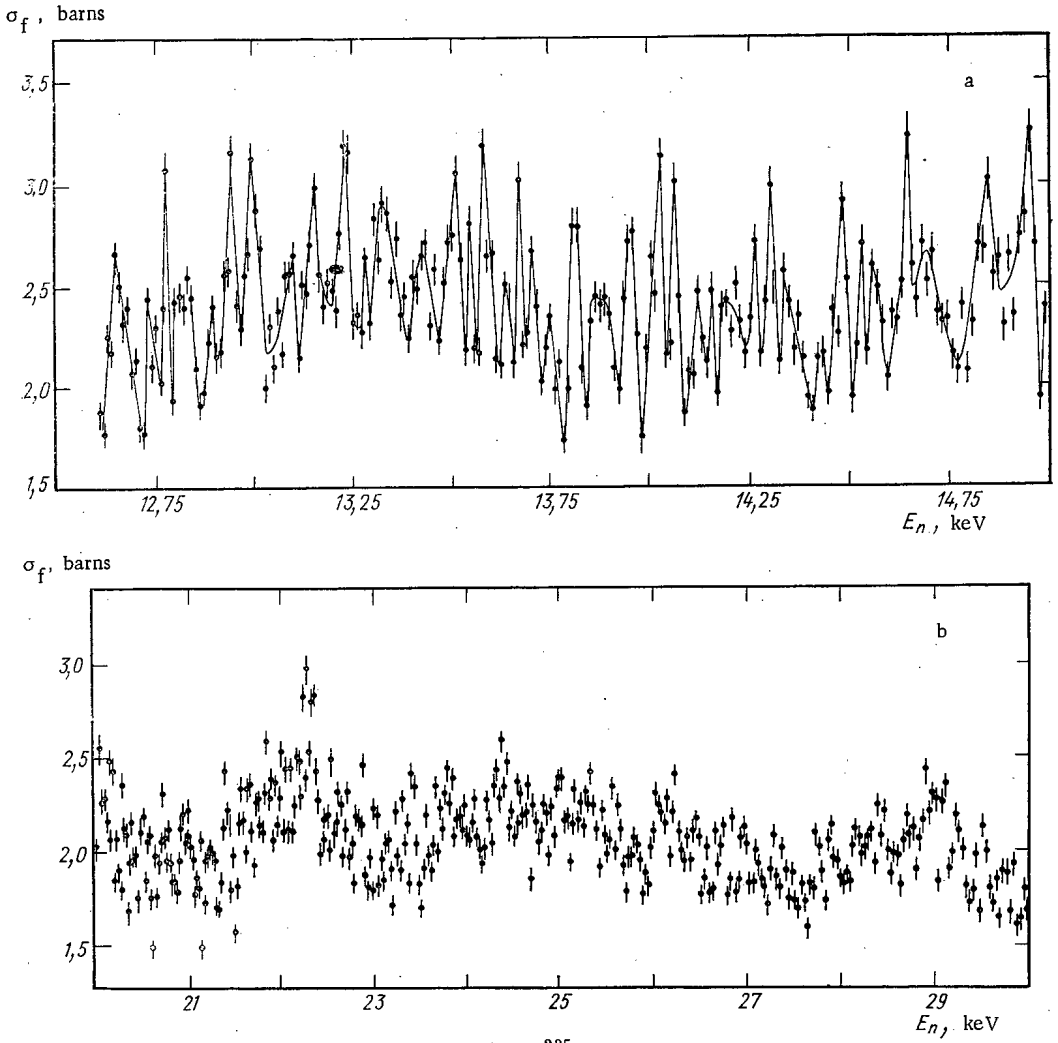

Fig. 4. Structure in the U^{235} fission cross section [55].

We consider still another example. In that same Pu^{240} target nucleus in which there was first observed a periodic, i.e., very systematic, structure in the cross section for subthreshold fission (see above and [5]), a correlation was observed in the relative location of resonance levels [50]; an anomalously large number of resonances were separated by an energy interval of 213 ± 1 eV. The position of levels separated by this interval are shown in Fig. 3; there is even a sequence of six equidistant levels. It was shown in [50] by means of statistical analysis that the factor for accidental production of this correlation is a quantity of the order of 10^{-3}. A like correlation was also observed in a number of heavy and medium nuclei. Evidently, we are observing here an unexpected and as yet unexplained phenomenon of ultrafine structure, i.e., a correlation of the order of tens and hundreds of electron volts. More thorough measurements at high resolution of the kind which is being done now and which is being planned for the immediate future will help to define more accurately the nature of this phenomenon including an independent check of its authenticity and a check for preservation of the "selection" of fixed spacing in various energy ranges and in various nuclei.

Earlier indications of the existence of an "ultrafine structure" (with a spacing of 70-90 eV) were obtained through analysis of the relative locations of resonance levels with relatively large neutron widths mainly in even–N target-nuclei [51] and through the positions of the neutron levels themselves (with respect to the threshold energy) [52, 53]. Since the scales of the observed ultrafine structure are quite similar in order of magnitude, it is highly probable that the appearance of some general mechanism is being observed in heavy even–N nuclei (Th^{232}, U^{238}, Pu^{240}, etc) which can be studied in other, lighter nuclei.

Thus the consideration of the data for even–even target-nuclei reveals three trends.

1. For a part of the experiments, satisfactory agreement between results can be noted; for example, this is illustrated in the determination of the radiation widths Γ_γ for the isotope U^{238} (below 1 keV).

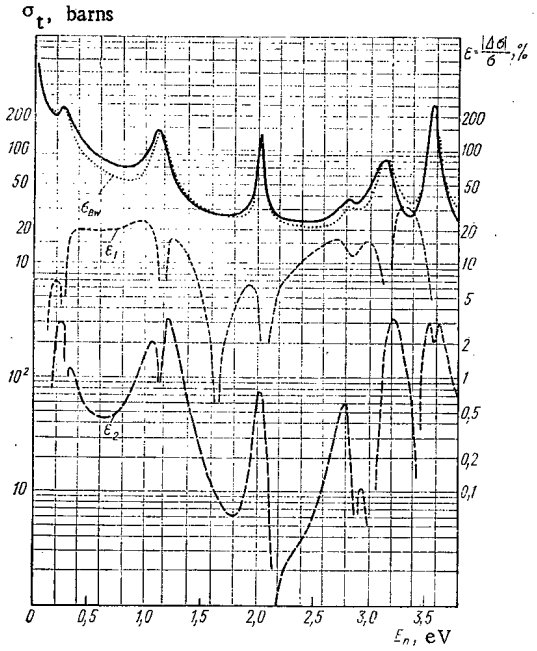

Fig. 5

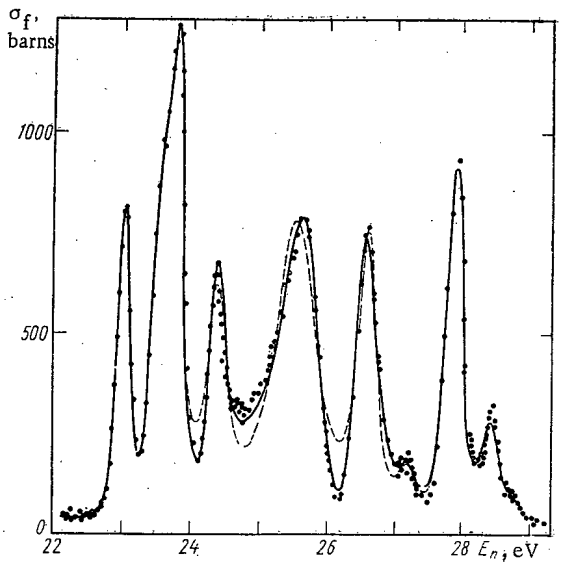

Fig. 6

Fig. 5. Deviation of experimental total cross section for U^{235} (solid curve) from that calculated from the one-level formula (σ_{BW}). Their relative difference ε_1 is compared with the relative difference between the experimental cross section and that calculated from a simplified multilevel formula [56].

Fig. 6. Experimental U^{235} fission cross section in the region 22-28 eV and theoretical calculations using the one-level (dashed curves) and multilevel (solid curve) formulas [56].

2. At the same time, other parameters are not in agreement, such as the neutron widths in different papers and $\bar{\Gamma}_\gamma$ for Pu^{240}. This situation is often encountered first.

3. Despite the generally satisfactory description of the properties of a system of neutron levels by a statistical ensemble, deviations from statistics are noted in many papers, which makes a representative model of the nonstatistical effects and an estimate of the contribution of such effects to the uncertainties in resonance parameters pressing problems.

We now consider data for another group of heavy nuclei, the odd-N fissile nuclei.

Cross Sections of Nuclei Fissioned by Slow Neutrons

A thorough analysis of the average fission cross sections σ_f for the isotopes U^{235} and Pu^{239} (below 20 keV), and also for U^{233} and Pu^{241} (below 1 keV), was carried out in [1], in which the entire region of investigated cross sections for each isotope is broken down into a large number (20-30) of intervals and the spread of the individual results for σ_f (within an interval) around the average value is studied. By eliminating the oldest and most highly divergent data from the averaging process, the recommended cross section values given in [1] were obtained. However, these values, determined for relatively broad energy intervals, do not reflect the "structure" with a spacing of the order of 100 eV observed in the fission cross sections of U^{235} and Pu^{239} [54, 55].

The cross section is shown in Fig. 4 for the ranges 12-15 keV (a) and 20-30 keV (b) [55]. The rise in the cross section in the region of 22 keV is clearly visible. Because of the presence of structure, the fission cross section measured in a narrow energy range turns out to be dependent on instrumental resolution. This circumstance throws doubt on the use of the U^{235} cross section in the region of 10-100 keV as a standard, which has been the practice until recently.

An original method for the comparison of cross sections was developed in [56] – the results of various measurements are averaged by means of a Gaussian function (of width 0.15 $\sqrt{E}$) in such a way that the difference in experimental resolutions is almost completely smoothed out and then the deviations of the resultant "smoothed cross sections" from the averaged values are found. This method makes it possible to

TABLE 2. Comparison of the Ratio $\alpha = (\Sigma 2g\Gamma_n\Gamma_\gamma/\Gamma)/(\Sigma 2g\Gamma_n\Gamma_f/\Gamma)$ for U^{235} in the Region 30-40 eV from Results of Various Authors [2, 71]

	Reference [66]			Reference [70]		Reference [68]			Reference [63]			Reference [71]		
E, eV	$2g\Gamma_n$, mV	$2g\Gamma_n\Gamma_f/\Gamma$, mV	$2g\Gamma_n\Gamma_\gamma/\Gamma$, mV	$2g\Gamma_n\Gamma_f/\Gamma$, mV	$2g\Gamma_n\Gamma_\gamma/\Gamma$, mV	$2g\Gamma_n$, mV	$2g\Gamma_n\Gamma_f/\Gamma$, mV	$2g\Gamma_n\Gamma_\gamma/\Gamma$, mV	$2g\Gamma_n$, mV	$2g\Gamma_n\Gamma_f/\Gamma$, mV	$2g\Gamma_n\Gamma_\gamma/\Gamma$, mV	$2g\Gamma_n$, mV	$2g\Gamma_n\Gamma_f/\Gamma$, mV	$2g\Gamma_n\Gamma_\gamma/\Gamma$, mV
30,86	0,52	0,15	0,36	0,16	0,35	0,49	0,17	0,32	0,39	0,16	0,23	0,40	0,17	0,23
31,55	—	—	—	—	—	—	—	—	0,01	0,01	0,00	—	—	—
32,07	1,95	0,90	1,01	1,03	0,88	1,87	1,08	0,75	1,49	0,87	0,60	1,83	0,87	0,95
33,52	1,92	0,62	1,24	0,71	1,15	1,82	0,77	1,03	1,47	0,62	0,82	1,86	0,70	1,16
34,34	2,20	0,88	1,22	0,98	1,14	2,18	1,07	1,07	2,18	1,03	1,10	2,12	0,85	1,27
34,83	0,90	0,40	0,49	0,69	0,20	1,25	0,92	0,32	0,60	0,48	0,12	0,90	0,35	0,55
35,17	4,50	2,75	1,62	3,24	1,16	4,55	2,95	1,46	5,47	4,28	1,07	4,76	3,10	1,67
36,6	—	—	—	—	—	—	—	—	0,05	0,04	0,01	—	—	—
37,4	—	—	—	—	—	—	—	—	0,04	0,04	0,00	—	—	—
38,31	0,55	—	—	—	—	0,56	0,48	0,08	0,40	0,34	0,06	0,66	0,39	0,27
39,41	2,55	1,24	1,18	1,45	1,00	2,46	1,43	0,96	3,32	1,69	1,52	2,78	1,28	1,50
39,90	0,46	—	—	—	—	0,31	0,27	0,04	0,38	0,29	0,09	0,40	0,25	0,15
40,51	0,45	—	—	—	—	0,41	0,33	0,08	0,47	0,38	0,09	0,53	0,38	0,15
Partial sum:		6,94	7,12	8,26	5,88		8,39	5,91		9,22	5,47		7,41	7,40
Total sum	15,95	—	—	—	—	15,90	9,47	6,11	16,27	10,23	5,71	16,24	8,34	7,90
Ratio α	1,03			0,71		0,71			0,59			1,00		

observe such systematic effects as a dip in σ_f because of neutron penetration through a filtering structural material [56, 57] and various "time groups" [56, 58]. The differences in the energy scales of most of the spectrometers were established as well as the fact that there are important deviations in the U^{235} and Pu^{239} fission cross sections in the regions between resonance levels; the cross sections measured on spectrometers with electron accelerators [57, 59, 60] are higher than the σ_f measured by means of an underground nuclear explosion [58]. The region between resonance levels is important for the choice of the proper description of a cross section by means of multilevel formulas, which, in their turn, are important for calculations of temperature effects in reactors, etc.

It is frequently said at the present time that the cross sections measured in experiments using nuclear explosions are more reliable than those measured in other ways. However, the one-time nature of an experiment using underground nuclear explosions doesnot permit proper monitoring of background conditions and of the dynamic range of the recording instruments, which must operate under very high current overload conditions at early times as well as severe shock conditions, etc. Since multilevel analysis of σ_f depends strongly on the quality of current experimental data, disagreement in the regions between resonances obviously calls for special simultaneous measurements of several cross sections (σ_f, σ_c, σ_s, α).

The importance of considering interference between levels can be demonstrated by a study of the U^{235} total cross section in the region 0-4 eV (Fig. 5) and of the fission cross section for the same isotope in the region 22-28 eV (Fig. 6) [56]. The relative difference ($\varepsilon_1 = \Delta\sigma/\sigma$) between the actual σ_t and that calculated by the Briet–Wigner one-level formula (σ_{BW}) shown in Fig. 5 (by the dashed curve) has a value ranging from 20-30% (scale on the right). The difference between the measured cross section σ_t and that calculated by a multilevel formula is as little as a few percent (the quantity ε_2 in Fig. 5) even if some simplifying assumptions are used in the calculation of interference between levels [56]. Note that the correct multilevel description of the U^{235} cross section in this region, i.e., a description consistent with the presently accepted values of the spins of the levels [61], was firstgiven in [62].

In the energy region above 20 eV, the experimental points agree better with the multilevel description [56] than with the one-level approximation (see Fig. 6). The number of levels included in cross section calculations is reduced by the use of the multilevel formalism. This is illustrated by Fig. 7 [2] where the location of U^{235} neutron levels is shown for the same energy region, 22-27 eV, based on data from [63-69], in two of which mutilevel analysis was used. This analysis helps to avoid the introduction of a considerable

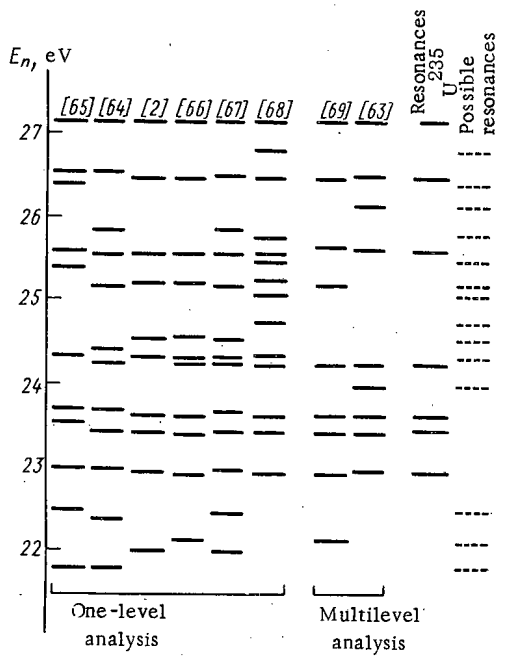

Fig. 7. Location of U^{235} neutron resonances in the energy region 22-27 eV from the data in various papers in which the one-level [64-68] and the multilevel [63, 69] approximations were used. On the right is indicated the location of reliably established levels as well as levels whose existence is not completely established (dashed lines) [2].

TABLE 3. Fission Widths of U^{235} Levels with Spins Known from Direct Measurements

Resonance energy, eV	Spins	T_t value (mV) from: [62]	[71]	[70]	[56]
0,29	3*	99	100	—	—
1,135	4*	112	115	—	—
2,04	3*	10	15	—	—
2,77	(4)	160	143	—	55,0
3,15	(3)	79	97	—	94,9
3,62	(4)	43	49	—	51,1
4,84	4	4	3,9	—	4,2
5,50	(4)	23	24	—	200
6,20	—	260	85	—	191,9
6,39	3	—	11	9	9,8
8,78	3	—	76	84	123,0
11,66	4	—	9	4	4,9
12,39	3	—	24	28	25,6
19,29	4	—	58	60	62,8
23,40	(4)	—	7	6	6,0
32,07	4	—	57	53	70,7
33,52	4	—	22	23	34,6
34,34	4	—	29	38	61,0
35,17	4	—	119	126	150,0
39,41	3	—	45	55	70,3

number of "virtual resonances" characteristic of one-level fitting, i.e., the introduction of levels for which a physical interpretation is difficult (they only appear because of an inadequate formalism). One ought therefore be cautious with respect to some conclusions in papers where multilevel analysis was not used, especially if the subject involved is the observation of grouping in radiation widths [63] or in ratios of partial widths [64, 70, 71].

The present state of the U^{235} data is characterized both by a spread in the parameter values for individual levels and by differences in the cross sections themselves. An illustration of this for the region 30-40 eV is given in [2]. Table 2 gives values of the parameters $2g\Gamma_n$, $2g\Gamma_n\Gamma_\gamma/\Gamma$ taken from [63, 66, 68, 70, 71], and the integral quantities $\Sigma 2g\Gamma_n$, $\Sigma 2g\Gamma_n\Gamma_\gamma/\Gamma$, and $\Sigma 2g\Gamma_n\Gamma_t/\Gamma$ are given in the last two lines (the next to last line gives the sum over the strongest resonances only). Since the two sums characterize the U^{235} capture and fission cross sections in the region under consideration, it is clear that the ratios of these quantities (i.e., of α) differ by more than 25% according to the data from the various authors (the value of α varies from 1.03 to 0.59).

In multilevel analysis, it is always desirable to know the spins of the neutron levels. Until recently, such data was not satisfactory because the number of known spins could be counted on the fingers and because an indirect method was often used to determine the spins of U^{235} levels from the multiplicity of capture γ-rays. Direct measurements of spins made recently (by neutron scattering [72]) did not give an unambiguous confirmation of the spins found by γ-ray methods and from data on the variation in the number of secondary neutrons [73] and average kinetic energy of fragments [74].

Among the possible systematic effects inherent in indirect methods for determining the spins of levels in fissile nuclei is the interference from fission γ-rays which are correlated with the quantities Γ_f or $\alpha \approx \Gamma_\gamma/\Gamma_f$ [75]; in contrast to nonfissile nuclei where indirect methods give an unambiguous value for the spins, the results of such methods are quite unreliable for U^{235}.

Table 3 presents data on the spins of the U^{235} resonances obtained in direct measurements [72] (lower part of the table) and from an analysis of the intensity of radiative transitions [76] (upper part of the table). This second method is also free of the defects of the multiplicity method (see above); the data in Table 3 can therefore be considered as the most up-to-date direct results. Also given are less reliable spin values from direct measurements (in parentheses) and from interference analysis [56] (values with asterisks) as well as fission widths from multilevel [56, 62] and one-level [70, 71] analyses. It is clear from the first four values in Table 3 that relatively large (~100 mV) and relatively small (~10 mV) fission widths are encountered for both level spins. The average values Γ_t = 45 mV ($J = 3^-$) and Γ_t = 47 mV ($J = 4^-$) do not

TABLE 4. Pu^{239} Resonance Parameters in the 60-100 eV Region from Various Papers [2, 71]

Level	James [80]					Farrel [80]					Reference [79]					Reference [71]		
	E, eV	Γ_n, eV	Γ_{f_1}, mV	Γ_{f_2}, mV	J	E eV	Γ_n, mV	Γ_{f_1}, mV	Γ_{f_2}, mV	J	E, eV	Γ_n, mV	Γ_{f_1}, mV	Γ_{f_2}, mV	J	E, eV	$2g\Gamma_n$, mV	Γ_f, mV
1	57,44	—	—	—	—	57,30	19,7	1040	—	0	57,00	14,47	—1554	28	0	57,8	9,37	402
																58,6	3,91	712
																59,6	12,8	135
2	60,94	30	5930	—	0	62,70	13,37	—4250	—	0	61,86	26,25	7102	20	0	61,7	1,46	160
3	—	—	—	—	—	63,16	0,69	—54	—	1	63,02	0,70	80	—	1	63,4	8,4	108
4	—	—	—	—	—	65,40	0,80	—39	—	1	—	—	—	—	—	—	—	—
5	65,71	—	—	—	—	65,75	7,57	—127	—	1	65,71	9,17	28,5	—	1	66,2	18,36	84
6	66,57	—	—	—	—	66,75	4,21	—	1355	0	65,50	13,66	2380	1510	0	—	—	—
7	—	—	—	—	—	68,05	0,014	—250	—	1	—	—	—	—	—	69,9	2,9	40
8	74,05	—	—	—	—	74,19	3,32	92	—	1	74,05	3,37	—26	—	1	—	—	—
9	74,95	—	—	—	—	74,97	16,4	148	—	1	74,94	22,78	—87	—	1	75,6	36,6	82
10	—	—	—	—	—	77,80	0,35	—	2000	0	—	—	—	—	—	—	—	—
11	78,95	0,107	140	—	1	78,60	0,008	50	—	1	78,97	0,04	2	—	1	—	—	—
12	81,36	5,39	—456	416	0	81,1	8,54	1950	—	0	80,92	4,95	963	582	0	—	—	—
13	82,68	0,50	29,5	—	1	83,62	0,22	—74	—	1	82,67	0,39	10	—	1	82,7	6,8	72
14	85,48	7,86	37	—	1	85,40	1,48	48	—	1	85,49	7,45	9,4	—	1	—	—	—
15	85,22	57,6	2686	571	0	85,60	43,5	—1916	—	0	85,53	53,4	—2010	55	0	85,7	38,7	802
16	96,49	(6,68)	1467	—	0	—	—	—	—	—	96,54	20,66	842	1816	0	—	—	—
17	100,25	(5,60)	—	5949		—	—	—	—	—	101,75	9,05	—4823	25	0	—	—	—

*One-level analysis.

fit the grouping of Γ_t values around average values equal to 87 ± 20 and 26 ± 6 mV discussed in [71]. In that paper, the grouping was associated with the spin dependence for Γ_t predicted in [77] (Γ_t is respectively 81 and 32.5 mV for J equal to 3^- and 4^-).

The situation with respect to Pu^{239} levels is more definite because direct measurements of spins and data for γ-ray spectra from resonance capture of neutrons [78] are more easily explained (the spins of the levels in the compound nucleus Pu^{240}, which are 0^+ and 1^+, have very different spectroscopic factors which can be measured relatively easily; in addition, the existence of a radiative transition to the 0^+ ground state is unambiguous evidence that $J = 1^+$ because the $0 \rightarrow 0$ transition is forbidden). In particular, the spin $J = 1^+$ was determined for the first neutron level (at $E_0 = 0.3$ eV) through observation of a direct transition from it while $j = 0^+$ followed from indirect considerations in an analysis of the interference structure of the cross section [79].

At the present time, spins have been uniquely determined for the majority of Pu^{239} resonances in the energy region below 200 eV. Furthermore, multilevel analysis of the Pu^{239} fission cross section by the various authors is in agreement in the main as has been shown for the region 60-100 eV [2]. In three independent papers, the resonances are distributed relatively identically with respect to interfering groups (with the same J) with the introduction of two interfering channels for $J = 0^+$ being necessary (Table 4). At the same time, there is not complete agreement in the various papers for several levels (2, 6, 11, 13, and 14, Table 4); however, this is not very strongly reflected in the integral distributions of the partial widths and in the average values (a review of these distributions was made earlier in [81], for example). The results of multilevel analysis diverge even more strongly from the parameters given by one-level fitting to the cross sections.

As an example, data from [71] is given in the last columns of Table 4 for the same energy range of Pu^{239} neutron levels. One can speak of corresponding results only for levels 5 and 9. In the other cases, the neutron widths in the one-level analysis are greater (levels 3, 7, and 13), and the fission widths are less (levels 1, 2, and 15), than in the multilevel analysis, or "virtual" levels with very significant neutron widths are introduced (between 1 and 2) and broad levels (6, 10, and 12) are omitted, i.e., levels which act as a background in the fission cross section ($\Gamma_f > 1000$ mV). Because of this transformation of parameters in one-level fitting of those cross sections where interference effects are clearly present, one should not overestimate the physical significance of one-level parameters. They should be treated as a first crude approximation in the description of a cross section for practical calculations.

A similar effect is observed in the analysis of U^{235} cross sections, as was seen above. A recent one-level analysis as Saclay of new data for σ_f [82] gave the following parameters for the region 0-150 eV: $\overline{\Gamma}_\gamma = 42.6$ mV, $\overline{\Gamma}_f = 73.4 \pm 8.0$ mV, and number of degrees of freedom $\nu = 2.8$. At the same time, multilevel analysis of σ_f, σ_t, and σ_c [56] in the region 0-50 eV led to the value $\overline{\Gamma}_\gamma = 150$ mV with the width distribution being better described by two relations with $\nu = 2$; $\Gamma_f = 300$ mV (27 levels) and $\overline{\Gamma}_f = 63$ mV (55 levels).

TABLE 5. Values of α for Various Portions of the Pu^{239} Cross Section Based on Neutron Resonance Parameters [102] and Comparison with Direct Measurements

Energy range, eV	Capture			Fission			Ratio	
	$\Sigma\sigma_0\Gamma_\gamma$, $J=0^+$, barn-eV	$\Sigma\sigma_0\Gamma_\gamma$, $J=1^+$, barn-eV	$\Sigma\sigma_0\Gamma_\gamma$, $J=0^+;\ J=1^+$, barn-eV	$\Sigma\sigma_0\Gamma_f$, $J=0^+$, barn-eV	$\Sigma\sigma_0\Gamma_f$, $J=1^+$, barn-eV	$\Sigma\sigma_0\Gamma_f$, $J=0^+;\ J=1^+$, barn-eV	$\alpha(E)$ (calculated)	$\alpha(E)$ (experiment) [6]
100—200	112	824	936	687	482	1169	0,801	0,80±0,08
200—300	33	936	969	540	565	1105	0,877	0,91±0,09
300—400	58	478	536	164 *	303	467	1,147	1,13±0,11
400—500	14 *	219 *	233	328	254	582	0,401	0,49±0,06
500—600	53	475	528	668 *	285	953	0,553	0,69±0,07
600—650	1	300	301	68 *	70	138	2,18	1,62±0,17 (E_n = 600 - - 700 eV)

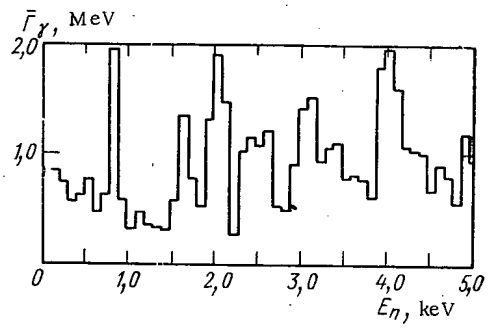

Fig. 8. Ratio of the fission and capture cross sections for Cm^{244} [94] (Assuming $\bar{\Gamma}_\gamma$ = 37 mV).

To conclude the discussion of the first neutron resonance region in Pu^{239}, one should cite the preliminary data of the Columbia University group (see [43], p. 54), who observed a variation in kinetic energy of the fragments from fission of different spin states of this nucleus. The difference in kinetic energies found for the first positive level of Pu^{239} (E_0 = 0.3 eV) and the negative level which contributes to the thermal point is in agreement with the observed variation of the number $\bar{\nu}$ for these levels in [73]. In [83], however, a marked change in the number $\bar{\nu}$ was not observed for resonances with different spins (in contrast to the data of [73] and [84]), and it was shown [85] that the difference between data for $\bar{\nu}$ cannot be ascribed to any simple discriminatory property of the fission chambers used in [73, 84]. It is obvious that additional measurements are necessary to resolve the contradiction in the $\bar{\nu}$ data [73, 83, 84]. A conference of IAEA experts at Studsuik (1970) recommended such investigations be made as quickly as possible because of their great physical and applied importance [86].

Data for the remaining fissile isotopes, including Pu^{241} [87-89], is as yet not as abundant as that for the isotopes discussed above. We shall therefore confine ourselves to the remark that in the case of U^{233}, cross-section measurements [90, 91] gave similar results, but analysis of those cross sections led to several differing parameters for the levels [92] as was also true in the case of Pu^{241}.

In particular, very different numbers for the degrees of freedom ν were obtained – 1.5 [87] and 2.8 [89] – for the distribution of fission widths in Pu^{241} although the one-level approximation was used in both papers. Because of the clear lack of coordination in the methods for cross-section analysis and because of the increasing number of nuclei for which the fission cross section in the resonance region has been measured recently (Th^{229} [93], Pu^{238} [43], $Cm^{244-248}$ [94], and Cf^{249} [47]), attempts are being made not only to analyze the cross sections by means of multilevel formulas of a different type [95], but also to develop methods of comparing and recomputing the parameters which were obtained through different multilevel formalisms [96, 97].

It has been pointed out [95] that as long as the data for any isotope is sparse, relative "agreement" is usually observed, and such a situation is considered satisfactory for some time; however, new repeated (or more precise) measurements are often quite surprising. At the present time, such a situation is developing in the analysis of data for the resonance region of heavy nuclei.

We discuss for each specific nucleus an example of how rapidly the situation is changing. Data on the ratio of the fission and capture cross sections ($1/\alpha$) for Cm^{244} [94] is shown in Fig. 8. A distinct "intermediate structure" is visible although its appearance was not evident in earlier work on this same nucleus [46] or from theoretical evaluations. The presence of local "structure" in the cross section means that resonance properties change quite significantly with a change in neutron energy by a few hundred electron volts and the transfer of average values (and width distributions) from one region to another is impossible because it leads to large errors. We demonstrate this by the quantity α for Pu^{239}.

Intermediate Structure in Pu^{239} Fission Cross Section

The observation of modulation in fission widths (i.e., intermediate structure in σ_f) in nuclei undergoing subthreshold fission (see above) brought about the consideration of the Pu^{239} nucleus, in which fission

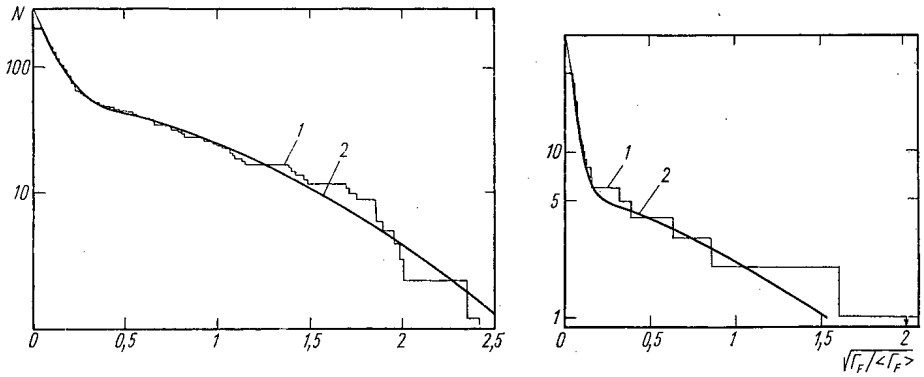

Fig. 9. Distribution of fission widths for neutron resonances in Pu^{239} [101]: above – a comparison of the integral distribution of Γ_f (curve 1) for the region 0-660 eV with a theoretical distribution (curve 2) made up of two components – two distributions with the parameters N = 171 levels, $\overline{\Gamma}_f$ = 35.5 mV, ν = 1, and N = 58, $\overline{\Gamma}_f$ = 2270 mV, ν = 1.4. Below – a comparison of the Γ_f distribution (curve 1) for the region 550-660 eV with a theoretical distribution (curve 2) consisting of two components – two distributions with the parameters N = 26, $\overline{\Gamma}_f$ = 7 mV, ν = 1, and N = 6, $\overline{\Gamma}_f$ = 1800 mV, ν = 1.

through a channel with $J = 1^+$ can be considered as approaching the threshold [1] (see the reviews [41, 98]). Correlation analysis of the fission cross section for this isotope was repeated [99] and a structure with a spacing of ~450 eV was confirmed. However, the reality of such a structure was partly placed in doubt because of [100] where it was found that structure in U^{235}, for example, may be the consequence of statistical fluctuations.

To solve this question, special measurements of the Pu^{239} total and fission cross sections using a cooled sample [101, 102] were made with the linear accelerator at Saclay. The energy dependence of the cross section obtained in this experiment was the following: strong levels were absent in the cross section in the region 600-900 eV; it was as though the cross section were cut off [101]. In order to explain this effect quantitatively, subsequent analyses were made in some papers not only of σ_f but also of the total cross section and neutron scattering. Thus, the distribution of the fission widths for all resonance levels was constructed in [101] for each 110 eV energy interval (0-110, 110-220, 220-330 eV, etc.). Such a distribution is shown in Fig. 9 (below) for the last interval, 550-660 eV; further analysis is yet to be done. The authors [101] concluded that the decomposition of this distribution into two components make it possible to obtain the average fission widths: $\overline{\Gamma}_f(1^+)$ = 7 eV and $\overline{\Gamma}_f(0^+)$ = 1800 mV. Such a decomposition was carried out in the other intervals. For them, there are direct determinations of the spins of the levels [102] for which similar values were obtained.

In doing a multilevel analysis of Pu^{239} cross sections in the region below 160 eV [79] (see Table 4 also), it was found that each width $\Gamma_f(0^+)$ in turn can be represented in the form of a sum of two Γ_f (and, correspondingly, two Γ_f distributions having the number of degrees of freedom ν = 1 and average values Γ_{f_1} = 218 mV and Γ_{f_2} = 1464 mV). The conclusion was derived from the experimental fact that every $\Gamma_f(0^+)$ must be represented in the form of a sum of independent fission widths Γ_{f_1} and Γ_{f_2}; otherwise, a satisfactory description of the observed interference effects is not obtained.

One should especially note the strongly varying behavior of the average fission width $\Gamma_f(1^+)$ (which is clear from a consideration of both parts of Fig. 9). The authors of [101, 102] consider this as a direct indication of the appearance of the expected modulation of $\Gamma_f(1^+)$ because of a complex fission barrier. In addition the quantities $\sigma_0\Gamma_\gamma$ and $\sigma_0\Gamma_f$ were calculated [102] for different spin states (and various energy intervals) and the quantity $\alpha = \Sigma\sigma_0\Gamma_\gamma/\Sigma\sigma_0\Gamma_f = \overline{\sigma}_\gamma/\overline{\sigma}_f$ was obtained, which makes it possible to analyze the contribution of various spin-dependent effects to this reactor constant of great practical importance.

The individual components of such a calculation are shown in Table 5, the last column of which gives the average values found by direct measurement [6]. As is clear from the table, the quantity α undergoes large changes in the range 400-500 eV (very low value) and the range 600-650 eV (very high value). In the first of these ranges, the integral capture falls sharply (by a factor of two), and in the second, the integral fission decreases even more sharply (boldface numbers in Table 5). Since fission through a channel with

TABLE 6. Basic Parameters of Modern Electron Accelerators (and some other installations) Used in Time-of-Flight Spectroscopy [95]

Device and location	Flight path, m	Pulse length, nsec	Particle energy, meV	Current per pulse, A	Power, kW
Mechanical selector, Brookhaven (USA)	22—48	5000	—	—	—
Mechanical selector, Kiel University (West Germany)	21,5	1000	—	—	—
Electron accelerators:					
San Diego (USA)	16—230	20	60	10	—
Livermore (USA)	4—250	15	140	10	30
Washington (USA)	—	5	100	—	—
Oak Ridge (USA)	20—2000	2—1000	140	15	50
Troy (USA)	10—250	—	>100	15—20	—
Geel (Belgium)	up to 200	20	65	4	5
Saclay (France)	50—200	10	>60	—	6—8
Harwell (England)	5—300	100	45	—	—
Nevis synchrocyclotron, Columbia University (USA)	up to 200	10	550 (protons)	—	20
Nuclear explosions, Los Alamos (USA)	~ 250	100—200	—	—	Five explosions in seven years
Pulsed reactor, Dubna (USSR) [21, 64, 71]	up to 1000	~ 4000	—	—	—

$J = 1^+$ is actually decreased, a portion of the fluctuation effect can be assigned to the expected phenomenon (but not the entire effect, as has been pointed out [102]). However, the main contribution to the variation in α (from the data in Table 5) comes not from the channel with $J = 1^+$ but from the marked variations in fission through the channel with $J = 0^+$: in the ranges 300-400 eV and 600-650 eV with a maximum at 500-600 eV as well as the fluctuation in capture at 400-500 eV noted above (these values are designated by an asterisk in Table 5). It is therefore impossible to consider the question of the fundamental reason for the strong variations in α to be definitely solved.

However, it is now clear that limitation to any narrow energy region (of the order of 100 eV) in the analysis of the distribution of partial widths and cross sections (and their ratios) is equivalent to the introduction of significant systematic error into the results. One can hope to obtain sufficiently good extrapolation of the distributions of partial widths into a region of unresolved resonances only by studying structure on a scale of hundreds of electron volts. One should further remember that even at energies of several kiloelectron volts in nuclei like Pu^{239}, levels excited by neutrons with orbital momentum $L = 1$ (p waves), about which there is less information than for s neutrons ($L = 0$), begin to play a significant role.

A quantitative description of intermediate structure in the Pu^{239} cross section is contained in [103] where the level parameters are determined for the second potential well (of the double-humped fission potential) – the so-called levels of the second class [41]. Using these results, the effect of intermediate structure on the Doppler coefficient of a fast-neutron reactor was analyzed [104]. It was concluded that this effect is large for Pu^{239} and that very detailed information about intermediate structure was necessary.

* * *

In conclusion, it should be pointed out that the increasing level of experimental measurements of neutron cross sections in the resonance region is associated with the construction of a whole series of new linear electron accelerators and the use of underground nuclear explosions. A few more high-intensity linear accelerators have begun to operate only recently and one has succeeded in measuring the cross sections of such short-lived nuclei as U^{237} and isotopes of curium and californium, for example, in underground nuclear explosions. The relative capabilities of the three basic types of spectrometers based respectively on mechanical selectors, nuclear explosions and linear accelerators have been discussed in review papers [1, 95]. It was shown there that only linear accelerators (and similar devices) are capable of giving the maximum information in the region of several kiloelectron volts because the resolution of the associated spectrometers is comparable in order of magnitude with the Doppler broadening of the resonances (Fig. 10).

TABLE 7. Measurements (1 – in progress, 0 – planned) at Various Neutron Spectrometers [95]

Measurement	Mechanical selectors		Electron accelerators								Other	
	Brookhaven	Kiel	San Diego	Livermore	Washington	Oak Ridge	Troy	Geel	Saclay	Harwell	Columbia University	Los Alamos
Cross sections												
total	—	1	1	1	1	1	1	1	1	1	1	—
capture	—	—	1	1	—	1	1	1	1	1	1	1
scattering	—	—	—	1	0	0	0	1	1	1	—	1
fission	—	—	—	1	—	1	0	1	1	1	1	1
Constants:												
α	—	—	—	1	—	1	0	—	0	1	—	0
γ	—	—	—	0	—	1	1	—	0	0	—	—
	1	—	1	1	—	1	1	1	1	0	—	—
γ-Ray spectra	—	—	1	1	—	0	—	1	1	—	—	—
γ-Ray multiplicity	—	—	—	—	—	1	—	—	0	1	—	0
Polarization, aligned nuclei												
Cross sections of radioactive samples:												
total	—	1	—	—	—	1	1	—	—	—	—	—
capture	—	—	—	—	—	—	—	—	—	—	—	1
fission	—	—	—	1	—	1	—	0	—	0	—	1
Standard cross sections	—	—	1	0	0	1	0	1	1	1	1	—
Mass and energy distribution of fission fragments	—	—	—	—	—	0	—	0	1	—	1	1
Self-indication	—	—	1	0	—	0	0	0	0	0	1	0

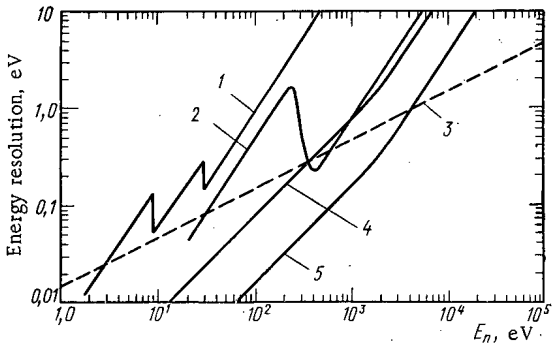

Fig. 10. Comparison of the resolution of the three basic types of spectrometers for various energies: mechanical (1), device associated with nuclear explosion (2), and spectrometer with 40 m (4) and 200 m (5) flight path associated with linear electron accelerator. Curve 3 is an estimate of the Doppler broadening of resonance lines [95] (A = 240).

The parameters of such a spectrometer shown in Fig. 10 (pulse length 25 nsec and flight path 200 m) are, in a certain sense, conventional; the parameters of most of the modern linear accelerators are shown in Table 6. It is clear that they have comparable resolutions (although the power is different).

We now see how these capabilities are being used and what experiments are being performed now or will be performed in the immediate future. Table 7 indicates that measurements of the cross section σ_f and of the constants α and $\bar{\nu}$ will be continued and expanded. From the data that has been presented, it is clear that only several independent measurements can assure reliable information about an important reactor constant; a broad front of neutron research is therefore absolutely necessary.

The information obtained with modern selectors is treated and analyzed at a corresponding level, i.e., with the use of large high-speed computers including the use of magnetic disc memories. The progress made could have been more significant if differences in the analysis programs used had been eliminated in advance and the various formalisms for theoretical interpretation of the cross sections unified. Recently, comparisons have been made of resonance parameters obtained through the various formalisms [96, 105-107], and it has been shown that only joint use of all cross sections (as was done in the case of Pu^{239}) can give results of definite physical significance. There is hope that the approximate description of cross sections needed for practical reactor construction along with better understanding of statistical (and other) behavior of s neutrons will be achieved in coming years.

However, further expansion of information (for neutrons with L = 1, 2, etc.) and understanding of a different kind of fine structure and effects requires even more intense neutron sources than those now existing, as already noted [108], and even better energy resolution. Since there remains the essential problem of measurement and analysis of resonance parameters for many fissile nuclei in the energy region above 50-100 eV, the question of comparison and evaluation of data will cease to be an urgent one and the various fine-structure effects will become the subject of forthcoming theoretical investigations.

LITERATURE CITED

1. G. James, Proc. Second Conf. Nuclear Data for Reactors (Helsinki, 1970), Vol. 1, IAEA, Vienna (1970), p. 267.
2. P. Ribon, ibid., Vol. 1, p. 571.
3. RENDA – Compilation of EANDC Requests for Neutron Data Measurements, W. Haussermann and S. Schwarz (1968). Cited in [2].
4. P. Greebler et al., Proc. Second Conf. Neutron Cross Section and Technology, NBS Special Publication 299, Vol. 1, Washington (1968), p. 291; see [1], Vol. 1, p. 17.
5. S. I. Sukhoruchkin, At. Energ., 28, 38 (1970); 31, 245 (1971).
6. S. I. Sukhoruchkin, see [1], Vol. 1, p. 307.
7. P. Ribon, CEA-N-1149 (1969). Cited in [2].
8. I. Gart et al., Phys. Rev., B134, 985 (1964).
9. M. Ashgar et al., Nucl. Phys., 76, 196 (1966).
10. L. Bollinger et al., Phys. Lett., 8, 45 (1964).
11. E. Haddad et al., GA-6272 (1965). Cited in [2].
12. I. L'Heriteau and P. Ribon, Third Conf. Neutron Cross Sections and Technology (USA, 1971). Report III-19.
13. L. Forman, ibid., Report VI-16.
14. G. Carraro and W. Kolar, see [1], Vol. 1, p. 403.
15. G. Carraro and W. Kolar, see [12], Report VI-23.
16. F. Rahn et al., see [12], Report VI-2.
17. M. Asghar, C. Chaffey, and M. Moxon, Nucl. Phys., 85, 305 (1966).
18. F. Firk et al., Nucl. Phys., 41, 614 (1963).
19. G. Rohr, H. Weigmann, and I. Winter, see [1], Vol. 1, p. 413.
20. N. Glass et al., see [4], Vol. 1, p. 573.
21. Kh. Maletski et al., "Radiation widths of P^{238} neutron resonances," Report at the Soviet – French Seminar on Nuclear Data (Dubna, 1970); At. Energ., 32, 49 (1972).
22. I. Rosen et al., Phys. Rev., 118, 687 (1960).
23. E. Silver et al., see [12], Report VI-3.
24. M. C. Moxon, AERE-R-6074 (1969). Cited in [22].
25. S. Friesenhahn et al., NASA CR-72745 (1970). Cited in [22].
26. M. Fricke et al., see [12], Report II-11.
27. T. Pitterle, see [1], Vol. 2, p. 687.
28. L. Abagjan et al., see [1], Vol. 2, p. 667.
29. W. Davey, Nucl. Sci. Engng., 39, 337 (1970).
30. T. Byer and V. Konshin, see [12], Report III-7.
31. W. Kolar and K. Bockoff, see [4], Vol. 1, p. 519; J. Nucl. Energy, 22, 299 (1968).
32. M. Cao et al., see [4], Vol. 1, p. 513.
33. H. Weigmann and H. Schmid, J. Nucl. Energy, 22, 317 (1968).
34. R. Hockenbury et al., see [12], Report VI-4.
35. D. Ramakrishna and M. Navalkar, see [1], Vol. 1, p. 533.
36. Yu. Abov, Session of Academy of Sciences of the USSR, on Peaceful Uses of Atomic Energy [in Russian], Izd-vo AN SSSR, Moscow (1955), p. 294.
37. P. Egelstaff et al., Nucl. Energy, 6, 303 (1958).
38. R. Cote et al., Phys. Rev., 114, 505 (1959).
39. N. Pattenden and V. Rainey, J. Nucl. Energy, 11, 14 (1959).
40. V. Strutinsky, Nucl. Phys., A95, 420 (1967).
41. I. Lynn, Proc. Symp. Physics and Chemistry of Fission, IAEA, Vienna (1969), p. 249.
42. G. James and G. Slaughter, Nuclear Phys., A139, 471 (1969).
43. T. Young and M. Silbert, NCSAC-31 (EANDE-US-143-"U") (1970), p. 70.
44. G. Auchampaugh et al., see [12], Report VI-6.
45. V. Strutinsky and H. Pauli, see [41], p. 155.
46. M. Moore et al., see [1], Vol. 1, p. 527.
47. M. Silbert et al., see [12], Report VI-5.
48. F. Poortmans et al., see [12], Report VI-11.
49. W. Havens, Jr., Progress in Fast Neutron Physics, Univ. Chicago Press (1963), p. 215.

50. K. Ideno and M. Okubo, J. Phys. Soc. Japan, 30, No. 3, 620 (1971).
51. S. I. Sukhoruchkin, Yadernaya Fizika, 10, 496 (1969).
52. S. I. Sukhoruchkin, Nucl. Data for Reactors, IAEA, Paris (1966).
53. S. Sukhoruchkin, see [4], Vol. 2, p. 923.
54. C. Bowman et al., see [1], Vol. 2, p. 65.
55. C. Bowman et al., see [12], Report V-7.
56. G. Krebs et al., see [1], Vol. 2, p. 789; see [12], Report III-8.
57. M. Cao et al., see [4], Vol. 1, p. 481.
58. W. Brown et al., Proc. Conf. Neutron Cross Section and Technology, Washington (1966), p. 971.
59. G. de Saussure et al., ORNL-TM 1804 (1967).
60. F. Brooks et al., AERE-ND/GEN 35 (1966).
61. R. Schermer et al., Phys. Rev., 167, 1121 (1968).
62. I. V. Kirpichnikov et al., At. Energ., 16, 216 (1964).
63. I. Cramer, Nucl. Phys., A126, 471 (1969).
64. Van Shi-di et al., Physics and Chemistry of Fission, Vol. 1, IAEA, Vienna (1965), p. 287; JINR Preprint P-2024 (1965).
65. C. Bowmann et al., Phys. Rev., 130, 1482 (1963).
66. A. Michandon et al., Nucl. Phys., 69, 545 (1965).
67. I. Schmidt, KFK 120-EANDC-E-354 (1966). Cited in [2].
68. D. Drawbaugh and G. Gibson, see [52], Vol. 2, p. 251.
69. F. Adler and D. Adler, see [4], Vol. 2, p. 967.
70. M. G. Cao et al., J. Nucl. Energy, 22, 211 (1968).
71. Yu. V. Ryabov et al., JINR Preprint P3-4992 (1970).
72. F. Poortmans et al., see [1], Vol. 1, p. 449.
73. S. Weinstein et al., Phys. Rev. Letters, 22, 195 (1969); see [41], p. 477.
74. S. Bochvarov, E. Dermendzhiev, and N. Kashukeev, see [41], p. 465.
75. C. Bowman et al., see [43], p. 112.
76. R. Chrien et al., see [12], Report VI-20a.
77. N. O. Bazazyants and I. V. Gordeev, At. Énerg., 13, 321 (1962).
78. R. Chrien et al., see [1], Vol. 1, p. 377.
79. H. Derrien et al., see [1], Vol. 1, p. 481.
80. G. James, J. Nucl. Energy, 22, 263 (1968); J. Farrel, Phys. Rev., 165, 1371 (1968).
81. A. Michaudon, see [4], Vol. 1, p. 427.
82. I. Blons et al., see [12], Report VI-8a.
83. L. Weston and I. Todd, see [12], Report VI-9.
84. Yu. V. Ryabov et al., Reports at the International Symposium on Nuclear Structure [in Russian], D-3893, Dubna (1968), p. 88.
85. E. Dermendzhiev and Ts. Panteleev, JINR Preprint PZ-5081 (1970).
86. D. Colvin, see [1], Vol. 2, p. 195.
87. I. Blons et al., see [1], Vol. 1, p. 469, see [12], Report VI-8b.
88. M. Moore et al., Phys. Rev., B135, 945 (1964).
89. W. Kolar et al., see [12], Reports VI-25, VI-26.
90. W. Kolar et al., see [1], Vol. 1, p. 387.
91. M. Cao et al., see [1], Vol. 1, p. 419.
92. R. Joly, see [1], Vol. 2, p. 919.
93. I. Felvinei and E. Melkonian, BNL-50276; (T-603) (1970), p. 60.
94. G. Keyworth and M. Moore, ibid., p. 136.
95. M. Moore, see [12], Report VI-1.
96. F. Adler and D. Adler, see [1], Vol. 2, p. 777.
97. G. de Saussure et al., see [1], Vol. 2, p. 757.
98. I. Lynn, see [1], Vol. 1, p. 93; A. V. Ignat'yuk, Structure of the Fission Barrier (Proceedings of the Fifth Winter School on Nuclear Theory and High-Energy Physics) [in Russian], Part 2, Leningrad (1970), p. 317.
99. G. James and V. Patrick, see [4], Vol. 1, p. 391.
100. G. de Saussure et al., Phys. Letters, 31B, 413 (1970); see [41], p. 307.
101. I. Blons et al., see [1], Vol. 1, p. 513.
102. I. Trochon et al., see [1], Vol. 1, p. 495.
103. Y. Kikuchi, Trans. Amer. Nucl. Soc., 13, No. 1, 312 (1970).

104. I. L'Heriteau and G. Neviere, see [12], Report VI-7.
105. A. A. Luk'yanov, see [21], Parameters for Multilevel Analysis of Cross Sections in the Resonance Region [in Russian].
106. D. Harris, see [12], Report VI-33.
107. G. Auchampaugh, see [12], Report III-6.
108. G. V. Muradyan et al., see [1], Vol. 1, p. 603.

THE URANIUM INDUSTRY IN THE INDUSTRIALLY DEVELOPED CAPITALIST COUNTRIES AND IN THE DEVELOPING NATIONS IN 1970

V. D. Andreev

Geological prospecting and exploration work was cutback to a certain extent below the very high 1969 level, in the uranium mining industry of the industrially advanced capitalist nations and in the developing nations during 1970, accompanied by a further increase in uranium ore mining and in the production of uranium ore concentrates, and an intense program of building new mines and new ore beneficiating plants.

The principal consumer category for uranium ore concentrates was that of full-scale nuclear power generating stations.

A considerable acceleration of the rates of development of nuclear power as an industry occurred in 1970. Worldwide consumption of fuel energy resources over the 1966-1970 period increased by an average of 7%, as against the 4.8% rate of increase in the 1961-1965 period, and the demand for electric power rose 9% each year on the average. The demand for all forms of fuel and electric power ran well ahead of supply, for the first time in the past 15 years. Some areas were teetering on the verge of a fuel crisis, necessitating the mobilization of all available power resources. The rise in the prices of coal, petroleum, and petroleum products that accompanied this development contributed to an improvement in the economically competitive position of nuclear power stations as compared to power stations burning fossil fuels. In most of these areas it has become feasible to build larger power stations burning nuclear fuel than the presently existing power stations running on fossil fuels. The installed capacity of nuclear power stations in the capitalist countries may rise from 18 million kW at the end of 1970 to a level of 118 million kW in 1975, and up to 300 million kW in 1980 and 610 million kW in 1985 [1]. In recent years the economic advantages of reactors burning slightly enriched uranium and cooled by ordinary water have come to the fore. Typical of these reactors are low building and investment costs and relatively high uranium consumption rates. The installed capacity of reactors cooled by ordinary water might possibly increase from the 1970 level of 11 million kW to a level of 248 million kW in 1980 [2].

According to the last development forecast released by the International Atomic Energy Agency, which takes into account the most recent trends in nuclear power development, the demand for uranium ore concentrates on the part of nuclear power stations in the industrially advanced capitalist countries and in the developing nations will rise from 10,900 tons U_3O_8 in 1970 to 33,600 tons U_3O_8 in 1975, 66,200 tons in 1980 (making a total of 390,000 tons U_3O_8 over the 1970-1980 decade), and to a level of 117,900 tons U_3O_8 in 1985 (or 870,700 tons U_3O_8 over the 1970-1985 period). It is acknowledged that, should full-scale plutonium reactors enter the picture as a major factor, the uranium demand for the period extrapolated to 1980 should be figured at 7% lower than these figures [2].

Overall (Geological) Uranium Reserves. According to the incomplete data available, the total increase in commercial uranium reserves in the capitalist countries amounted to roughly 550,000 tons U_3O_8 (with 119,000 tons U_3O_8 from mining operations taken into account) for the past five to six years, i.e., the amount almost doubled (Table 1).

The net increase in commercial uranium reserves in the the USA reached the level of 38,100 tons U_3O_8 in the year 1970 (with mining of 49,900 tons U_3O_8 taken into account) compared to 11,800 tons in 1968 (with mining of 23,600 tons U_3O_8 taken into account), and compared to the 1969 level of 39,000 tons (with mining of

Translated from Atomnaya Energiya, Vol. 31, No. 6, pp. 610-618, December, 1971. Original article submitted August 10, 1971.

TABLE 1. Geological Uranium Reserves in the Industrially Advanced Capitalist Nations and in the Developing Nations, Thousands of Tons U_3O_8 [2-6]

Nation	1965		1970	
	Total	Commercial reserves included	Total	Commercial reserves included
USA	1 342,6[1]	176,9[2]	1 800,0[3]	353,8[4]
Canada	997,8	190,5[5]	1 079,8	210,5[5]
S. Africa	127,0	127,0	403,8	181,4
Sweden	680,4[6]	...	680,4[6]	...
Australia	17,4	13,6	300,0	120,0
Spain	273,1	10,0	281,2	10,0
Argentina	33,5	4,5	146,1	16,7
India	15,0	...	80,7	...
France	72,6	33,6	72,3	40,8
Nigeria	—	—	70,0[7]	23,6
Portugal	23,6	6,4	34,0	8,7
Italy	...	1,4	28,6[8]	1,4
Gabon	4,5	4,5	21,0	12,2
Morocco	22,7	5,4	22,6[9]	5,4
Angola	13,6	...	13.6	...
Central African Republic	—	—	11,8	9,5
Congo Kinshasa	5,4	5,4	5,4	5,4
Japan	2,4	—	6,5	2,5
Greenland	4,5	...	24,0[10]	...
Mexico	1,5	...	5,0	1,2
Other	28,0[11]	3,1	116,0[12]	3,7
Total	3 675,6	582,3	5 208,0	1 010,6

[1]Including 127,000 tons U_3O_8 obtainable as by-product in phosphoric acid production.

[2]Same, 18,100 tons U_3O_8.

[3]In ores that can be profitably mined and processed at uranium concentrate market prices up to 66 dollars/kg U_3O_8. Includes 276, 600 tons U_3O_8 obtainable as by-product in phosphoric acid production and from tailings in copper smelting production (based on production figures extrapolated to the year 2000).

[4]Same, 81, 600 tons U_3O_8.

[5]With losses in mining and beneficiation (25 %) taken into account.

[6]With 35% extraction of uranium contained in schists.

[7]According to other estimates, upwards of 100,000 tons U_3O_8.

[8]Primarily as by-product in production of zirconium, titanium, and other elements.

[9]As by-product in phosphoric acid production.

[10]Inferred reserves estimated at 180,000-270,000 tons U_3O_8.

[11]West Germany, Italy, Turkey.

[12]Turkey, Brazil, West Germany Malagasy Republic, No information available on extent of uranium reserves in SW Africa, Mozambique, Egypt, Tunisia, Pakistan, and several other countries.

50,800 tons U_3O_8 taken into account). As of December 31, 1970, uranium reserves in the USA at occurrences considered profitable for exploitation at the then current market price of uranium concentrate of 17.6 dollars/kg U_3O_8 (which assumes not less than 0.15-0.17% U_3O_8 content in the ore) was estimated at 223,300 tons U_3O_8 [3]. It was pointed out, in this estimate, that much of the information coming into the USAEC on uranium reserves during 1970 from private firms had not yet been processed.

Possible additional inferred reserves at occurrences profitable for exploitation at a price not higher than 17.6 dollars/kg U_3O_8 were estimated as of the end of 1970 at 344,500 tons U_3O_8, in other words 90,700 tons of U_3O_8 more than at the end of 1969 [3].

The dynamics of probe and exploration drilling in the USA are illustrated by the following data, given in thousands of tons [7]:

TABLE 2. Uranium Ore Mining, in Millions of Tons

Country	Average U_3O_8 content in ore, %	1959	1967	1968	1969	1970
USA †	0,21 ‡	6,2	4,8	5,4	5,3	5,8
Canada*	0,12	12.7	2,8	2,8	3,1	3,1
Union of South Africa* *	0,034	22,3	9,5	12,3	12,6	13,0
France	0,23‡	0,6	0,7	0,6	0,6	0,6
Gabon	0,4	—	0,1	0,1	0,1	0,1
India	0,07	...	...	0,1	0,1	0,1
Australia	0,17	0,7	—	—	—	—
Total*	...	42,5	17,9	21,3	21,8	22,7

* Estimate.
† Shipments from mines.
‡ In 1970.
* * Processed at mills.

TABLE 3. Production of Uranium Concentrates, Tons U_3O_8 [2, 5-7, 37-39]

Country	1959	1965	1968	1969	1970
USA	14 870	8 967	11 159	11 058	11 600
Canada	14 420†	3 292	3 750	4 037	4 082
South Africa	5 850	2 674	3 513	3 602	3 737
France‡	860	1 265	1 377	1 493	1 493
Gabon	—	580	450	550	550
Australia	1 013	250*	175*	175	150
Spain	—	65	65	65	65
Portugal*	...	40	95	95	95
India*	...	...	40	70	90
Argentina	12	47	40	70	70
Sweden*	9	18	60	60	60
West Germany	3	20**	...	...	...
Malagasy Republic	105	121	33	—	—
Japan*	...	2	...	...	...
Congo Kinshasa	2 110	—	—	—	—
Total*	39 500	17 350	20 800	21 300	22 050

* Estimate.
† Shipment.
‡ Content of U_3O_8 in ore mined (1959 figures: concentrates).
* * Including concentrates made from imported ore.

	1966	1967	1968	1969	1970
Prospecting drilling	549	1658	4949	6243	5490
Exploration drilling	732	1625	2296	2862	1677

The volume of prospecting and exploration drilling carried on in the USA in 1970 dropped 21% below the 1969 level, but still stayed 2.9 times higher than the 1957 level. The average depth of the boreholes drilled was: 68 m in 1966, 110 m in 1967, 125 m in 1968, 119 m in 1969, and 122 m in 1970. Despite forecasts to the opposite effect, no further increase in the drilling depth took place in the last two years. The number of firms engaged in drilling dropped from 126 in 1969 to 116 in 1970. Twenty oil exploitation companies accounted for 48% of the total volume of drilling in 1970, as against 31% in 1969.

The bulk of the exploratory drilling done in 1970 was confined to three states: Wyoming (4.7%), Texas (25.9%), and New Mexico (22.1%). Colorado and Utah, which until recently occupied a prominent place in the USA uranium mining industry, have now dropped to a secondary position. The overall volume of drilling in those states was 3.7 times smaller in 1970 than in Texas, where five years ago almost no drilling at all had been done.

Average drilling costs were estimated at 4.92 dollars per meter headway (from 1.64 to 9.83 dollars/m headway, depending on drilling depth and local conditions). The average cost of logging operations at boreholes was determined at 43 cents/m headway. The cost of drilling operations in 1970 was figured at 35.6 million dollars, the cost of logging operations in 1970 was figured at 3.1 million dollars, as compared to respectively 45 million dollars and 3.9 million dollars in 1969. Specific costs were therefore estimated at 77 cents/kg U_3O_8 in 1970 and 96 cents/kg U_3O_8 in 1969 (this includes the cost of logging operations) [8]. Specific costs are much lower at the large occurrences. For example, specific costs at one of the occurrences in the Grants district (state of New Mexico) with reserves of 18,200 tons U_3O_8 with an average U_3O_8 content of 0.46%, amounted to no more than 16 cents/kg U_3O_8 [9].

The specific increase in commercial uranium reserves in the USA in 1970 amounted to ~7.0 kg U_3O_8/m drilled, compared to the 1969 figure of 5.6 kg U_3O_8/m drilled and the 11.2 kg U_3O_8/m drilled for the 1948-1966 period.

The average uranium oxide content in the ores of profitable grades is 0.17%. Nine of the largest occurrences account for well over 40% of the reserves. Of the reserves 82% lie at depths less than 240 m down. Of the reserves 49% lie at depths to 105 m, and 56% of the ores can be won by strip mining. The Grants district accounts for 41%.

In the coming years a fall-off in the level of prospecting and geological exploration work is anticipated in the USA. According to the latest information available from 52 private concerns and reported by USAEC, a volume of 23,770,000 m of drilling work is scheduled throughout the country for the next four years (1970-1973). According to a questionnaire circulated the previous year, plans call for drilling a total of 33,406,000 m over the 1969-1972 period. Expenditures of 120 million dollars, or five dollars/m headway, were set aside for the purpose for 1970-1973. The volume of prospecting drilling amounts to 15,250,000 m (64%), and the volume of exploration drilling amounts to 8,520,000 m (36%) [10]. USAEC expressed confidence that

TABLE 4. Production Costs of Uranium Concentrates at Grants New Mexico Plant* [42]

Year	Ore processed, 10^3 tons	Average U_3O_8 content, %	Extraction to concentrate, %	Production of concentration, tons U_3O_8	Production cost†		Price, dollars /kg U_3O_8
					dollars/ton	dollars per kg U_3O_8 in concentrate	
1964/65	955,7	0,213	95,0	1933	24,70	12,210	17,600
1965/66	963,4	0,207	94,4	1886	23,90	12,210	17,600
1966/67	1028,4	0,210	94,7	2042	23,81	11,990	17,028
1967/68	1225,1	0,200	94,3	2318	23,56	12,452	16,676
1968/69	1163,3	0,187	93,1	2027	22,58	12,958	15,664

* Plant built in 1958, capacity 3084 tons ore per day, ore mined by open-cast method (90 to 260 m).

† Including amortization writeoffs (dollars per kg U_3O_8): 2.53 for 1964/65 2.508 for 1965/66, 1.76 for 1966/67, 1.936 for 1967/68, 1.848 for 1968/69.

payable (commercial) uranium reserves in the country will see a fast swing upward in the coming years.

Actual reserves of payable-grade uranium ores in Canada increased by 16% in the past three years. Possible additional reserves are estimated at 208,700 tons U_3O_8. Actual (reliably inferred) reserves falling in the category from 22 to 33 dollars/kg U_3O_8 are estimated at 117,900 tons U_3O_8, and possible additional reserves are now estimated at 154,200 tons [2]. A mid-1970 report provided information on discovery of an occurrence in Northern Ontario province (~25 km east of the familiar Quirke district, in the Elliott Lake uranium province) with inferred reserves of 270,000 to 320,000 tons U_3O_8 [11]. Later on, however, no information appeared to confirm this report, or shed any further light on the subject. On the whole, the level of prospecting and exploration work going on in Canada in 1970 was markedly below the level attained in previous years.

Estimates of payable uranium reserves in the Union of South Africa showed no essential changes in recent years. The underlying premise, however, is that the current price for gold (34 dollars an ounce) will remain unchanged. Should this price rise appreciably, as stipulated by many specialists as a necessary prerequisite for liquidating the crisis in the capitalist currency and credit system, uranium reserves in that country (the uranium is won, as a rule, as a by-product in gold mining and refining operations) will have to be revised upwards. Calculations were reported for reserves present at an occurrence 48 km southwest of Johannesburg: 17 million tons of ore with an average U_3O_8 content of 0.06%, which means mining and working of this ore would be profitable at concentrate prices of ~20 dollars/kg U_3O_8, i.e., at a level far higher than the current price on the world market [12].

Sensational discoveries in Australia have been attracting attention. Prospecting for uranium in that country has been steadily expanded in recent years, and results have been quite fruitful. The increment in commercially payable uranium reserves in the country in 1968 amounted to 4000 tons U_3O_8, topped by the 1969 figure of 10,000 tons, while tentative data for 1970 place the amount at as high as 100,000 tons [2, 4, 7, 13].

Reserves at the Nabarlek occurrence 270 km east of the town of Darwin (in the Northern Territory), and 280 km from the famous Rum Jungle deposit, are estimated at 8000 tons U_3O_8, with an average content of ~2.0% U_3O_8 in the ore. It is assumed that five of the 483 deposits discovered are deserving of further scrutiny. Eight million dollars have been earmarked for a detailed investigation of the occurrence in the 1971-1974 period [13]. The ore lies at a shallow depth, which opens up prospects for low-cost strip mining in the cost range not higher than 2.2 dollars/kg U_3O_8 [14].

Reserves at the Ranger occurrence loacted 50 km from Nabarlek are estimated at 71,000 tons U_3O_8, just considering high-grade ores of high uranium content (averaging 0.32% U_3O_8). The ore lies at depths from 11 to 125 m, which leaves it accessible to open-cast mining[4, 15]. Actual and probable reserves at the Jim-Jim occurrence located 24 km south of Ranger and 100 km west of Nabarlek are estimated at 25,000 tons U_3O_8 with an average U_3O_8 content of 0.45% in that ore. The uranium content in assayed samples from the six boreholes sunk run from 1.04 to 6.35% U_3O_8. This ore lies at depths of 35-50 m [16-18].

Geological reserves at the occurrences mentioned in the province of Northern Territory are estimated at 300,000 tons U_3O_8 [4].

It is assumed that the occurrence discovered in the vicinity of Radium Hill (in South Australia) is highly promising. The uranium content in assayed samples runs from 0.23 to 0.91% U_3O_8 [19]. Reserves at the Mt. Painter occurrence (in South Australia) have increased from 1.0 million to 2.5 million tons of ore with 0.09% average U_3O_8 content [20].

Proven reserves at the Westmoreland occurrence 35 km from the Gulf of Carpentaria and 370 km northwest of Mt. Aisa (in Queensland), in the Red Tree mineralization zone, increased to 9300 tons U_3O_8, while the reserves at Valhalla increased to 1700 tons U_3O_8, with an average U_3O_8 content of 0.14% in this ore; a possible discovery of another 10,000 tons U_3O_8 at Long Rocket (20 km from Red Tree) is reported [21, 22].

Possibilities of a further appreciable increase in Australia's uranium reserves are being regarded as highly promising.

In France, following a revision of the existing data, uranium reserves were revised downward 1200 tons in 1969 (with an increase of 300 tons U_3O_8 with mining taken into account) below the 1968 increase of 6500 tons (increased again by 7600 tons U_3O_8 with mining taken into account) [6]. Actual and possible uranium reserves in the country (considered payable up to 22.0 dollars/kg U_3O_8) at the end of 1969 were estimated by the French Atomic Energy Commissariat at 63,000 tons U_3O_8. Their distribution over individual occurrences was as follows (data in thousands of tons U_3O_8): La Crouzille 18.9, Herault 12.8 Forez-Morvan 8.1, Vendee 8.7, plus 14.1 for reserves at occurrences in the Massif Central belonging to private concerns, and 0.8 in Brittany [6, 23].

Actual reserves in Gabon (at rates to 22.0 dollars/kg U_3O_8) amounted to 16,500 tons U_3O_8 in mid-1970, compared to 5000 tons back in 1961, although over 5000 tons U_3O_8 had been mined in the intervening period. Possible additional reserves of payable grades were estimated at 5900 tons U_3O_8 [23]. The same reserves in Niger were estimated at 35,200 tons U_3O_8 as of mid-1970, and in the Central African Republic at 9400 tons. Consequently, France controlled actual and possible additional reserves of uranium (figured at 22.0 dollars/kg U_3O_8 as payable) in amounts running as high as 165,000 tons U_3O_8 [23]. French geologists terminated uranium prospecting efforts in Haute-Volta and in Cameroun [24].

Prospecting and geological exploration work in African countries are also being undertaken by West German firms: since 1970 (in collaboration with Portugal) in Angola and in Mozambique, since 1969 in Somalia (on 10,000 km^2 of territory in the Bur-Aqaba region), since 1968 in Ghana, since 1969 in Southwest Africa, and since 1970 in the Malagasy Republic; prospecting possibilities in Togo were also studied [25].

Italian prospecting firms have been contracted for prospecting operations in Somalia (at sites 210 km west of Mogadishu), in Kenya, and in the Congo Democratic Republic (capital Kinshasa). In 1970, Italy obtained a concession for prospecting for uranium, thorium, and rare earths in Zambia (in the northwest corner of the country, over 63,350 km^2 of territory) [26, 27].

Japan and France signed an agreement, in 1970, on joint financing of prospecting and geological exploration operations in Niger, specifically in the Akokan district. The cost of these operations is estimated at 4 to 6 million dollars [28].

The presence of a very large uranium occurrence in Southwest Africa has been confirmed. Despite the low grade of the uranium ore (below 0.1% U_3O_8), a decision has been announced to begin preparations for strip mining. It is projected that a minimum of 1000 tons U_3O_8 can be produced annually in the form of concentrate from this occurrence [29, 30].

The Argentina AEC reported the discovery of what are purported to be the country's largest uranium occurrences to date, at Sierra Pintada (950 km west of Buenos Aires). Three thousand boreholes were sunk in two years of explorations. Reserves are calculated at 10,000 tons of U_3O_8 with average U_3O_8 content of 0.1%. Beginning with 1973, it will be at this occurrence that Argentina will be mining the bulk of its uranium [31].

Proven uranium ore reserves in Mexico totalled 4.6 million tons with a content of 3157 tons U_3O_8 [32]. Problems in bringing occurrences located in the states of Chihuahua, Nuevo Leon, Durango, and Sonora into the market are being examined.

Proven uranium reserves in the state of Bihar (India) have been estimated at 65,400 tons at the end of 1970, and of these 16,300 tons are in ores with U_3O_8 contents of 0.05% and higher [33].

An agreement has been reached on exploration of uranium occurrences at Buller Gorge (New Zealand) [34].

Uranium prospecting activities have been resumed in Italy, particularly in the Alpine regions (1100 m of drilling per year) [35].

Uranium prospecting operations in the Tirschenrut area (Oberpfalz), where 300 to 500 tons U_3O_8 have been discovered to date, are now in progress in West Germany; prospecting operations are also underway at Weisenstadt (in the Fichtelgebirge range) with 50 to 60 tons estimated, and at Stockheim (Oberfranken) with several hundred tons estimated [25].

An 18-month study and survey of uranium occurrences in central and eastern districts of Greek Macedonia has been scheduled. UNO development funds have made available 331,000 dollars for these efforts, making a total funding of 557,000 dollars for this purpose [36].

Prospecting in Austria was concentrated, in 1970, in the northern areas of Lower Austria, in the southern districts of Carinthia, and in the western districts of the Tyrol [27].

The study of methods of obtaining uranium from sea water has been continuing (Great Britain, Japan).

Uranium Ore Mining in 1970. This was based on tentative data available, rose 4% over the 1969 level and 55% over the 1965 level. But it remained 47% below the 1959 level, which was the peak level on record (see Table 2). Most of the ore was mined in four countries. Uranium ore mining was begun in late 1970 in Niger (the first capacity rating for the quarry at Arly was 350,000 tons a year).

The average U_3O_8 content in ore mined in the USA fell from 0.25% in the early Sixties to 0.21% in 1970 (a 16% drop), but rose in France from 0.16% in 1965 to 0.23% in 1970 (a 44% rise), and remained practically the same in most other countries.

There were 239 mines in operation in the USA in 1969, as compared to 800 mines operative in 1963. Two thirds of all the ore is accounted for by 18 of these mines. Strip mining accounts for 41% of the ore, i.e., much more than in previous years. The states featuring most intensive mining are New Mexico (46%), Wyoming (23%), and Colorado (10%). The importance of Wyoming and Texas has been increasing in recent years. Uranium ore mining capacities seem to be increasing, in the last three years, by a rate of 6500 tons of ore per day (2.5 million tons a year), or by more than 1/3 [2, 7].

Three mines were operative in Canada in late 1970, as compared to 25 in 1959, and only one mine was operating at full capacity, while a second was being worked at 67% capacity, a third at 50% capacity. It was assumed earlier that a considerable increase in the productivity of the existing uranium mines in that country was to be anticipated in the next five years, both by reopening and reactivating old mines and by building new ones. However, under conditions of supply exceeding demand, sharpened market competition, and lower prices, and a generally poorer competitive position vis-a-vis South African, French, and to an extent American firms, many Canadian firms tended to bow out in the competition (predominantly because of the lower grade of the ores), and were forced to postpone their plans for expanded mining operations.

Eleven mines were in operation in the Union of South Africa in 1970, as against 27 in the 1959-1960 period, and two mines went into operation, one with a capacity of 690,000 tons of ore per year, the other with a yearly capacity of 435,000 tons of ore. Four mines with a total capacity of 5.6 million tons of ore annually are being built. In addition, the capacity of one mine will be increased in 1973 by 0.3 million tons of ore per year, another by 1.2 million tons of ore per year. The total productivity of the South African mines in the period up to 1975 will increase by more than 7.9 million tons of ore, or by 50% over the productivity of the mines operative in 1969 [2, 6, 7].

New mines were constructed in Spain, Argentina, and Mexico. A decision was reached to build the world's largest uranium quarry at Rossing in Southwest Africa, with a capacity as high as 5 million tons of ore per year [16]. Plans call for building large uranium quarries in the province of Northern Territory in Australia. The possibilities of building uranium mining enterprises in other countries are being given active study.

Consequently, the total capacity of the uranium mines and uranium quarries in the industrially developed capitalist countries and in the developing nations may increase by 15 to 18 million tons of ore per year over the coming five years.

Production of Uranium Concentrates. Production of uranium concentrates in the countries referred to increased by 750 tons U_3O_8 (4%) in 1970 over the 1969 level, and by 4700 tons U_3O_8 (or 27% over the 1965 level) (see Table 3).

A program of deliveries of uranium ore concentrates to the government was completed in the USA. Over the course of 29 years, a total of ~295,000 tons U_3O_8 has been purchased, at a total cost of about six billion dollars; 46% of these were imported shipments, mostly from Canada and from the Union of South Africa. No subsequent purchases to replenish government stores are proposed for the coming years. Moreover, an announcement has been made on realization of over 45,000 tons U_3O_8 from those supplies for the industrial-scale nuclear power stations. It is expected that this will hold back the expansion of production of atomic raw material expected in the mid-Seventies.

A uranium concentrates production plant went on stream at Rey Ponte (Texas) in the USA in 1970, with a capacity of 907 tons of ore per day (~500 tons U_3O_8), the plant at Shirley Basin (Wyoming) had its production capacity expanded by 454 tons of ore per day (300 tons U_3O_8 per year), and a plant at Ford (Washington) with a capacity of 454 tons of ore per day (350 tons U_3O_8 per year) was put back on stream. At the same time, a plant at Grant Junction (Colorado) was closed down, and later dismantled. Construction of four plants is in progress (two in the state of Wyoming, one in Texas, the fourth in the state of Utah), and these are scheduled to go on stream in 1971-1973. Construction of two more plants has been put off for the time being. The total capacity of existing uranium ore beneficiation plants in the United States of America has increased from 13,600 tons U_3O_8 in 1969 to 17,200 tons U_3O_8 in 1972, and will far surpass all real needs for uranium concentrates in that country [2, 5-7].

Uranium concentrates production costs in the USA are estimated currently in the range from 6.6 to 13.2 dollars/kg U_3O_8, depending on the scale of mining operations, ore quality, the depth at which ore veins are located, amortization conditions, and so forth. At the present time, the vice-president of one leading uranium ore firm estimates typical uranium concentrates production costs in the United States of America (for ore mined by open-cast methods) in 1968 at 13.2 dollars/kg U_3O_8, including (in dollars/kg U_3O_8): prospecting and exploration costs of 1.76, ground rental costs of 0.88, mining costs of 6.60* (in this item, amortization accounts for 24%, wage payroll for 46%, materials, power, taxes, miscellaneous for 31%); ore shipment to the concentrates production mill, production of concentrates per se, and costs for shipping and marketing concentrates add up to 3.96 dollars/kg U_3O_8. This puts the total production costs (including ore shipping costs) at ~10.7 dollars/kg U_3O_8. These costs were estimated somewhat earlier at ~13.0 dollars /kg U_3O_8, including (in dollars/kg U_3O_8): mining costs of 6.05, costs for shipping ore to the concentrates production mill 1.10, ore comminution costs of 0.88, ore grading and storage costs of 0.88, leaching costs of 1.54, ore separation and extraction of 1.76, concentration costs of 0.55, drying and packaging costs of 0.33, costs for disposal of wastes and gangue 0.11, i.e., totalling 20% higher [40, 41].

Data on the actual production costs at one of the largest uranium concentrates processing mills in the USA are listed in Table 4 (administrative and management costs, federal and local taxes, are left out of account in these tabulated data).

Production costs for uranium concentrates at Falls City (Texas) relating to the group of medium-capacity plants (907 tons of ore per day) amounted to 9.812 dollars/kg U_3O_8 in 1964, as a result of processing of 98,200 tons of ore (average U_3O_8 content 0.168%) and extraction of 160 tons of U_3O_8, and in the first quarter of 1968 6.358 dollars/kg U_3O_8 as a result of processing 72,000 tons of ore (average U_3O_8 content 0.175%) and extraction of 119 tons of U_3O_8, including amortization writeoffs that amount to 0.286 dollar, administrative and management costs and deductions of 0.594 dollar for prospecting and exploration work at an average price of 13.728 dollars/kg U_3O_8 for 1568 tons of concentrate delivered in the 1968-1970 period [43].

According to data presented by specialists employed by one oil company, characteristic production costs at existing plants in the USA run at 12 dollars/kg U_3O_8. As a rule, however, these data do not include the costs recorded in past years in connection with prospecting, exploration, and putting occurrences into productive operation, ground rents, and also amortization writeoffs. The characteristic production costs for uranium concentrates at new plants with capacities of 500 tons U_3O_8 annually, which may be constructed

* Fluctuations are quite considerable within the scope of individual mills: from 1.1 to 13.2 dollars/kg U_3O_8 even in the case of ore from the same uranium deposit.

in the early Seventies, are calculated at an average of 18.04 dollars/kg U_3O_8 for the operating conditions likely to prevail for the decade, and include (in dollars/kg U_3O_8): prospecting and exploration costs of 1.43, costs associated with making up basic capital investment costs, preparatory and initiating operations 3.74, direct operating costs (including depreciation) 10.12, ground rent 2.20, costs associated with stoppage of production 0.55. The point of departure in these calculations was provided by the following assumptions: capital costs 10% of annual, duration of prospecting and exploration work three years, bringing occurrence into production, construction of mines and plant (including preoperational period) three years; one year counted as total production stoppage time. The possible 50% increase in costs is accounted for by an appreciable rise in the cost of land, in costs for prospecting and exploring occurrences, in investment capital coming at steeper costs, etc. [44-46]. Concentrates production costs at least one of the new plants to be built in the USA were figured at ~10.0 dollars/kg U_3O_8 [47, 48].

In 1970 plans called for placing an experimental pilot U_3O_8 extraction facility into operation at a copper smelting plant at Bingham Canyon (Utah) in the USA, with the object of thereby making a feasibility determination for prospects of producing uranium as by-product from copper refining tailings. The present predicted production costs are quite optimistic: 6.6 to 8.8 dollars/kg U_3O_8 in concentrate form [49].

The Candian Government has come forth with a regular support program for the development of the uranium industry. As a supplement to the ~9000 tons U_3O_8 already purchased, the government has accepted the obligation of acquiring another 2940 tons of U_3O_8 over the 1971-1974 period at a price level of 13.2 Canadian dollars/kg U_3O_8 [16].

Production costs of uranium concentrates at Candian mills, with costs already transferred to the earlier products, fluctuated between 8.1 and 15.6 dollars/kg U_3O_8, averaging out at 11.8 dollars/kg U_3O_8. Production costs for uranium concentrates in 1968 amounted to 8.36 dollars/kg U_3O_8 for the Rio Aglom Mines Company, and 8.91 dollars/kg U_3O_8 for Denison Ltd. It is assumed that these costs increased by 0.66 dollars/kg U_3O_8 over the 1969-1971 period. All of the existing plants reported profits at the going price of 11 to 15 dollars/kg U_3O_8 [50-54].

Construction work on two uranium concentrates mills with a total capacity of 327 tons U_3O_8 annually was completed in 1970, in the Union of South Africa. Two more mills, with a total capacity of 818 tons U_3O_8 annually, are scheduled to go into production in 1971. Taking into cognizance the planned expansion of some of the existing plants, and the construction of new plants, the total capacity of this country's uranium industry is expected to increase, by the mid-Seventies, to a level of 8000 tons U_3O_8 per year, or double the level attained at the end of 1969 [2, 5-7].

Since costs for mining auriferous –uraniferous ores are included in the main production costs, while the cost of the uranium concentrates mills are completely subsumed in the prices of the concentrates set by intergovernmental agreements, production costs at existing South African plants amounted to 7-8 dollars /kg U_3O_8 in the early Sixties, dropping to as low as 4.5-5.0 dollars/kg U_3O_8 at the present time [56, 57].

Concentrates production costs at the new South African mills are estimated at 8.8 to 16.5 dollars/kg U_3O_8, if the occurrence is being worked primarily for gold production, and at 12.1 to 18.7 dollars/kg U_3O_8, if uranium is regarded as the primary product of the operations [50].

A uranium concentrates production mill with a capacity of 750 to 875 tons U_3O_8 per year was put on stream at Arly (in Niger), in January, 1971. Concentrates containing 79% U_3O_8 are being produced there. It is expected that plant capacity will be doubled in 1974 [2, 58].

According to data reported by French economists, capital investments in an enterprise with a capacity of 1800 tons U_3O_8 in concentrate on a yearly basis (i.e., a plant such as the one built at Arly), handling uranium ore obtained by strip mining, should amount to ~36 million dollars, which includes direct costs of building the open-cast quarry and preliminary costs before starting operations totalling 25%, capitalization of the concentrates production mill 42%, construction of highways and living quarters for workers, etc., 33%. Direct operating costs are figured at 11 dollars/kg U_3O_8, including: mining costs 24%, beneficiation costs 61%, general costs 10%, concentrates shipping costs 3%, miscellaneous expenses 2% [35].

Plans call for resuming operations at the large Mary Kathleen plant in Australia (Queensland) starting in 1972 [59]. It is expected that concentrates from the Nabarlek occurrence will begin arriving at Mary Kathleen starting in 1973 or 1974, and shipments from the Ranger occurrence will begin arriving starting in 1976 [15, 60]. By the late Seventies, production at the first of these occurrences will have attained the level

of 7500 tons U_3O_8, at the second 3500 tons U_3O_8, and in Australia as a whole: 15,000 tons U_3O_8 per year [4, 60, 61].

The planned plant capacity for the Rossing uranium concentrates mill (in Southwest Africa) amounts to 5000 tons U_3O_8. Construction is expected to be completed in the mid-Seventies [16].

Work has started on an experimental facility with a capacity of 50 tons of ore per day at Ningyo-Toge (Japan). It is anticipated that as much as 130 tons U_3O_8 in concentrates form will be produced there in 1974 [62].

An experimental production facility with a daily capacity of 4.5 tons of ore has been put on stream at Lahore (Pakistan); ores from the Dera-Gazi deposit that has been worked for the past few years are being processed there [63].

Sweden is making efforts to lower production costs of uranium concentrates from its own low-grade ores, from the present level of 29-33 dollars/kg U_3O_8 to a level of 20-22 dollars/kg U_3O_8. But the actual possibilities of getting the uranium occurrences in that country into profitable working are very slim [64].

A plant for production of uranium concentrates, with an annual capacity of 300 tons U_3O_8, is being built at Ciudad Rodrigo in Spain (province of Salamanca). Production of atomic raw materials is scheduled to be increased to a level of 500 tons U_3O_8 per year, which should fully meet the country's own requirements.

In 1970, the plant at Jaduguda (India) was brought up to its design capacity of 1000 tons of ore per day, which makes it possible to produce ~100 tons of U_3O_8 per year [33].

Uranium concentrates production capacities are expected to be expanded by 1973 in the following countries (with figures given in tons of U_3O_8): in Portugal up to 270, in Mexico 180, in Italy 110, and in Argentina 80 [2].

While developmental plans for the uranium industry in the advanced capitalist countries and in the developing nations will be carried out primarily within the stipulated periods, in the mid-Seventies the capacity of existing uranium concentrates mills in those countries will have attained the level of 50 to 55 thousand tons of U_3O_8.

In connection with the glut of uranium concentrates on the market, prices for uranium concentrates in the USA were at the level of 13.0 to 13.5 dollars/kg U_3O_8 under immediate-delivery conditions, and 14 to 14.5 dollars/kg U_3O_8 where conditions specify delivery in the mid-Seventies, with clauses dealing with a price increment depending on changes in labor costs and materials costs during that time period. At the beginning of 1971, this price has declined to 12.5 to 13.0 dollars/kg U_3O_8 in the USA, and to 11.5 to 12.0 dollars/kg U_3O_8 in Western Europe [65]. Some experts feel that the development of the occurrences in Australia will make it possible to hold prices at the 15-16 dollars/kg U_3O_8 level during the second half of the Seventies, even if there should be an appreciable rise in demand. Levels of 22 dollars/kg U_3O_8 are expected to appear only in the Eighties [66].

LITERATURE CITED

1. Nucl. Engng. Intern., 15, No. 173, 933 (1970).
2. Uranium: Resources, Production and Demand, Paris–Vienna, ENEA-IAEA (1970), p. 34.
3. Nucl. Industry, 18, No. 5, 37 (1971).
4. Nucleonics Week, 11, No. 36, 1 (1970); No. 44, 4 (1970); 12, No. 1, 2, 3 (1971); North Miner, 56, No. 24, 1 (1970).
5. V. D. Andreev, At. Energ., 29, 313 (1970).
6. Rapport Annuel 1969, Paris, AEC (1970), pp. 91-93.
7. J. Sherman, Engng. and Mining J., 172, No. 3, 108-111 (1971).
8. USAEC. "The nuclear industry – 1970," Washington (1970), pp. 37-46.
9. Nucleonics Week, 12, No. 10, 1 (1971).
10. Appl. Atomics, No. 765, 5 (1970).
11. Nucleonics Week, 11, No. 24, 6 (1970).
12. Ibid., 12, No. 19, 8 (1971).
13. Financial Times (August 14, 1971), p. 10.
14. Nucl. Industry, 17, No. 9, 33 (1970).
15. Ibid., 17, No. 11/12, 89 (1970).

16. Ibid., 18, No. 1, 48-50 (1971).
17. North. Miner, 57, No. 12, 1 (1971).
18. Mining J., 276, No. 7086, 477 (1971).
19. Nucl. Engng. Intern., 16, No. 178, 303 (1971).
20. Nucleonics Week, 11, No. 26, 7 (1970).
21. North. Miner, 56, No. 24, 1 (1970).
22. Nucl. Engng. Intern., 16, No. 181, 449 (1971).
23. Appl. Atomics, No. 778, 6 (1970).
24. Ibid., No. 773, 5 (1970).
25. Atomwirtschaft, 15, No. 4, 154 (1970).
26. Nucleonics Week, 11, No. 26, 7 (1970).
27. Atomwirtschaft, 15, No. 9/10, 413 (1970).
28. GEA Bulletin (June, 1970), p. 1.
29. Rio Tinto Zinc Corp., Press release dated May 19, 1971.
30. Financial Mail (May 21, 1971), p. 657.
31. Nucleonics Week, 11, No. 32, 8 ((1970).
32. Appl. Atomics, No. 779, 2 (1970).
33. Government of India, Department of Atomic Energy, Press release dated December 10, 1970.
34. Nucl. Engng. Intern., 16, No. 178, 305 (1971).
35. Brennstoffe–Warme–Kraft, 23, No. 1, 13 (1971).
36. Financial Times Commodity New Report (May 25, 1971).
37. Bureau of Mines, Commodity Data Summaries, Washington (1971).
38. Nucleonics Week, 11, No. 27, 8 (1970).
39. Appl. Atomics, No. 783, 4 (1970).
40. R. Stochr, Conference on Nuclear Fuel, Oklahoma City (1969), p. 128.
41. Electr. World, 167, 93 (1970).
42. Atomic Energy Clearing House, 15, No. 33, 6 (1969).
43. Nucl. Industry, 15, No. 9, 24-25 (1968); Engng. and Mining J., 169, No. 12, 104 (1969).
44. Nucleonics Week (December 2, 1969), p. 2.
45. Engng. and Mining J., 170, No. 3, 168 (1969).
46. World Business (July, 1969), p. 12.
47. Nucleonics Week (December 25, 1969), p. 5.
48. Nucl. Industry, 17, No. 1, 18 (1970).
49. Ibid., 17, No. 5, 54 (1970).
50. The Outlook for Nuclear Energy and the Uranium Industry, New York (1968), pp. 63-65, 132.
51. Mining J., 274, 89 (1970).
52. Appl. Atomics, No. 743, 5 (1969).
53. North. Miner, 55, 6 (1969).
54. Nucleonics Week (April 17, 1969), p. 6.
55. The Australian Mineral Industry – 1964. Review. Canberra (1965), p. 289.
56. Appl. Atomics, No. 608, 10 (1967).
57. Mining Annual Review – 1968, London (1969), p. 273.
58. Atomwirtschaft, 16, No. 5, 216 (1971).
59. Nucleonics Week, 12, No. 8, 6 (1971).
60. Nucl. Engng. Intern., 16, No. 181, 449 (1971).
61. Ibid., 16, No. 180, 369 (1971).
62. Atoms in Japan, 13, No. 7, 17 (1969).
63. Nucl. Engng. Intern., 16, No. 180, 372 (1971).
64. Engineering (January 8, 1971), p. 688.
65. Atomwirtschaft, 16, No. 15, 2 (1971).
66. Nucleonics Week, 12, No. 15, 2 (1971).

ABSTRACTS

DISTRIBUTION OF ACTIVATION PRODUCTS IN THE COOLANT LOOP OF A BOILING-WATER REACTOR

A. Ya. Kramerov and Yu. V. Chechetkin

UDC 621.039.524.4:621.039.543

We discuss a procedure for calculating the distribution of activation products in the coolant loop of a boiling-water reactor such as the AÉS VK-50. The coolant flow is complicated by the presence of two phases having different physical constants. The equations describing the behavior of two-phase flow include boundary conditions for the interaction of one phase with the other and with solid walls, mechanical equations, and the equations of conservation of energy and mass in each phase. In addition it is necessary to take account of the redistribution of coolant activation products between steam and water as functions of many factors such as the degree of radiolysis, the pH and temperature of the system and surfaces of contacting media, the time of contact, the neutron distribution over the height of the reactor, etc. The system of equations which takes account of all these factors is so complicated as to be useless for practical calculations. A more promising approach is to use a system of equations describing two-phase flow as the flow of a homogeneous medium with effective local properties obtained by appropriate averaging. The simplicity and convenience of the calculation in this case depends on the form of the neutron distribution over the core height Φ_2.

In general the increase in activity ΔA in the core is given by

$$\Delta A = \frac{\lambda N}{3.7 \cdot 10^{10} M} \int_0^h \sigma_{act} \Phi_z \gamma_z S_z e^{-\lambda \tau_z} dz, \quad (1)$$

where λ is the decay constant of the isotope under consideration; N is Avogadro's number; M is the molecular weight of the coolant; σ_{act} is the activation cross section normalized to the fission spectrum flux; h is the core height; γ_2 is the density of the steam–water mixture at section z; S_z is the cross-sectional area of a fuel assembly at section z; and τ_z is the time for the steam–water mixture to flow from the core inlet to section z.

The activation of the coolant can be calculated by using the average value $\Phi_z = \Phi_{av}$ as constant over the length of a fuel assembly. This ordinarily underestimates somewhat the average volume steam contant $\bar{\varphi}$, but leads to simple expressions for the weight steam content x in terms of the average volume steam content and for the rate of circulation in terms of x etc.

Equation (1) can then be written

$$\Delta A = \frac{N}{3.7 \cdot 10^{10} M} \Phi_{av} G (1 - e^{-\lambda \tau_c}); \quad (2)$$

$$\tau_c = \frac{h}{w_0} \left\{ \frac{\Delta i_u}{\Delta i} + \frac{r}{b \Delta i} \ln \left[1 + \frac{b \Delta i}{r} \left(1 - \frac{\Delta i_u}{\Delta i} \right) \right] \right\}, \quad (3)$$

where τ_c is the steam–water transit time through the core; w_0 is the coolant velocity; G is the flow rate of the steam–water mixture through the core; Δi is the increase in enthalpy in the core; r is the heat of vaporization; and b is a constant [1].

The simple expressions obtained for calculating the AÉS VK-50 coolant activity can also be used for other reactors of similar type. Satisfactory agreement is found between the experimental data and the calculations.

Translated from Atomnaya Énergiya, Vol. 31, No. 6, p. 619, December, 1971. Original article submitted March 11, 1971.

LITERATURE CITED

1. A. Ya. Kramerov and Ya. V. Shevelev, Nuclear Reactor Engineering Calculations [in Russian], Atomizdat, Moscow (1967).

THE ASYMPTOTIC NEUTRON SPECTRUM AND THE EFFECT OF "FICTITIOUS" ABSORPTION

V. P. Gorelov, E. V. Malinovskaya, and V. I. Yuferev

UDC 621.039.51.12

By assuming that the reaction cross sections are velocity-independent the operator form of the transport equation may be written as

$$\hat{L}[\varphi(x)]=\hat{S}[\varphi(x)]. \tag{1}$$

Here x is a point in phase space $\{\mathbf{r}, \Omega, u\}$, where $u = \ln E_0/E$ is the lethargy;

$$L[\ldots]=\Omega\nabla\ldots+\Sigma_{tr}(\mathbf{r})\ldots-\frac{\Sigma_{es}(\mathbf{r})}{4\pi}\int_0^u du'\int d\Omega' g_{es}(u'-u)\ldots-\frac{\Sigma_{in}(\mathbf{r})}{4\pi}f(u)\int_0^u du'\int d\Omega'\ldots;$$

$$\hat{S}[\ldots]=\frac{\nu_f\Sigma_f(\mathbf{r})}{4\pi}X(u)\int_0^\infty du'\int d\Omega'\ldots;$$

Σ_{tr}, Σ_{es}, Σ_{in}, and Σ_p are respectively the transport, elastic scattering, inelastic scattering, and fission cross sections; $g_{es}(u'-u) = ae^{-\beta(u-u')} + b\delta(u-u')$ is the synthetic elastic scattering kernel proposed in [1]; f(u) is the inelastic scattering spectrum; f(u)du = f(E)dE, where according to the evaporation model $f(E) = (E/T_1^2)e^{-E/T_1}$; $T_1 = 0.23$ MeV for mass number $A \sim 240$; X(u) is the fission spectrum; X(u)du = X(E)dE, where $X(E) = 2\sqrt{E}e^{-E/\theta}/\sqrt{\pi\theta^3/2}$; $\theta \approx 1.32$ MeV.

The solution of Eq. (1) must satisfy the usual continuity conditions at boundaries between media, and the condition for an inflow of neutrons across the outer surface: $\varphi(\mathbf{R}, \Omega, u) = 0$ for $\Omega, \mathbf{n} < 0$, where $\mathbf{R}$ is the radius vector to the outer surface and $\mathbf{n}$ is the normal to the outer surface at point $\mathbf{R}$.

Formally Eq. (1) can be regarded as an inhomogeneous equation with a source

$$\hat{L}[\varphi(x)]=\eta(x), \tag{2}$$

where

$$\eta(x)=\hat{S}[\varphi(x)].$$

The general solution of Eq. (2) can be written as the sum of the general solution of the homogeneous equation $\hat{L}[q(x)] = 0$ and a particular solution of the inhomogeneous equation $\hat{L}[H(u)\Psi(\mathbf{r}, \Omega)] = \hat{S}[H(u)\Psi(\mathbf{r}, \Omega)]$;

$$\varphi(\mathbf{r}, \Omega, u)=H(u)\Psi(\mathbf{r}, \Omega)+q(\mathbf{r}, \Omega, u). \tag{3}$$

The function $q(\mathbf{r}, \Omega, u)$ satisfies the condition $\int d\Omega \times \int_0^\infty duq(\mathbf{r}, \Omega, u) = 0$ and represents a correction to the asymptotic spectrum H(u).

If the system under consideration consists of layers the spatial-angular part of the asymptotic spectrum can be found as in [2]. Within a single layer the first approximation to the asymptotic neutron energy spectrum can be written in the form

Translated from Atomnaya Énergiya, Vol. 31, No. 6, p. 620, December, 1971. Original article submitted May 13, 1971.

$$H(E)=\frac{1}{\lambda}\left\{\nu_f\Sigma_f\frac{2}{\sqrt{\pi}\theta^{3/2}}\sqrt{E}\,e^{-E/\theta}+\frac{\nu_f\Sigma_f 2}{\lambda\sqrt{\pi}\theta^{3/2}}\left[b\sqrt{E}\,e^{-E/\theta}+0{,}1\,(0{,}1E)^{\beta-1}b^{-\left(\frac{3}{2}-\beta\right)}\right.\right.$$

$$\left.\left.\times\left\langle\gamma\left(\frac{3}{2}-\beta,\frac{E}{\theta}\right)-\gamma\left(\frac{3}{2}-\beta,\frac{10}{\theta}\right)\right\rangle\right]+\frac{\Sigma_{in}}{T_1^2}Ee^{-E/T_1}\left(\frac{10}{\theta}\right)^{-3/2}\left\langle\gamma\left(\frac{3}{2},\frac{E}{\theta}\right)-\gamma\left(\frac{3}{2},\frac{10}{\theta}\right)\right\rangle\right\}. \quad (4)$$

Here $\gamma(a, x)$ is the incomplete γ function; λ characterizes the effective number of secondary neutrons per mean free path and is equal to

$$\lambda=\nu_f\Sigma_f+\Sigma_{es}g(0)+m\Sigma_{in}, \quad (5)$$

where $m=\int_0^\infty f(u)du\int_0^u H(u')du'$.

The definition of λ in the form (5) explains the appearance of σ_x in the pseudo capture cross section which is introduced to describe the experimental quantity $(\lambda-\Sigma_{tr})$ for use in the one-group theory.

From (5) the fictitious absorption cross section Σ_x is defined as $\Sigma_x=(1-m)\Sigma_{in}$. This confirms the conclusion in [3] that Σ_x is related to the spectral effect of inelastic scattering.

Calculation of the one-group constants by using the spectrum H(E) shows that the definition of λ in the form (5) improves the agreement with experiment.

LITERATURE CITED

1. D. V. Shirkov, in: Reactor Physics and Heat Engineering [in Russian], Atomizdat, Moscow (1958), p. 62.
2. V. P. Gorelov and V. I. Yuferev, Zh. Vych. Matem. i Matem. Fiz., No. 1, 11 (1971).
3. L. Codd et al., in: Advances in Nuclear Engineering [Russian translation], Izd-vo Inostr. Lit., Moscow (1958), p. 289.

EFFECT OF NONISOTHERMICITY ON STABILITY OF FREE-FALLING WATER FILMS

G. P. Dubrovskii, A. Ya. Didenko, and L. S. Kokorev

UDC 621.039.51

At the present time, falling-film columns are gaining wide acceptance in the metallurgical and chemical process industries, and in the power industry (desalinating plants, cooling of control systems, and reactor shielding). The stability of a liquid film flowing down over the heating surface is both interesting and important in this context. Hydraulic resistances, heat transfer, and heat burnout are largely governed by the state of the liquid film on the heat-transfer surface, in disperse-annular flow of a two-phase stream, and by the conditions of heat and mass transfer between the falling film and the vapor core.

This article cites results of an experimental investigation of the range of stable existence of a film falling freely over the outer surface of an electrically heated cylindrical rod.

The experiments were conducted over a range of variation in process parameters: liquid flowrate at the inlet 0.8 to 30 g/sec, corresponding to the variation in "reflux density" from 10.2 to 382 kg/m·h heat loading to $2\cdot10^6$ W/m^2, length of heat-generating portion of effective section 40, 90, 140, 190, 240, 290, 340 mm.

Translated from Atomnaya Énergiya, Vol. 31, No. 6, p. 621, December, 1971. Original article submitted February 18, 1971.

The inlet temperature of the water in the operating channel was maintained constant in all the experiments, and close to the saturation temperature. The experiments showed that a local disruption of a liquid film falling freely over the heated surface at heat loadings less than those required for the onset of liquid boiling is possible. The resulting hot spots on the dried-out heat-generating surface can attain temperatures of hundreds of degrees, and thermal stresses severely deform the working area of the surface.

The effect of a disruption of the liquid film is aggravated when subcooling of the liquid is increased up to the saturation temperature.

The "burn-in" of the heated surface leads to increased film stability through improved wettability. In the case of a rapid transition to developed boiling, the liquid film becomes more stable, and local disruptions (dry spots) already formed in the film are "washed away."

The heat burnout incurring boiling of a free-falling film was also investigated. Under all the sets of conditions investigated, heat burnout took place at nonzero liquid flowrates in the film in the critical cross section.

The results of this work show that it is not only burnout heat loads that are dangerous in film cooling, but also loads close to the onset of liquid boiling, and this must be taken into account in the design of systems relevant to the problem.

THERMODYNAMIC PROPERTIES OF MOLTEN ALLOYS IN THE SYSTEM URANIUM – LEAD

V. A. Lebedev, A. M. Poyarkov,
I. F. Nichkov, and S. P. Raspopin

UDC 536.7+669.45'822

Measurements were taken of the emf of galvanic batteries of type U_{solid}/fused electrolyte + 5 wt.% UCl_3/U – Pb_{liquid}, over the temperature range from 660 to 870°C. The results of the measurements were reduced to a single standard state (γ-uranium). The emf between the uranium and saturated solutions of uranium in molten lead was independent of the uranium content in the alloys (5 to 15 wt.%) and independent of the electrolyte composition (KCl–NaCl or KCl–LiCl based melts), but varied with temperature according to the equation:

$$E = 0.403 - 0.251 \cdot 10^{-3} T \pm 0.002 \text{ V}.$$

Partial enthalpies and the entropy of γ-uranium in the compound UPb_3, an equilibrium composition with the saturated solutions, were constant over the range of temperature studied, and were respectively -27.9 ± 1.4 kcal/g·atom and -17.4 ± 1.4 esu/g·atom. For the partial free energy of uranium in that compound, the following equation would be valid:

$$\Delta\bar{G}_U = -27.900 + 17.4 \cdot 10^{-3} T \pm 0.3 \text{ kcal/g·atom}$$

Using the data so obtained, as well as the information on uranium solubility in lead [1], we can successfully arrive at the thermodynamic properties of uranium solutions in molten lead. The activity coefficient of the uranium in these solutions, with respect to γ-uranium, varies with the temperature according to the equation

$$\lg \gamma_U = 2.977 - \frac{2366}{T} \pm 0.08.$$

When the state of molten uranium is taken as the standard state, the equation for the activity coefficient of the uranium (k_U) acquires the form $\log k_U = 3.717 - 3396/T \pm 0.08$.

Translated from Atomnaya Énergiya, Vol. 31, No. 6, pp. 621-622, December, 1971. Original article submitted December 14, 1970.

The dissolution of molten uranium in lead is accompanied by the release of a significant amount of heat (15.5 kcal/g · atom) and by a decline of 17.0 esu/g · atom in excess entropy, attesting to the formation of stable, ordered groupings of atoms of the solute with the solvent atoms in the metallic melt. Negative deviations from Raoult's law are typical of the low-temperature activity of uranium in solution, while positive deviations from Raoult's law are typical at high temperatures. The activity of molten uranium in uranium solid solutions with lead is close to the atomic fraction, at temperatures in the order of 900°K.

LITERATURE CITED

1. R. Teitel, J. Inst. Metals, 85, 409 (1957).

ALBEDO OF γ-PHOTONS ON GRAPHITE CYLINDERS

N. V. Krasnoshchekov, A. N. Kuz'menko, and D. B. Pozdneev

UDC 621.039.51.17

Monte Carlo calculations were made of the spectral–angular and integrated characteristics of γ-photons emitted by He^{203}, Cs^{137}, and Co^{60} and backscattered by cylindrical graphite reflectors. Geometries of a mononormal source and an isotropic source of primary radiation placed at the center of the base of the cylinder are examined. The calculations are carried out for the case of cylindrical reflectors of radius r and height d equal to 0.1, 0.2, 0.6, 1.0, and 2.5 free-path lengths of the primary γ-photons.

The effect of changes in radius on the albedo is most substantial in the case of large-thickness reflectors ($\geqslant$0.6 mean free-path lengths). This is manifested in the energy spectra and in the angular distributions of the backscattered photons. Systematic data are presented on the differential numerical current albedo $A(\theta)$ and energy albedo $A_E(\theta)$ as functions of the variables r and d and of the energy of the primary γ-photons.

The dependence of the integrated current numerical albedo and energy albedo on r and d are described, with accuracy to within ±10%, by the empirical formulas:

$$A(r, d) = A(r, \infty)(1 - e^{-\alpha d}); \quad (1a)$$

$$A_E(r, d) = A_E(r, \infty)(1 - e^{-\alpha_E d}), \quad (1b)$$

where A(r, d) and A_E(r, d) are the integrated numerical and current albedo from a scatterer of radius r and thickness d; A(r, ∞) and A_E(r, ∞) are the same, but in the case of a scatterer of infinite thickness, so that, in turn,

$$A(r, \infty) = a + b(1 - e^{-\beta r}); \quad (2a)$$

$$A_E(r, \infty) = a_E + b_E(1 - e^{-\beta_E r}). \quad (2b)$$

The values of α and α_E can be found from the empirical formulas

$$\alpha = \alpha(0) - k\sqrt{r}; \quad (3a)$$

$$\alpha_E = \alpha_E(0) - k_E\sqrt{r}. \quad (3b)$$

In Eqs. (1)-(3), α, α_E, β, β_E, a, a_E, b, b_E, k, and k_E are all empirically derived values of the variables.

The data cited are useful in calculations of A(r, d) and A_E(r, d) based on formulas (1)-(3), for different energies and different source geometries.

Translated from Atomnaya Énergiya, Vol. 31, No. 6, p. 622, December, 1971. Original article submitted April 28, 1971.

MEASUREMENT OF ABSORBED RADIATION DOSE BY DEGRADATION OF LUMINESCENCE IN ANTHRACENE *

V. N. Doroshenko, I. N. Chervetsova, and A. M. Kabakchi

UDC 541.15:539.12.08

The present work was undertaken to test the possibility of using the degradation of luminescence in anthracene to determine the absorbed dose in an organic material in contact with metals or other solids. We investigated the luminescence spectra obtained by irradiating 1-5 mm thick anthracene crystals, films 0.06-0.16 mm thick, and thin (<100 nm) layers adsorbed on aluminum surfaces with Co^{60} γ-rays. The characteristic bands in the luminescence spectra 404, 422, 444, 480 nm maintain positions in going from crystals to films, and differ trivially for the adsorbed layers before and after irradiation. A difference in the intensity distribution in the individual luminescent bands is observed. We studied the dependence of the degree of quenching of the luminescence radiation on the absorbed dose by measuring $\Delta J/J_0 = (J_0 - J)/J_0$, %; J_0 and J are respectively the integrated intensities of luminescence in the 400-500 nm region before and after irradiation. It was found that $\Delta J/J_0$ varied the same way with dose for all samples studied. The results are shown in Fig. 1 as a graph of $\Delta J/J_0$ against $\log l$, where l is the thickness of the layer in angstrom units. The graph shows that for layers of luminescent material from 100 nm to 5 mm thick the degree of quenching is independent of the crystal thickness. The luminescent material was surrounded by a homogeneous layer to ensure electron equilibrium and was in contact with a metallic backing of low atomic number.

The quenching of the luminescence of a 0.1 cm thick crystal film of anthracene irradiated between metallic plates of the same thickness determines the ratio of the dose absorbed in this heterogeneous system to the dose in a single crystal of anthracene. The data obtained (1.08 for aluminum, 1.3 for nickel, and 1.65 for gold) are in good agreement with values reported in the literature. The experimental results show that degradation of luminescence can be used in the 0.2-3 Mrad range to determine the absorbed dose in an organic layer in contact with a solid.

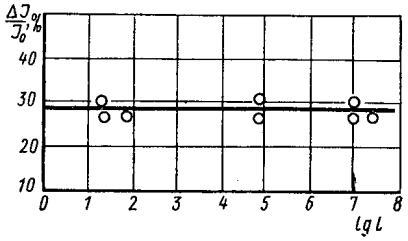

Fig. 1. Degree of degradation of luminescence of anthracene as a function of the thickness of the crystal layer.

SPECTRAL METHOD OF MEASURING COATING THICKNESS†

P. L. Gruzin, A. M. Rodin, and E. V. Skachkov

UDC 621.039.84

Problems associated with the utilization of monoenergetic electrons in backscatter thickness, in place of the more commonly used radioisotope β-ray sources, are investigated in the work described in this article.

*Translated from Atomnaya Énergiya, Vol. 31, No. 6, pp. 622-623, December, 1971. Original article submitted April 28, 1971.

†Translated from Atomnaya Énergiya, Vol. 31, No. 6, pp. 623-624, December, 1971. Original article submitted April 22, 1971.

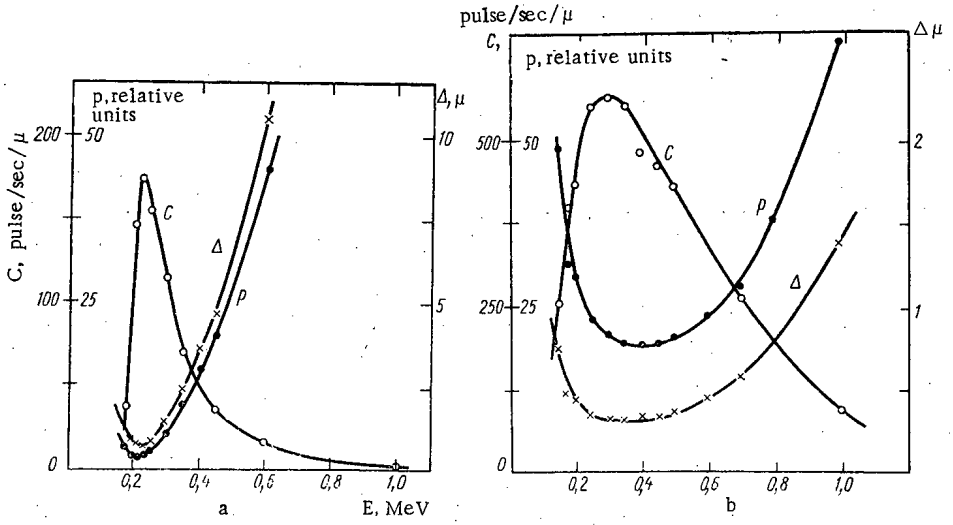

Fig. 1. Dependence of precision characteristics of energy of arriving electrons: a) organic coating on copper substrate; b) tantalum coating on copper substrate; ○) average sensitivity of thickness measurements (C); ×) average statistical error in thickness measurements (Δ); ●) quantity proportional to instrumental bias error in thickness measurements (p).

A monochromator built around a twin-lens magnetic spectrometer and an isotope source of $Sr^{90} + Y^{90}$ β-particles of type BIS-10, activity 500 μCi, was used in order to generate a beam of monoenergetic electrons. The momentum resolution was 3.5% for a source 10 mm in diameter. The backscattered electrons were recorded by a type DDS 18/2A cooled silicon semiconductor detector. The intensity and spectral distribution of the backscattered electrons were measured. The instrumental spectra were processed by introducing corrections for electron backscatter from the detector material, on an M-20 computer. The following combinations of substrate and coating materials were selected as specimens:

1) Z of base >Z of coating (base copper, coating organic, coating thickness 165-205 μ).

2) Z of base <Z of coating (base copper, coating tantalum, coating thickness 9-12 μ).

The dependence of the average sensitivity and of the average absolute statistical error and average instrumental bias error in the measurements of the coating thickness in both groups of specimens on the energy of the incident electrons was investigated. The results are plotted graphically for normal beam incidence ($\gamma = 0°$), for the angle θ at which the detector was placed is reckoned from the normal to the specimen). Clearly, the average sensitivity peaks at E^{C}_{opt}, while the average absolute statistical error and the average instrumental bias error are minimized at the energies E^{Δ}_{opt} and E^{p}_{opt}, respectively. Comparisons of those errors in the measurements of coating thickness when monoenergetic electrons of appropriate optimum energy were made in the same geometry ($\gamma = 0°$, $\theta = 20°$), and also in the case where a radioisotope source of β-particles was employed, with the flux of the monoenergetic electrons and the flux of β-particles on the specimens assumed the same. If the most probable energy of the β-ray spectrum of the isotope selected for comparison was close to the optimum energy, the instrumental bias error was found to be ≈4 times less in the case of the combination copper base–organic coating, in the case of monoenergetic electrons, and the statistical error was found to be ≈3 times less, again in the case of monoenergetic electrons for that combination. In the case of the combination tantalum coating–copper substrate, these errors were found to be respectively ≈1.5 times less and ≈1.7 times less. But when the isotopes $S^{90} + Y^{90}$, a combination frequently encountered in backscatter thickness gages, was selected for comparison, the improvement in the errors was respectively ≈12 times and ≈8 times in the case of the combination copper base–organic coating, and respectively ≈1.9 times and ≈2 times in the case of the combination copper base–tantalum coating.

A DIRECTIONAL THERMAL NEUTRON EMITTER

V. I. Fominykh and O. A. Migun'kov

UDC 621.039.555

A 15 cm diameter paraffin sphere with a Po – Be source is used to produce a thermal neutron flux. Such a thermal neutron source has two shortcomings: 1) it has a complex spectrum consisting of a small number of thermal neutrons, together with a large number of fast neutrons; 2) only the neutrons emitted at a certain solid angle are utilized.

In the proposed directional thermal neutron emitter – the "Projector" – the thermal neutron flux is increased and its quality is improved by using a source of monoenergetic low-energy neutrons and a hydrogenous reflector.

The emitter consists of a block of paraffin moderator whose inner surface serves as a reflector. An open tube containing the neutron source and a cylindrical moderator is coaxial with the reflector. Various types of neutron sources can be used in the emitter. The dimensions of the cylindrical moderator are determined by the thickness x necessary to thermalize the source neutrons, and the layer y necessary to slow down the neutrons to energies ~1 keV (Fig. 1). The emitter was compared with a 15 cm diameter paraffin sphere by using a long counter (Table 1). A miniature proportional boron counter was used to investigate the distribution of the thermal flux from the emitter along the axis and in the transverse direction.

The thermal flux was measured at a point on the axis 50 cm from the center of the source by manganese–nickel foils. Knowing the thermal flux and the total flux of source neutrons it is possible to determine the total flux of source neutrons Q necessary to produce a unit thermal flux at a given point on the axis of the emitter (Table 2).

TABLE 1. Composition of Neutron Flux, %

Neutron source	Sphere		"Projector" emitter	
	thermal neutrons	epithermal neutrons	thermal neutrons	epithermal neutrons
Po—Be (α, n)	11	89	46	54
Po—B (α, n)	11	89	51	49
Cf^{252}	—	—	51	49
Sb—Be (γ, n)	—	—	69	31

TABLE 2. Total Flux of Neutron Sources

Type of emitter	"Projector" emitter			Sphere
Type of source	Po—B (α, n)	Cf^{252}	Sb—Be (γ, n)	Po—Be (α, n)
Q, neutrons/sec	$2{,}3 \cdot 10^4$	$1{,}9 \cdot 10^4$	$1{,}7 \cdot 10^4$	$2{,}6 \cdot 10^5$

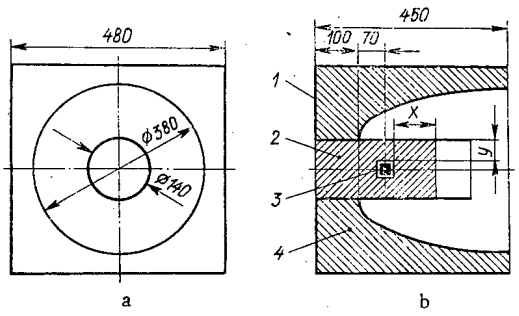

Fig. 1. Schematic diagram of emitter and cross section of thermal neutron beam at distance of a) 50 and b) 100 cm from the neutron source. 1) case; 2) paraffin block; 3) neutron source; 4) reflector.

Translated from Atomnaya Énergiya, Vol. 31, No. 6, p. 624, December, 1971. Original article submitted January 29, 1971. Original article submitted January 29, 1971; revision submitted May 27, 1971.

APPLICATION OF THE METHOD OF ALTERNATING IRRADIATION CONDITIONS TO NEUTRON ACTIVATION DETERMINATIONS OF ALUMINUM, MAGNESIUM, AND SODIUM IN PYROLYTIC GRAPHITE*

N. A. Kryzhenkova, M. G. Valieva,
E. M. Lobanov, and M. M. Usmanova

UDC 543.53

Monitoring the impurity content level in pure pyrolytic graphite is of single importance when pyrolytic graphite is used in the nuclear power industry, in semiconductor devices, and in other allied areas.

This paper discusses the possibility of determining aluminum, magnesium, and sodium from the radioactive isotope of sodium formed from the original stable isotopes as a result of competing reactions.

The method of alternating irradiation conditions for decoding and quantitative determination of three-component activity induced in those reactions yields an inadequate manifestation of each component in the transition from one set of irradiation conditions to another.

The mathematical processing is based on the solution of a system of linear equations describing these successive irradiations. The decoding technique is justified without requiring superposition of similarity conditions when the experiment is conducted under the various sets of conditions.

The boundary relations for the concentrations of the analytical components at which the procedure is applicable are derived. The possibilities of obtaining coarser results as a result of the effect of thermalization of the neutron flux were investigated. Standardization and accuracy of the method in the instrumental variant of neutron activation analysis applicable to pyrolytic graphite are discussed.

METHOD FOR DETERMINING ACTIVATION ENERGY IN THE PROCESS OF DIFFUSION OF A GAS EMBEDDED IN METAL†

L. B. Begrambekov, V. A. Kurnaev,
A. A. Pisarev, V. M. Sotnikov,
and V. G. Tel'kovskii

UDC 533.15

On the basis of the solution of the one-dimensional diffusion equation on a semiinfinite line with zero boundary conditions, it is shown that, in the case of a linear temperature rise (in the target temperature) after cessation of ion bombardment, and in the case of a constant temperature T_1 established after linear heating, the activation energy for diffusion of particles Q can be determined on the basis of the following formulas if the particles becoming embedded in the course of the ion bombardment, before the target warms up, fill up a layer of metal of thickness $\Delta p = p_2 - p_1$ evenly (here p_1 and p_2 are respectively the minimum and maximum ranges of the particles, expressed in terms of the number of lattice constants of the metal):

$$p_{av}^2 aQ = Fk_0RT^2 \exp\left[-\frac{Q}{RT}\right] \text{ (in linear temperature rise);} \quad (1)$$

$$Q = RT_1 \ln\left[Fk_0 (t - t_1) p_{av}^{-2}\right] \text{ (constant temp.);} \quad (2)$$

*Translated from Atomnaya Énergiya, Vol. 31, No. 6, p. 625, December, 1971. Original article submitted April 19, 1971.

†Translated from Atomnaya Énergiya, Vol. 31, No. 6, pp. 625-626, December, 1971. Original article submitted April 12, 1971.

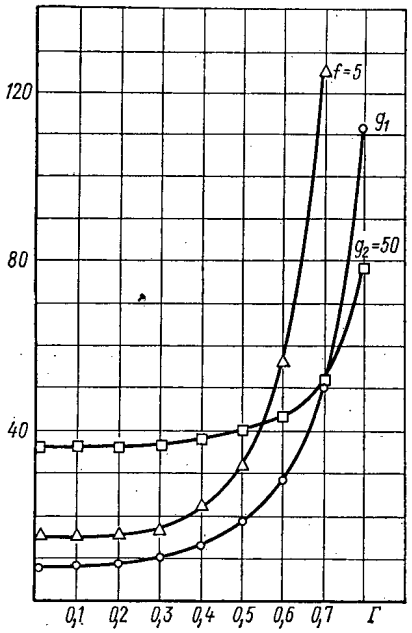

Fig. 1

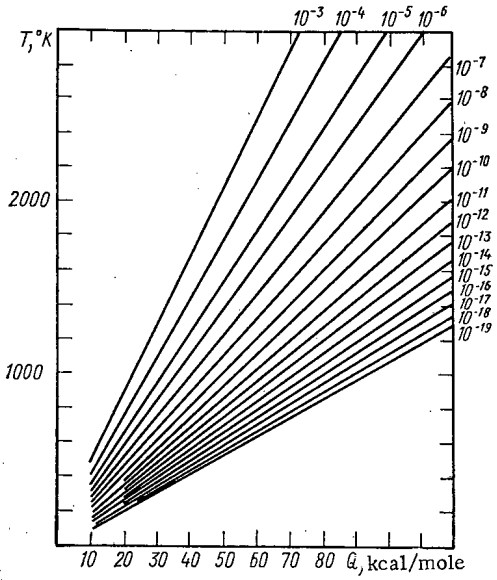

Fig. 2

Fig. 1. Dependence of parameters f and g on the relative half-width of the initial distribution Γ.

Fig. 2. Dependence of characteristic temperature T on energy of activation for diffusion Q at different values of ratio C.

Here $p_{av} = (p_2 + p_1)/2$; T is the characteristic temperature; t is the characteristic time; a is the heating rate in the linear temperature rise; k_0 is the lattice vibration frequency; R is the universal gas constant; F is a parameter dependent on the relative half-width of the initial distribution of particles with respect to depth in the metal $\Gamma = p_2 - p_1/2p_{av}$; t_1 is the time temperature T_1 is arrived at. In the linear temperature rise case the value of Q can be found by recording one of the three characteristic temperatures at which the rate of evolution of gas from the metal into a vacuum is either maximized ($T = T_{max}$) or becomes e times less than the maximum temperature ($T = T_{e1}, T_{e2}$). In the case of constant temperature, Q can be calculated on the basis of one of the characteristic times at which the rate of gas evolution is either maximized ($t = t_{max}$ or becomes e-fold less than the maximum temperature ($t = t_{e1}, t_{e2}$). If Q is determined on the basis of the instant at which the maximum rate of evolution of gas from the specimen appears into a vacuum occurs $j = j_{max}$, then $F = 1$, and if it is determined on the basis of the instant when $j = (1/e)j_{max}$, then $F = g_1, g_2$.

Figure 1 displays the dependences of f and g_1, g_2 on Γ. The two branches g_1 and g_2 correspond to the ascending and descending portions of the time dependence j. In the linear temperature rise case, the value of Q can be determined more conveniently with the aid of Fig. 2, on the basis of Eq. (1), where the parameter is the ratio $C = p_{av}^2 a/Fk_0$.

By combining different variants of equations (1) and (2), we can obtain expressions which do not contain p_{av}, k_0, or a in the linear temperature rise case, and t_1 in the constant temperature case.

ON THE TRAJECTORIES OF PARTICLES IN AN ISOCHRONOUS CYCLOTRON IN THE PRESENCE OF ACCELERATION. III

Yu. K. Khokhlov

UDC 621.384.611

In choosing the geometry of the dees for a projected cyclotron [1], one must be certain that the electric field of the gaps will not shift the frequency of the radial betatron oscillations in the region of the parametrical resonance $\nu_x = 1$. In conjunction with this, the experiment examines two primary mechanisms of the influence of the gaps on ν_x: a) the effect, which is determined by relative increase of kinetic energy, $\Delta W/W$, and b) the effect, which is defined by the rate of change in the increase of ΔW at the moment of the crossing of the gap by the trajectory of the center of the bunch, $\varepsilon = (\Delta W)'/\omega_c$. The experiment is a direct continuation of the preceding experiments [2, 3]. Interest in effect "a" is stimulated by [4].

An attempt to describe effect "a" in the limit of a linear approximation according to the relative deflection x/R of the trajectory which is under examination from the corresponding closed equilibrium trajectory leads to erroneous results. This is explained by the fact that the neglected nonlinear members of the type $(x/R)^2$ and others have exactly the same order of magnitude as the members being considered of the type $(\Delta W/W) \cdot (x/R)$. In order to circumvent this difficulty, the experiment examines small deflections from the open, actually existing trajectory of an accelerated particle. For such a trejectory $(x/R)^2 \ll (\Delta W/W) \cdot (x/R)$, as a result of which the use of a linear approximation becomes possible.

The influence of the factors $\Delta W/W$ and ε/W on the frequency ν_x is examined in linear and quadratic approximations. It is shown that as a consequence of the symmetrical orientation of the dee system relative to the magnetic system, the corrections linear in $\Delta W/W$ to SpM $(\pi/0)$ are equal to zero. In the case of strictly isochronous movement of particles, the corrections linear in ε/W are also equal to zero. Corrections quadratic in $\Delta W/W$ decompose, in turn, into focusing orbital corrections and defocusing boundary corrections. The sum of these corrections has a rather quickly focusing character, i.e., shifts the frequency ν_x to the side from the dangerous value $\nu_x = 1$. The correction quadratic in ε/W has a purely defocusing character, i.e., in principle can be examined as a possible cause of parametrical resonance or pulsation. However, the numerical value of this correction is very small (and quickly decreases with an increase of energy). Thus, the conclusion is drawn that in a cyclotron of the type described in [1] the factors $\Delta W/W$ and ε/W do not represent a real danger.

In the concluding section of the experiment corrections which are caused by the final width of the gap are calculated. They were negligibly small.

LITERATURE CITED

1. I. Ya. Barit et al., Paper of the P. N. Lebedev Physics Institute, Academy of Sciences, USSR, No. 15 [in Russian] (1969).
2. Yu. K. Khokhlov, At. Énerg., 29, 39 (1970).
3. Yu. K. Khokhlov, At. Énerg., 30, 451 (1971).
4. V. P. Dmitrievskii, V. V. Kol'ga, and N. I. Polumordvinova, Paper of the Joint Institute of Nuclear Research, No. 13-4496 [in Russian] (1969), p. 36.

Translated from Atomnaya Énergiya, Vol. 31, No. 6, p. 626, December, 1971. Original article submitted February 13, 1971.

COMPARATIVE SPEED OF RESPONSE OF REACTOR SCRAM SYSTEMS IN PERIOD CONTROL AND POWER CONTROL

V. I. Kazachkov and A. S. Alpeev

UDC 621.039.538

One of the main criteria in judging the effectiveness of power reactor scram systems is speed of response. This parameter is of particular importance when the reactor is operating at power levels close to the reactor's power rating.

Protection by power control limits the upper range of deviation of the power setpoint and is characterized by the coefficient $\varkappa = N_{sc}/N_{sp}$, which is the ratio of the power scram level N_{sc} to the specified level N_{sp}. A power trip of the scram system therefore comes about whenever the reactor power exceeds the level $\varkappa N_{sp}$, for whatever reason.

Protection by a period trip limits the rate of power rise, and is characterized by a certain scram period T_{sc}, i.e., the scram system is tripped by period whenever the period T becomes shorter than T_{sc}.

The first type of scram response involves a power surge beyond the power setpoint in response to any external conditions whatever, when the period $T > T_{sc}$. The second mode of scram response involves a rate of power rise greater than permissible in response to any external conditions whatever when the period $T < T_{sc}$.

In the first scramming mode it is only the power protection channel that is activated. In the second scramming mode it is not only the power protection channel, but also the period protection channel, that goes into action. It would be of interest to clear up which channel becomes energized first, under what conditions. This would enable us to estimate the feasibility of parallel utilization of power-level trip and period trip channels for concrete sets of reactor operating conditions.

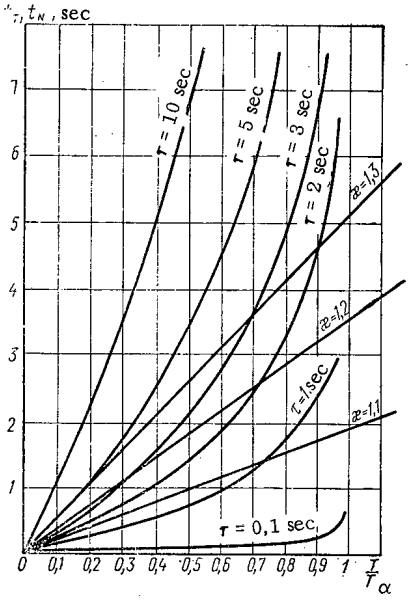

Fig. 1. Response time of power trip protection system t_N and response time of period trip protection system t_T, as functions of time constant τ of differentiating circuit, reactor warmup time T, and ratio of scram power level to power setpoint $\varkappa$.

Translated from Atomnaya Énergiya, Vol. 31, No. 6, pp. 627-628, December, 1971. Original article submitted January 6, 1971.

The power-level trip system and the period trip system differ only in their input measuring channels. At high power levels, the power-level protection measuring channel can be treated as essentially inertialess, i.e., having instantaneous response. But the differential amplifier used in the period trip channel cannot have a zero time constant, in principle. Moreover, it is precisely in that component of the period trip measuring channel that the time constant cannot be smaller than a certain value set by statistical fluctuation noise in the neutron flux and by the overall noise immunity of the period trip system [1]. Clearly, then, there exist certain conditions under which the power-level protection chanel (if the response time is reckoned from the time of onset of the reactor power rise, with reactor period $T < T_{sc}$, to the instant the signal is sent out from the measuring circuits to scram the safety rods).

For definiteness, we assume that the scram system has two settings: one for the power level $\varkappa N_{sp}$, the other for the period T_{sc}. At some time a scramming situation arises, as a result of which the power level begins to vary in accordance with the law

$$N = N_0 e^{-t/T},$$

where $T < T_{sc}$.

We now determine the time it takes to reach the power trip threshold t_N, as a function of the period $\varkappa N_0 = N_0 e^{-t_N/T}$. Hence,

$$t_N = T \ln \varkappa. \tag{1}$$

The response time of the power-level scramming system is a linear function of the period and of the logarithm of $\varkappa$.

The response time of the period scramming system is found from the equation for the output voltage U_{out} of the differential amplifier [1]:

$$U_{out} = \frac{K}{T}\left(1 - e^{-\frac{t}{\tau}}\right),$$

where K is a constant; T is the reactor period; τ is the time constant of the differentiating circuit.

At some $t = t_T$, the voltage across the output attains the value $U_0 = K/T_{sc}$, corresponding to the scram period: $\frac{K}{T_{sc}} = \frac{K}{T}\left(1 - e^{-\frac{t_T}{\tau}}\right)$. Solving this equation for t_T, we get

$$t_T = -\tau \ln\left(1 - \frac{T}{T_{sc}}\right). \tag{2}$$

The physical meaning of Eq. (1) resides in the fact that it makes sense to consider activation of the period trip only when $T < T_{sc}$. The case $T = T_{sc}$ has the purely theoretical interpretation that, in the limit, $t_T \to \infty$ in that case.

The period trip and power-level trip channels are activated simultaneously when

$$T \ln \varkappa = -\tau \ln\left(1 - \frac{T}{T_{sc}}\right). \tag{3}$$

Figure 1 shows the dependence of t_T and t_N on the ratio T/T_{sc} at different τ and $\varkappa$ values. It is clear from Fig. 1 that the power-level trip goes into action earlier than the period trip at the values $\varkappa = 1.2$ and $\tau = 5$ sec. It appears that period trip channels such that $\tau = 5$ sec should not be used parallel with power-level trip channels. The period trip channels exhibit lower noise stability than the power-level trip channels. Under the conditions indicated above, then, it would be better to increase the number of power-level trip channels while eliminating period trip channels.

Using Eqs. (1) and (2), we can estimate the relative speed of response of the power-level and period trip channels under any sets of conditions.

LITERATURE CITED

1. In: Control of Nuclear Power Plants, No. 1 [in Russian], Atomizdat, Moscow (1966).

REDUCTION OF SYSTEMATIC ERRORS IN MEASUREMENTS OF $\sigma_c^{238}/\sigma_f^{235}$

L. N. Yurova, A. V. Bushuev,
V. G. Bortsov, V. M. Duvanov,
and A. F. Kozhin

UDC 539.172.4

The ratio of the U^{238} radiative capture cross section to the U^{235} fission cross section in an experimental system can be determined by calibrating samples in a thermal neutron flux. Ordinarily two samples are used – one depleted in U^{235} and one enriched. The depleted uranium is used to reduce the background of U^{235} fission fragment radiation in recording captures in U^{238}. The use of enriched uranium indicators to estimate the U^{235} fission rate permits the neglect of U^{238} fission.

The introduction of indicators which differ in composition from the medium being studied perturbs the neutron distribution. Because of the difficulties of taking account of the systematic errors arising in this case it is necessary to minimize the perturbation introduced by the sample.

We propose to determine the $\sigma_c^{238}/\sigma_f^{235}$ ratio by using samples which have the same composition as the fuel elements. Information on both U^{238} capture and U^{235} fission is obtained from measurements of a single indicator which does not perturb the neutron distribution when placed in a fuel element.

Such experiments can be performed by γ-spectrometry. Measurement of the intensity of the γ-radiation from indicators in the region of the 74 keV U^{239} photopeak gives information on the capture rate, and the recording of hard γ-rays from fission products furnishes data on the fission rate. The radiation from fission fragments produces a background in measurements of the U^{239} activity, and the accurate determination of this background is the most difficult part of the experiment.

Ordinarily the following method is used. A sample of enriched uranium is irradiated in the thermal column and the relative intensity of the fission fragment radiation in two energy ranges is determined: 1) in the region of the 74 keV U^{239} photopeak and 2) in the high-energy region where there is no U^{239} radiation. By determining this ratio and measuring the intensity of the radiation from the main indicator in the high-energy region it is possible to find the background of fission fragment radiation in the first region.

Better accuracy can be achieved by measuring the activity of the indicator in both regions simultaneously. In this case it is not necessary to take account of the difference in the U^{239} and the fission fragment decay rates or to monitor the neutron flux in which the sample is irradiated.

The working formula has the form

$$\frac{\sigma_c(238)}{\sigma_f(235)} = \frac{\sigma_c^{th}(238)}{\sigma_f^{th}(235)\, g_{235}} \varepsilon p k,$$

where $\sigma_c^{th}(238)$ is the U^{238} capture cross section and $\sigma_f^{th}(235)$ is the U^{235} fission cross section for thermal neutrons; g_{235} is the Westcott factor.

Inaccuracies in the constants lead to an uncertainty of ~2% in the ratio of the cross sections. This limits the accuracy with which the $\sigma_c(238)/\sigma_f(235)$ ratio can be determined at the present time from measurements made by calibrating indicators in a thermal neutron flux; ε is a parameter which takes account of the contribution of U^{238} to the total activity of fragments when the indicator is irradiated in the system; p is a correction for the escape of fragments from the indicator during irradiation in the thermal column. In our case this correction is 1.011. It is assumed that during the irradiation in a fuel element the escape of fragments from the indicator is compensated by the influx of fragments from the fuel into the indicator.

Translated from Atomnaya Énergiya, Vol. 31, No. 6, pp. 628-629, December, 1971. Original article submitted January 13, 1971; revision submitted April 22, 1971.

The experimental parameter is determined by the expression

$$k=\frac{k_1-k_3}{k_2-k_3}=\frac{(A_1/A_2)^{ind}_{sys}-(A_1/A_2)^{sam}_{t.c.}}{(A_1/A_2)^{ind}_{t.c.}-(A_1/A_2)^{sam}_{t.c.}},$$

where $k_1 = (A_1/A_2)^{ind}_{sys}$ is the ratio of activities of the indicator in the energy range ΔE_1 under the 74 keV peak and in the high-energy region ΔE_2 after irradiation in the system under study. The region ΔE_2 of hard γ-radiation has only a lower bound; it must not contain bremsstrahlung produced by β-particles emitted in the decay of U^{239}; $k_2 = (A_1/A_2)^{ind}_{t.c}$ is the same ratio when the indicator is irradiated in the thermal column; $k_3 = (A_1/A_2)^{sam}_{t.c}$ is the ratio of the activities of the sample of enriched uranium in the ranges ΔE_1 and ΔE_2.

Thus a standard series of measurements must include three experiments: 1) an experiment with the indicator in the system to determine k_i; 2) an experiment with the indicator in the thermal column to determine k_2; 3) an experiment with an enriched sample in the thermal column to determine k_3. This series of experiments determines k_{1i}, k_{2i}, and k_{3i} at time t_i after the end of irradiation, and then k_i.

The composition and dimensions of the indicators are determined by the characteristics of the fuel elements of the system under study. The best measuring conditions, the smallest background from uranium decay products, and the maximum ratio of effect to background of fission fragment radiation are obtained by using indicators of minimum thickness.

It is advantageous to use uranium enriched to 90% in U^{235} since in measurements with such samples the contribution of the U^{239} radiation to the activity in the ΔE_1 range is negligible. Highly enriched samples perturb the neutron distribution in the thermal column, but this does not affect the value of k_3. This conclusion is confirmed by measurements of k_3 with samples of thickness 110 μ, 220 μ, and "zero" (a paper indicator with fragments collected on it).

The value of k_3 is weakly dependent on thickness for two reasons.

1. The γ-absorption cross section of uranium is not very different in the ΔE_1 and ΔE_2 intervals: σ_1 (at 80 keV)/σ_2 (at 1.5 MeV) = 1.75. The relatively weak γ-absorption in the range ΔE_1 is due to the fact that these energies are below the threshold of the photoelectric effect for the K shell of uranium (115.6 keV).

2. As the γ-rays pass through uranium and interact with the detector, some of the photons of the upper groups undergo Compton scattering and enter the ΔE_1 range. Electrons emitted in the β-decay of fission fragments form bremsstrahlung in the ΔE_1 range as they pass through uranium. Thus the absorption of radiation from the ΔE_1 range is more strongly compensated than that from the ΔE_2 range.

The simplest apparatus for performing the measurements described is a scintillation spectrometer. The most suitable detector is a thin NaI(Tl) crystal of rather large diameter with good amplitude resolution. The pulses from the detector are fed into two channels: the first, which is designed to record soft U^{239} photons, includes an amplifier, a single-channel analyzer for separating out the range ΔE_1, and a scaler; the second channel, for recording hard radiation from fragments, includes an integral discriminator and a scaler. It is convenient to tune the first channel with Bi^{207} γ-rays ($E_\gamma \approx 78$ keV), and the second with the Na^{22} line (1.28 MeV).

Preliminary experiments showed that after the indicator had been irradiated for 15 to 30 min the values of k_3 varied by less than 10% during the measuring process. Initially the fragments decay more rapidly than U^{239} and the ratio of effect to background in the ΔE_1 range increases, reaches a maximum after 30-40 min, and then begins to decrease slowly. In measurements with a natural uranium indicator placed in an experimental assembly of natural uranium and graphite this ratio varied from 3.5 to 5. The resolution of the detector for U^{239} γ-rays was 31%.

The $\sigma_c(238)/\sigma_f(235)$ ratio in this assembly was determined by the method described above and also in the usual way by recording neutron captures in U^{238} with U–Al alloy indicators containing uranium depleted 230 times in U^{235}, and U^{235} fissions with U–Al alloy indicators containing uranium enriched 90% in U^{235}. The results differed by 11-13%, confirming the importance of systematic errors.

Thus the method proposed permits measurements of $\sigma_c(238)/\sigma_f(235)$ with minimum systematic errors since all the information is obtained with a single indicator which does not perturb the neutron distribution in the system. It has been established that this method using a scintillation detector is suitable for measurements in systems fueled with natural or slightly enriched uranium.

EFFECT OF TEMPERATURE ON STRUCTURAL CHANGES IN Pu^{238} DIOXIDE IN SELF-IRRADIATION

I. I. Kapshukov, L. V. Sudakov, and G. N. Yakovlev

UDC 621.039.542.342+546.799

Changes in the crystal lattice constant of Pu^{238} dioxide in response to internal irradiation at liquid nitrogen temperature, at room temperature, and at 500°C, were investigated in the case of two series of specimens containing different amounts of impurities.

Thin-walled leaktight quartz capillaries containing 1 to 2 mg plutonium dioxide were used in the x-radiography. Excellent quality x-ray plates were taken after 30 to 40 min exposure to internal irradiation, in copper light at 35 kV and 20 mA x-ray conditions. The x-ray plates taken of specimens with a lower impurity content K_α (<1%) showed doublets remaining sharp and clearly defined all the way to the angles furthest back, which makes it possible to measure the crystal lattice constant of these specimens (series I) to within ±0.0005 Å. In the case of specimens containing iron impurity (series II), the quality of the x-ray plates was slightly lower, and the crystal lattice constant was determined to within ±0.001 Å in those cases. The quality of the x-ray plates suffered practically no change during the process of self-irradiation.* The results of the room-temperature investigation, as well as the data on the composition of the specimens, are given below [1]. The capillary with the specimen were exposed throughout the duration of the experiment in liquid nitrogen or in a furnace heated to 500°C, and were withdrawn for about one hour, once a day, to take the x-ray plates. Investigation of specimens of one series was begun immediately after the Pu^{238} dioxide crystallized, and was carried on in parallel at the three temperatures mentioned. The first x-ray plates were taken in 8-12 h.

The characteristic shape of the self-irradiation curves noted earlier [1] is clearly manifested in the case of specimens belonging to series I, at all three of the temperatures (see Fig. 1). Since the depth of the minimum investigated at room temperature on the kinetic curves is shallow, about 20 specimens fabricated from several batches of the dioxide, with impurity content ~1%, were investigated in order to draw unambiguous conclusions as to the existence of this minimum. In all instances, the maxima and minima on the kinetic curves showed up with particular clarity, and their differences in magnitude and position were very insignificant. In the case of specimens belonging to series II, the existence of depressions on the kinetic curves is beyond doubt [1]. It is clear from the diagram that the curves shift downward, as a whole, as the temperature rises, and that the characteristic points (maxima and minima) shift to the left. The same regularities stand out quite conspicuously in the case of specimens belonging to series II. These regularities are reminiscent of the temperature dependence of the crystal lattice constant of uranium dioxide irradiated by neutrons at temperatures 70°C and 400°C [2].

Curves of isochronous stepwise anneals up to 1000°C, after prolonged exposure of the specimens in liquid nitrogen, are similar to the curve reproduced in [1]; after the specimens were held at 500°C, the anneal curves are characterized by a monotonic decline in the crystal lattice constant.

The data obtained, as well as the results reported in [1], enable us to draw some qualitative inferences as to the relaxation phenomena occurring in the process of self-irradiation of Pu^{238} dioxide. Changes brought about in the crystal lattice constant during self-irradiation are due to the formation and relaxation of point defects (Frenkel pairs). The existence of a stationary state is indicative of a dynamical equilibrium between the formation and annihilation of point defects.

*Investigation of the shape and relative intensity of the lines of specimens in series I, carried out at room temperature with an x-ray diffractometer, revealed slight attenuation of intensity and some broadening of lines, the changes being monotonic in nature.

Translated from Atomnaya Énergiya, Vol. 31, No. 6, pp. 630-631, December, 1971. Original article submitted August 27, 1970; revision submitted April 5, 1971.

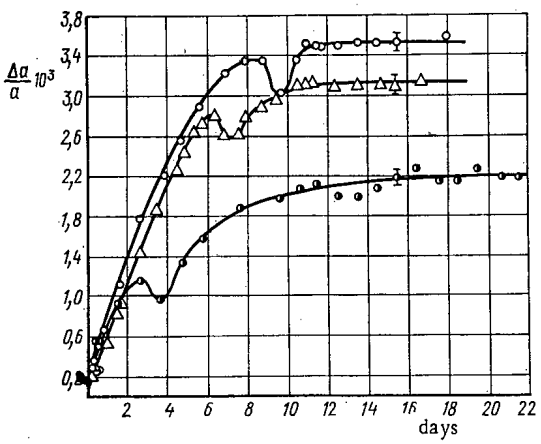

Fig. 1. Variation of crystal lattice constant of Pu^{238} dioxide in response to self-irradiation at liquid-nitrogen temperature (○), at room temperature (△), and at 500°C (◑).

According to the model advanced [1], relaxation processes go to completion in the crystal at temperatures below 500°C because of migration of interstitial ions through the lattice; vacancies are considered immobile. It is natural to assume that the principal result of a temperature rise will be acceleration of diffusion processes. The mobility of the interstitial ions increases, and as a consequence the rate of emergence of point defects from the lattice via recombination increases. In addition, as the mobility increases, the limiting permissible concentration of solitary interstitial ions in the lattice will drop, since the conditions governing the formation of dislocation loops of ions become more favorable. The net outcome of all this is that the self-irradiation curves end up lower with rising temperature (when the rate of formation of defects remains constant as annihilation of defects is accelerated), and the maxima on the curves shift leftward (formation of nuclei of dislocation loops sets in at a lower concentration of isolated interstices).

However, certain features of the experimental results resist explanation, when we assume that relaxation processes reduce to thermal annealing out of defects, as a whole. It is clear from Fig. 1 that the self-irradiation curves of Pu^{238} dioxide are located very close to each other at the temperatures −196°, 20°, and 500°C, even though the differences between the mobilities of the interstitial ions must be very great at those temperatures. The results of isochronal stepwise anneals showed [1] that no decline is observed in the crystal lattice constant, for all practical purposes, in annealing up to 200°C. This indicates that relaxation processes include, in addition to the thermal anneal, radiation anneal of flaws, and that the role played by radiation annealing out of flaws predominates at temperatures below 200°C.

The radiation anneal mechanism seems to reduce to activation of diffusion processes in regions of local heating (thermal spikes). Even though the α-decay events occur at different times in different parts of the crystal, diffusion processes will be activated by the internal irradiation an identical number of times (on the average) in all regions of the crystal. The formation of thermal spikes in response to recoil atoms was convincingly demonstrated in the case of NpO_2 by the method of the Mossbauer recoil effect on the Np^{237} nucleus [3, 4]. The second possibility in the activation of diffusion under irradiation is due to the appreciable kinetic energy of the defects forming (tens and hundreds of electron-volts). This energy is much greater than the mean kinetic energy of the crystal atoms, so that the defect will migrate through the lattice until equilibrium is attained, expending energy in collisions with atoms. Dynamic crowdions are especially favorable [5] for migration of the defect away from its site of formation. Under real conditions, both local heating and dynamical factors must act simultaneously on diffusion processes. It appears to be an impossible job to evaluate their contributions to radiation annealing separately, at the present time.

Comparison of results of self-irradiation of the dioxides of Pu^{239}, Pu^{240}, Am^{241}, and Pu^{238} at room temperature [6-8, 1] also furnish compelling arguments in favor of the predominant role played by radiation annealing under these conditions. If the relative change in the crystal lattice constant is expressed as a function of the relative number of decaying atoms, then the self-irradiation curves, despite the enormous differences in the specific activities of the α-emitters, will lie very close to each other. The major contribution made by radiation annealing will also account for the low value (0.15 eV) of the energy of activation of the displacement of interstitial ions, determined on the basis of the results of an isothermal anneal of Pu^{238} dioxide [9]. In that case the true (effective) temperature of annealing will appear to be much higher, thanks to radiation effects, than the temperature of the thermostat (300°, 400°C) employed in the experiments.

LITERATURE CITED

1. I. I. Kapshukov et al., At. Énerg., 27, 337 (1969).
2. L. Roberts et al., Proc. of the Third International Conference (Geneva, 1965) on the Peaceful Uses of Atomic Energy, Vol. 11, New York (1965), p. 464.

3. A. Stone and W. Pillinger, Phys. Rev. Lett., 13, 200 (1964).
4. J. Mullen, Phys. Lett., 15, 15 (1965).
5. S. T. Konobeevskii, Effect of Radiation on Materials [in Russian], Atomizdat, Moscow (1967).
6. C. Griffin et al., Proc. of the Third International Conference on Plutonium, London (1965).
7. T. Chicalla and L. Eyring, J. Inorg. Nucl. Chem., 30, No. 1, 133 (1968).
8. C. Keller, "Lanthanide–Actinide Chemistry," in: Adv. in Chem., Series No. 71, Amer. Chem. Soc., Washington DC (1967), p. 228.
9. I. I. Kapshukov, L. V. Sudakov, and G. N. Yakovlev, Fiz. Tverd. Tela, 12, No. 7, 2157 (1970).

TERNARY SYSTEMS CONTAINING SODIUM, POTASSIUM, AND CALCIUM CHLORIDES, AND URANIUM TRI- AND TETRACHLORIDE

V. N. Desyatnik, Yu. T. Mel'nikov, S. P. Raspopin, and V. I. Sushko

UDC 541.123.3.5:546.32'33'41'791.3'4

The absence of information on fusibility diagrams of ternary systems containing sodium, potassium, and calcium chlorides, and uranium tri- and tetrachloride, together with the need for information on the behavior of these melts in order to select corresponding electrolytes and to explain certain processes occurring during calcium–thermal reduction of chlorides, prompted our investigation of the fusibility diagram of the system $NaCl-UCl_3-UCl_4$, $KCl-UCl_3-UCl_4$, and $CaCl_2-UCl_3-UCl_4$.

The initial substances were prepared for these investigations. Sodium and potassium chlorides of cp grade were twice recrystallized, dried in vacuum, and then fused. Their melting points, determined by the differential thermal method, were 800 ± 2 and 770 ± 2°C, respectively. Uranium tetrachloride was prepared by the procedure described in [1], the trichloride was obtained by reducing UCl_4 with hydrogen by the reaction

$$UCl_4 + 1/2H_2 \rightarrow UCl_3 + HCl.$$

The melting point of uranium trichloride was 834 ± 2°C, the atomic ratio [Cl] : [U] = 3.05. Calcium chloride was obtained by the familiar method [2]; the melting point was 775 ± 2°C. All operations involving the highly hygroscopic uranium chlorides were performed in a dry chamber.

The primary crystallization surfaces of the ternary systems were studied by the differential thermal method with recording of the cooling curves. A sample (2.5-3.0 g) was placed in a quartz cell, sealed by a rubber bung; after evacuation, the cell was filled with purified argon, placed in a resistance furnace, and

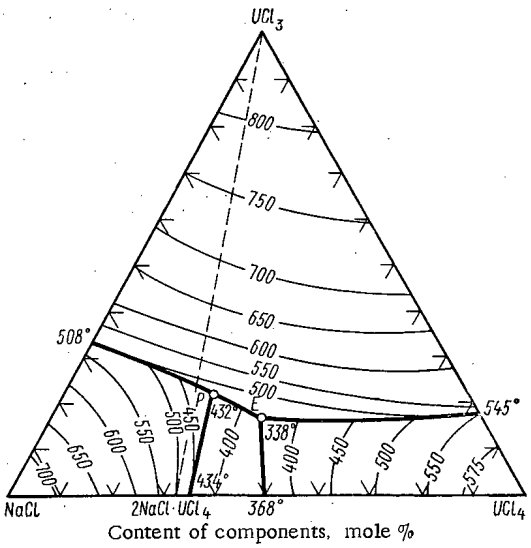

Fig. 1. Fusibility diagram of the system $NaCl-UCl_3-UCl_4$.

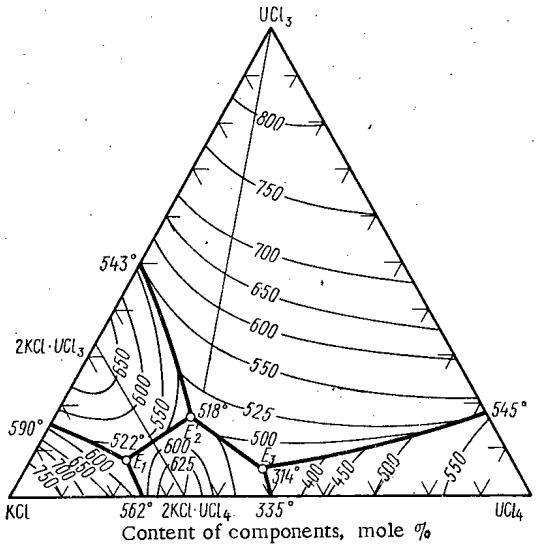

Fig. 2. Fusibility diagram of the system $KCl-UCl_3-UCl_4$.

Translated from Atomnaya Énergiya, Vol. 31, No. 6, pp. 631-633, December, 1971. Original article submitted December 7, 1970; revision submitted May 6, 1971.

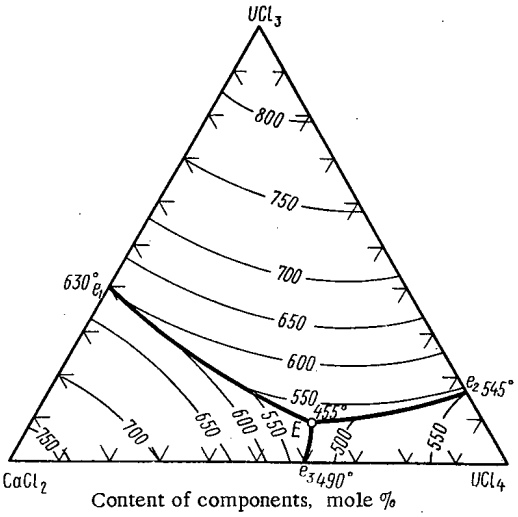

Fig. 3. Fusibility diagram of the system $CaCl_2-UCl_3-UCl_4$.

fused. The fused mixture was retained for 60-90 min to equalize the composition. The homogenized substance was cooled at a rate of 5-8 deg/min with simultaneous recording of the thermogram. Beryllium oxide crucibles were used for operations with uranium trichloride.

The thermograms were interpreted by known procedures [3-5].

To study the system $NaCl-UCl_3-UCl_4$ we used the binary systems $NaCl-UCl_3$ [6], $NaCl-UCl_4$ [7], and UCl_3-UCl_4 [8]. In the ternary system we studied nine polythermal cross sections which passed through the apex of the concentration triangle, corresponding to UCl_3, and the opposite side. Figure 1 shows the liquidus surface of the system, constructed from our interpretation of the thermograms. The primary crystallization surface is represented by the fields NaCl, UCl_3, UCl_4, and $2NaCl \cdot UCl_4$. Uranium trichloride forms the largest part of the area of the concentration triangle, $2NaCl \cdot UCl_4$ forms the smallest part. The system displays one eutectic and one peritectic point. The eutectic melts at 338°C and corresponds to the composition (mole %): NaCl 42.5, UCl_3 17.0, and UCl_4 40.5. The peritectic point at 432°C corresponds to the composition (mole %): NaCl 49.0, UCl_3 21.5, UCl_4 29.5.

To study the primary crystallization surface of the system $KCl-UCl_3-UCl_4$, we used data of previous investigations of the binary systems $KCl-UCl_3$ and $KCl-UCl_4$, which agree closely with results in [7].

Figure 2 shows the liquidus surface of the system $KCl-UCl_3-UCl_4$, consisting of five crystallization fields: KCl, $2KCl \cdot UCl_3$, UCl_3, UCl_4, and $2KCl \cdot UCl_4$. Like the previously described system, the largest area is occupied by uranium trichloride, the smallest area by the field of potassium chloride and $2KCl \cdot UCl_4$. The size of the crystallization fields may be assessed from the stability of the given compound in the melt.

It was found that the system $KCl-UCl_3-UCl_4$ contains two quasibinary cross sections: $UCl_3-2KCl \cdot UCl_4$ and $2KCl \cdot UCl_4 \cdot 2KCl \cdot UCl_3$. These divide the system $KCl-UCl_3-UCl_4$ into three secondary subsystems, each having one eutectic. The crystallization fields of KCl, $2KCl \cdot UCl_3$, and $2KCl \cdot UCl_4$ form a eutectic E_1 at 522°C, corresponding to the composition (mole %): KCl 74.5, UCl_3 7.5, UCl_4 18.0. The eutectic E_2, formed by the crystallization fields of $2KCl \cdot UCl_3$, and $2KCl \cdot UCl_4$, corresponds at 518°C to the composition (mole %): KCl 57.0, UCl_3 17.0, and UCl_4 26.0. The crystallization fields of $2KCl \cdot UCl_4$, UCl_3, and UCl_4 converge in the eutectic E_3 at 314°C. The composition of the eutectic E_3 is as follows (mole %): KCl 49.5, UCl_3, 5.5, UCl_4 45.0.

Figure 3 shows the fusibility diagram of the system $CaCl_2-UCl_3-UCl_4$, constructed from our interpretation of the thermograms.

The primary crystallization surface of the ternary system is represented by three fields which converge, forming a eutectic corresponding to the composition (mole %): $CaCl_2$ 34.0, UCl_3 10.0, UCl_4 56.0; the melting point is 455°C.

LITERATURE CITED

1. V. N. Desyatnik, I. F. Nichkov, and S. P. Raspopin, Izv. Vuzov. Tsvetnaya Metallurgiya, No. 5, 95 (1969).
2. Yu. V. Karyakin, Pure Chemical Reagents [in Russian], Goskhimizdat, Moscow (1947).
3. L. G. Berg, Introduction to Thermography [in Russian], Nauka, Moscow (1969).
4. A. Gaumann, Chimia, 20, Marz, 82 (1966).
5. F. Paulik, J. Paulik, and L. Erdey, Talanta, 13, No. 10, 1405 (1966).
6. C. Tipton, Sr., Reactor Handbook, Second Edition, Vol. 1, Materials (1960).
7. T. Kyroda and T. Suziki, J. Electrochem. Soc., Japan, 26, Nos. 7-9, 140 (1958).
8. V. N. Desyatnik et al., At. Energ., 26, 549 (1969).

SIMULTANEOUS RADIOMETRIC DETERMINATION OF URANIUM AND THORIUM IN SULFURIC ACID SOLUTIONS

V. V. Anosov, N. I. Gavrilov, and T. P. Smelkova

UDC 543.52:546.791 +546.841

Chemical methods for simultaneous determination of uranium and thorium in solutions are complex and laborious. In the case of radiometric methods, uranium and thorium are determined separately only in powdered specimens [1, 2]. We have developed a γ-spectrometric method for simultaneous determination of uranium and thorium in sulfuric acid solutions, which does not require complicated chemical treatment of the samples.

It was previously established that when equilibrial uranium ores are broken up in sulfuric acid solution with an H_2SO_4 content of more than 35 g/liter, the products of the decomposition of uranium to radium pass into solution in amounts equilibrial with uranium. In weaker solutions we observe sorption of UX_1 on the insoluble residue as poorly soluble sulfate compounds. Approximately 0.5% of the initial radium remains in solution. After separating the residue, the γ-emitters of the decomposition products of radon, still in solution, decompose in approximately 2 h. Of the uranium series, the solution now contains only one γ-emitter UX_1 with a considerable yield of γ-quanta. At an acidity of more than 35 g/liter, UX_1 is in equilibrium with U^{238}.

The content of γ-emitter U^{235} in a natural uranium mixture is 0.720%, and this amount of U^{235} is retained in a sulfuric acid solution. Thus, in a sulfuric acid solution UX_1 and U^{235} are γ-emitters, and the uranium content can be determined from their radiation intensity. Figure 1 shows a spectrogram of the γ-radiation of a uranyl nitrate solution; there is no difficulty in distinguishing the UX_1 lines with energies of 64 and 93 keV and the U^{235} line with an energy of 185 keV.

In naturally occurring compounds, thorium usually exhibits radioactive equilibrium. Therefore when thorium-containing ores are broken up in a sulfuric acid solution, RaTh (Th^{228}) is in equilibrium with the parent of the thorium series – Th^{232}. Mesothorium-1 (Ra^{228}), ThX (Ra^{224}), and ThB (Pb^{212}) remain almost completely in the residue, and in the solution, separated from the latter, only the products of decomposition of RaTh are accumulated. In the solution the γ-emitter is ThB in equilibrium with ThC and ThC″. Maximal sensitivity in the differential γ-measurements was obtained for ThB radiation in the 80 and 238 keV regions of the spectrum (see Fig. 1). To determine thorium we selected the 238 keV energy region, for which separation of uranium and thorium γ-radiation is better than at 80 keV.

TABLE 1. Measurement Sensitivity and Background in Channels

Sample	Content, g/liter	First channel pulse/min		Second channel (220-260 keV), pulses/min
		85–100 keV	170–200 keV	
U	1,0	410,8	182,8	26,8
Th	1,0	267,6	198,4	639,0
Background	—	18,2	28,7	22,8

Note: Sample volume 100 cm^3, size of NaI(Tl) crystal 40 × 40 mm.

The sulfuric acid solution obtained when ores containing uranium and thorium are subjected to attack by H_2SO_4 contains small amounts of Ra^{226} and Ra^{228}. Furthermore, Ra^{224} is accumulated relatively rapidly in a solution from RaTh. To exclude the effect of γ-radiation of the decomposition products of Ra^{226} and Ra^{228} and to establish the accumulation time of ThX, in order to make an appropriate correction, radium is removed by coprecipitation with barium. To the analysis sample are added 15-20 drops of barium chloride and the precipitate is filtered. During solution, filtration, etc., radon is removed from the liquor. The filtrate is then transferred to a beaker

Translated from Atomnaya Énergiya, Vol. 31, No. 6, pp. 633-635, December, 1971. Original article submitted October 15, 1970; revision submitted January 25, 1971.

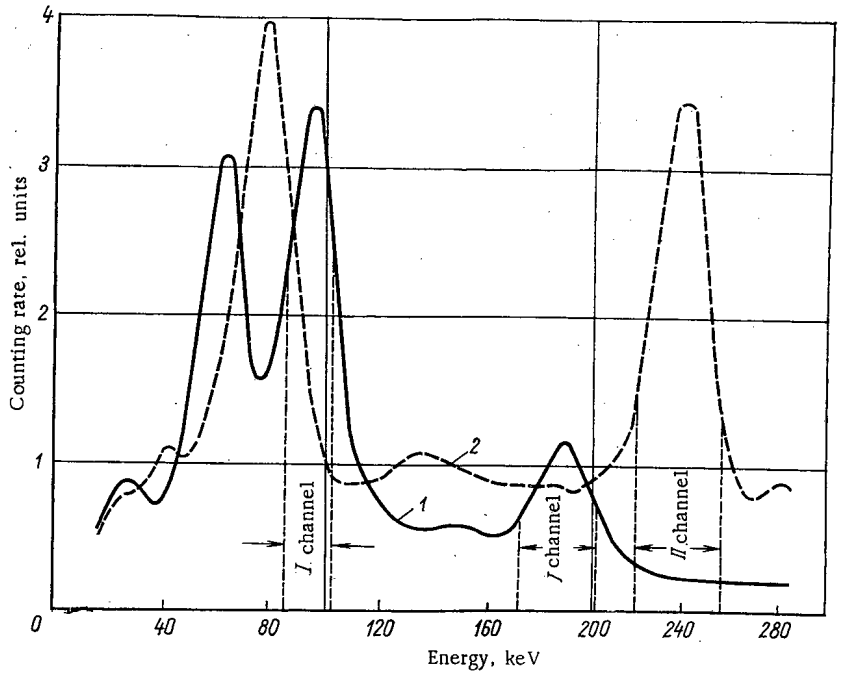

Fig. 1. Scintillation spectra of γ-radiation: 1) uranyl nitrate solution (UX_1 in equilibrium with U^{238}); 2) sulfuric acid solution of thorium (RaTh in equilibrium with the decomposition products).

for sample measurement, which is then sealed. After 3 days, when the γ-emitters $MsTh_2$ and the decomposition products of radon have decayed and mobile equilibrium is established between ThB and ThX, the activities of samples in two sectors of the γ-spectrum are measured: 93 and 238 keV or 185 and 238 keV. The sensitivity of uranium measurements at 93 keV is 2.2 times greater than at 185 keV (see Table 1); therefore to determine the uranium and thorium content in sulfuric acid solutions obtained after breaking up ores in which UX_1 is in equilibrium with U^{238}, it is desirable to measure the activities of the samples at 93 and 238 keV. If from solutions with less than 35 g/liter H_2SO_4 we remove preferentially uranium or thorium and the equilibrium between U^{238} and UX_1 is disturbed (because UX_1 is a thorium isotope), uranium and thorium are determined from the activities of samples in the 185 and 238 keV regions of the γ-spectrum. The window width at the photopeak of UX_1 is 15 keV, the values for U^{235} and ThB being 30 and 40 keV, respectively.

The number of elements determined in the specimens is calculated by the equation:

$$U = \frac{1}{p_1 - p_2}(A_1 - A_2); \tag{1}$$

$$Th = \left(\frac{p_1}{p_1 - p_2} A_2 - \frac{p_2}{p_1 - p_2} A_1\right) \cdot \frac{1}{1 - e^{-\lambda_{ThX} t_1}}, \tag{2}$$

where U and Th are the uranium and thorium contents of the sample in g/liter, respectively; A_1 is the activity of the sample in the corresponding channels (expressed as thorium equivalent); p_1 is the thorium equivalent of uranium in the corresponding channels; λ_{ThX} is the decay constant of ThX; t_1 is the accumulation time of ThX in the sample. The samples and standards are measured under the same geometrical conditions at equal volumes. Hence

$$p_i = \frac{Q_{Th} N_i^U}{Q_U N_i^{Th} k}; \tag{3}$$

$$A_i = \frac{Q_{Th} N_i^{sa}}{N_i^{Th} k}; \tag{4}$$

$$k = \frac{1}{e^{-\lambda_{RaTh} t_2}}, \tag{5}$$

where Q_U and Q_{Th} are the uranium and thorium contents of the standards, in g/liter, N_i^{sa}, N_i^U, and N_i^{Th} are respectively the counting rates for measurement of the sample and the uranium and thorium standards in

the corresponding channels, in pulses/min; k is a correction factor for decay of RaTh in the thorium standard; λ_{RaTh} is the decay constant of RaTh; and t_2 is the time elapsing since separation of RaTh from $MsTh_1$ in the thorium standard.

As the uranium standard we used a solution of uranyl nitrate in weak hydrochloric acid, in which UX_1 is in equilibrium with U^{238}. The thorium standard is prepared by dissolving the powdered thorium standard in sulfuric acid. Ra^{228} is removed from the solution by coprecipitation with barium, and the only γ-emitters remaining in the standard are those of the decay products of RaTh. The thorium content of the standard solution is determined chemically. The standard is used for measurements 25-30 days after hermetic sealing, when mobile equilibrium between RaTh and ThX is established in the solution. Analyses with the standard may be performed approximately after six months; in this case, accumulation of RaTh from $MsTh_1$ can be neglected.

A layer of the sample, 6 mm thick, may be regarded as a thin layer for γ-radiation of UX_1 (93 keV) when the solution has a salt content of up to 50 g/liter, and for γ-radiation of U^{235} up to 200 g/liter. In solutions in beneficiation plants the total salt content is usually less than 20 g/liter. To analyze solutions with a salt concentration of more than 50 g/liter, one must prepare standards with densities and chemical compositions similar to the sample being analyzed.

The threshold of sensitivity of determinations [2] for 100 cm^3 samples with a measurement period of 10 min in each channel for measurements at 93 and 238 keV is 0.015 g/liter for uranium and 0.01 g/liter for thorium; for measurements in the 185 and 238 keV regions of the γ-spectrum, it is 0.04 and 0.01 g/liter for uranium and thorium, respectively. In measurements of the activities of samples at 93 and 238 keV, the discrepancies between radiometric and chemical analysis of uranium and thorium for samples with uranium and thorium contents of 0.1-1.4 and 0.08-0.5 g/liter, respectively, are less than ±10%. The results of uranium and thorium determinations are unaffected by the presence of zirconium, rare earths, and other elements in the solution, although they complicate chemical analysis. Radiometric determinations of uranium and thorium by a single-channel analyzer are approximately four times more efficient than the chemical method and are far cheaper.

LITERATURE CITED

1. A. L. Jakubovich, E. I. Zaitsev, and V. V. Anosov, At. Énerg., 15, 224 (1963).
2. E. I. Zheleznova, I. P. Shumilin, and B. Ya. Yufa, Radiometric Methods of Analyzing Natural Radioactive Elements [in Russian], Nedra, Moscow (1968).
3. A. N. Nesmeyanov et al., Practical Manual of Radiochemistry [in Russian], Goskhimizdat, Moscow (1956).

HIGHLY EFFICIENT NEUTRON DETECTOR

I. V. Sanin, G. N. Markov,
A. I. Krivenko, and N. G. Ivchenko

UDC 539.1.074.4:539.125.5

By making use of the Cerenkov radiation generated during the motion of fast electrons in water, and the feasibility of producing radiators with a large volume of $Cd(NO)_2$ and NaCl solutions, we were able to produce a radiator for recording neutrons with a sensitivity of 0.03 neutron/cm^2 per detector pulse [1].

In the present paper we give results of an investigation of the characteristics of a Cerenkov detector with a radiator in the form of an NaCl solution (30 parts NaCl/100 g water) of dimensions 550 × 500 × 200 mm. The Cerenkov radiation that characterizes the capture of slowed neutrons by nuclei of chlorine and hydrogen (five captures by chlorine for each capture by hydrogen) was recorded with an FÉU-65 photomultiplier, placed at the center of the lateral face.

In order to eliminate the electrostatic fields in the radiator volume we used a circuit in which the photomultiplier was connected to a grounded photocathode [2]. The photomultiplier operated in a single-electron pulsed regime, i.e., it recorded pulses from individual photons [3].

We used a Pu – Be source of strength $1.85 \cdot 10^6$ neutrons/sec (+10%), placed 0.7 m from the detector; in measurements with this source we obtained 6860 pulses/sec, which defines the sensitivity; approximately 0.004 neutron/cm^2 · pulse. The recoil protons that are generated when fast neutrons are slowed down are not recorded, which defines approximately the same sensitivity of the Cerenkov detector for measurements of intensity of pulsed and static neutron fluxes. A small change of sensitivity in static measurements results in the recording of γ-quanta in reactions of the inelastic scattering (n, n') by oxygen, sodium, and chlorine (~20% for neutron energy ~10 MeV).

To record neutron absorption events, we use the γ-radiation of Cl^{35} with energy ~7 MeV. For water, the minimum energy that γ-quanta must have in order to register is ~0.5 MeV; therefore, the Cerenkov detector can be used on a background of intense γ-radiation with energy ~0.5 MeV. From the experimental results (see Fig. 1) with Co^{60} γ-sources (E_γ = 1.12 and 1.33 MeV) and Cs^{137} γ-sources (E_γ = 0.661 MeV), we see that the sensitivity for recording Cs^{137} γ-quanta is approximately 100 times worse than the sensitivity for recording neutrons from a Pu – Be source.

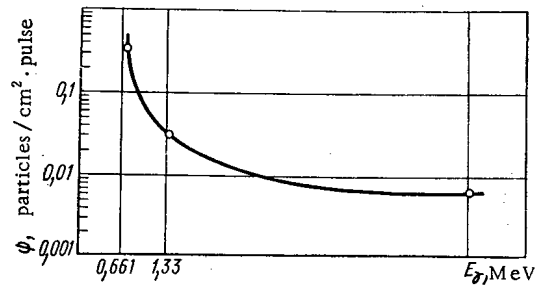

Fig. 1. Cerenkov-detector sensitivity as a function of γ-quanta energy.

The time distribution of pulses for measurements with a pulsed neutron source enables us to determine the neutron lifetime in a Cerenkov detector [4]. The lifetime ≃50 μsec and is determined by the NaCl concentration and by the absorption cross section of Cl^{35} thermal neutrons ($\sigma \approx 33$ barn).

The authors would like to thank S. V. Samylov and V. I. Semyachkov for helpful discussions and help with the measurements.

LITERATURE CITED

1. I. V. Sanin, G. N. Markov, and N. G. Ivchenko, At. Énerg., 27, 354 (1969).
2. F. Reines et al., Rev. Scient. Instrum., 25, 1061 (1954).

Translated from Atomnaya Énergiya, Vol. 31, No. 6, pp. 635-636, December, 1971. Original article submitted February 23, 1971; revision submitted April 6, 1971.

3. A. N. Pertsev, A. N. Pisarevskii, L. D. Sosnin, Zh. Prikl. Spektroskopii, 2, 369 (1965).
4. V. M. Gorbachev and Yu. S. Zamyatnin, At. Énerg., 3, 101 (1957).

FAST-NEUTRON RADIATION RESISTANCE OF SILICON SURFACE-BARRIER DETECTORS

I. I. Lazutkin, B. I. Sinitsyn,
O. P. Fedoseeva, and S. G. Tsypin

UDC 539.1.074

The effect on the operational characteristics of surface-barrier detectors (SBD) produced by protons of various energies [1-4] and by α-particles [5, 6] has been reported. The radiation resistance of SBD with respect to neutrons has hardly been investigated although the timeliness of such information is obvious, particularly when detectors are used in conjunction with radiators for neutron detection [7].

Our present purpose is a study of the change in the basic operating characteristics of an SBD – such as inverse current, intrinsic noise, energy resolution, capacity, resistance in the forward direction, and efficiency in collection of charge produced by 5.5 MeV α-particles – as a function of the fast-neutron flux (Fig. 1). The characteristics mentioned were measured over the reverse voltage range 0.15 V.

Fifteen mass-produced type DKP_S detectors were used which had the following characteristics: area, 50 mm^2; energy resolution for 5.5 MeV α-particles, 1-2%, and charge collection efficiency, 100%. The detectors were made from BKÉF-200 n-type silicon with a specific resistance of 200 Ω/cm. The maximum neutron flux incident on the detectos was $4 \cdot 10^{13}$ neutrons/cm^3. Five detectors were irradiated with a flux density of $2.2 \cdot 10^8$ neutrons/$cm^2 \cdot$sec, and ten with a flux density of $5.5 \cdot 10^8$ neutrons/$cm^2 \cdot$sec, with five of these held at a reverse voltage of 10 V during irradiation.

The inverse current of a detector began to increase markedly at a flux of $5 \cdot 10^{11}$ neutrons/cm^2, which agrees with published data. It should be pointed out that averaged results for five detectors are given in Figs. 2 and 3 (voltage was applied to the SBD during irradiation). The spread in the relative variation of the detector parameters after irradiation did not exceed 30% with the exception of the inverse current, for

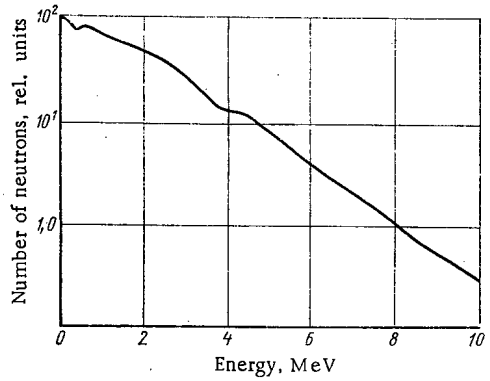

Fig. 1

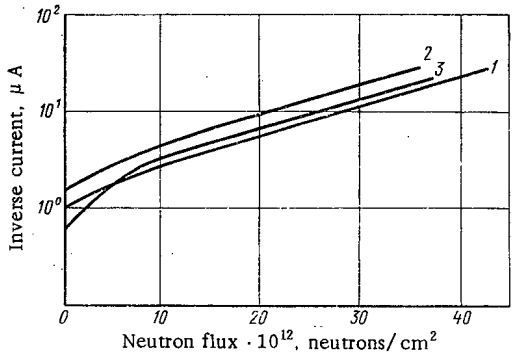

Fig. 2

Fig. 1. Neutron spectrum.

Fig. 2. Dependence of inverse current of an SBD at 10 V on the magnitude of the neutron flux D. Neutron flux densities: 1) $2.2 \cdot 10^8$ neutrons/$cm^2 \cdot$sec; 2) $5.5 \cdot 10^8$ neutrons/$cm^2 \cdot$sec; 3) $5.5 \cdot 10^8$ neutrons/$cm^2 \cdot$sec.

Translated from Atomnaya Énergiya, Vol. 31, No. 6, pp. 636-637, December, 1971. Original article submitted February 1, 1971; revision submitted April 19, 1971.

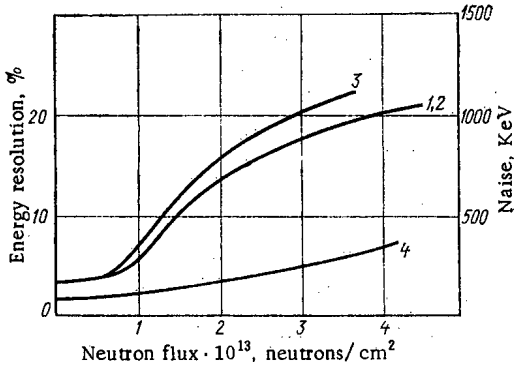

Fig. 3

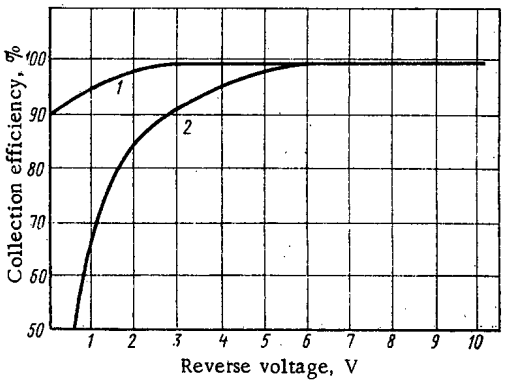

Fig. 4

Fig. 3. Dependence of SBD energy resolution (curves 1-3) and noise (curve 4) on D for V = 10 V: 1) P = $2.2 \cdot 10^8$ neutrons/cm^2 · sec; 2) P = $5.5 \cdot 10^8$ neutrons/cm^2 · sec; 3, 4) P = $5.5 \cdot 10^8$ neutrons/cm^2 · sec.

Fig. 4. Charge collection efficiency as a function of reverse voltage: 1) for an unirradiated detector; 2) for a detector exposed to $4.4 \cdot 10^{13}$ neutrons/cm^2.

which the spread can be 100%. The spread in the relative variation of the parameters increases with increasing integral radiation dose.

A marked increase in noise and degradation of the energy resolution (see Fig. 3) begins at a flux of $5 \cdot 10^{12}$ neutrons/cm^2, with the energy resolution worsening more rapidly than the increase in SBD noise, particularly at high fluxes. This can be explained by the post-radiation increase in the contribution to the energy resolution from fluctuations in collection of the charge produced throughout the volume of the detector by α-particles.

The parameter least sensitive to irradiation is the charge collection efficiency. For reverse voltages above 7 V, it does not vary as a function of the neutron flux of $4.4 \cdot 10^{13}$ neutrons/cm^2 (Fig. 4).

During irradiation, the series resistance of the detectors rose sharply (from 60 Ω to 40 kΩ at maximum flux), which is explained by the increase in resistance of the silicon in the undepleted region.

The increase in silicon resistance during irradiation leads to a decrease in the capacity of the detectors and to a change in the shape of the voltage-capacity characteristic. A marked reduction in capacity begins at a flux of 10^{12} neutrons/cm^2, and the reduction is more marked at lower operating voltages.

No significant difference was observed between the radiation resistance of detectors kept under reverse voltage during irradiation and that of those not under voltage. An increase in the flux density of the neutrons during irradiation by a factor of two did not change the degree of susceptibility to damage for detector characteristics when the fluxes were the same.

LITERATURE CITED

1. J. Coleman et al., IEEE Trans. Nucl. Sci., 15, 120 (1968).
2. J. Coleman et al., IEEE Trans. Nucl. Sci., 15, 363 (1968).
3. G. George, Nucl. Instrum. Methods, 25, 253 (1964).
4. A. S. Brykina et al., Kosmich. Issled., 2, 623 (1964).
5. A. E. Antropov et al., Kosmich. Issled., 5, 622 (1967).
6. G. Dearnaley, IEEE Trans. Nucl. Sci., 10, 106 (1963).
7. I. A. Baranov, Pribory i Tekh. Eksperim., No. 2, 181 (1964).

DEPENDENCE OF SCINTILLATION COUNTER OUTPUT PULSE HEIGHT ON RATIO OF EXIT WINDOW AND PHOTOCATHODE AREAS

B. K. Damitov

UDC 539.1.074.3

In solving some γ-ray spectrometry problems, it is necessary to couple a photomultiplier of small diameter to a scintillator having a large-area exit window. In that case, it is necessary to know the dependence of the output signal from the scintillation counter on the ratio of the areas of the photocathode and scintillator exit window. The case where a circular reflector with an opening is placed between the photomultiplier photocathode and the scintillator ("iris" detector) has been discussed [1]. Using certain assumptions, the authors of [1] obtained the dependence of the pulse amplitude V at the photomultiplier output on the ratio x of the area q of the reflector opening and the area q_0 of the crystal exist window:

$$\frac{1}{V}=\frac{2a\rho_s\rho_d}{Ak(1+a\rho_s)}+\frac{1-a\rho_s(1-2w+2a\rho_d w)}{Akaw(1+a\rho_s)}\cdot\frac{1}{x}. \quad (1)$$

Here, a is the transmittance of the crystal; A is the number of photons produced in the scintillator; ρ_s and ρ_d are respectively the coefficients of reflection of scintillation light for the walls and diaphragm; k is a constant of proportionality between the number of photons per scintillation and the pulse height of the signal at the counter output; and w is the mean value of the relative solid angle for the escape of scintillation light through the diaphragm.

When using a diaphragm, the geometric conditions for light collection are different from those which are obtained with direct coupling of photomultiplier and scintillator. It is therefore advisable to consider the case where a photomultiplier with a cathode of small area is optically coupled to a crystal having an exist window of large area without the use of light pipes or diaphragms. It has been shown [1, 2] that a cylindrical scintillator can be approximated by a scintillator of spherical shape like a photometric sphere.

To obtain the relation V = f(x), we assume that the crystal is transparent to its own radiation ($a = 1$), and we consider a flash of light at the center of the sphere. The photosensitive area σ is an opening in a sphere with surface area $(S + \sigma)$.

The incident light flux per unit area of the photosensitive surface σ consists of two terms:

$$I(D)=J(D)+\int \rho(B)\,I(B)\frac{dw(B)}{4\pi}, \quad (2)$$

where J(D) is the light flux from the source directly incident per unit area at the point D (unreflected light flux); $\int \rho(B)I(B)dw(B)/4\pi$ is the light flux incident per unit area at the point D as the result of reflection of scintillation light by walls with a reflection coefficient ρ_s; dw(B) is the solid angle subtended by the area element dS containing the selected point B.

Since the window is a small "perturbation" in a sphere with a diffuse reflecting internal surface, we assume that the window also reflects light in accordance with Lambert's law (coefficient of reflection, ρ_t). Then, solving Eq. (2) for the particular case of J(D), we obtain [3]:

$$I(D)=J(s+\sigma)\frac{1}{S(1-\rho_s)+(1-\rho_t)}, \quad (3)$$

where $J(S + \sigma)$ is the total energy in the light flash and $(1 - \rho_t)$ is the fraction of light passing through the window onto the photosensitive surface σ. Multiplying both sides of (3) by $\sigma(1 - \rho_t)$, we have

Translated from Atomnaya Énergiya, Vol. 31, No. 6, pp. 637-639, December, 1971. Original article submitted January 18, 1971.

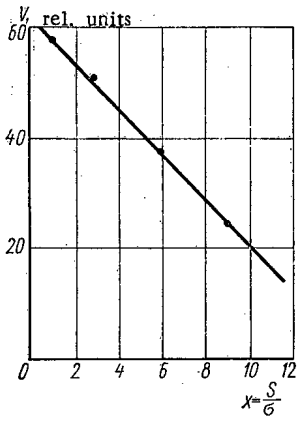

Fig. 1

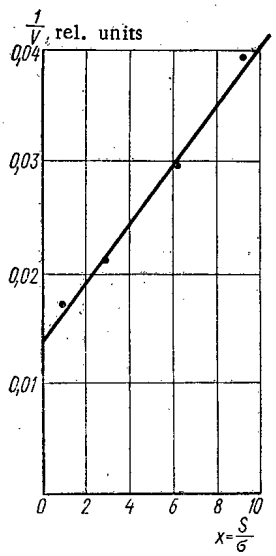

Fig. 2

Fig. 1. Dependence of signal amplitude V at output of scintillation counter on ratio of areas.

Fig. 2. Dependence of the inverse of the signal amplitude at the output of the scintillation counter, 1/V, on ratio of areas: ——) theoretical relation (6); •) experiment.

$$E=\frac{E_0\sigma(1-\rho_t)}{S(1-\rho_s)+\sigma(1-\rho_t)}, \tag{4}$$

where $E = I(D)\sigma(1 - \rho_t)$ is the energy delivered to the photocathode through the window in the spheres and $E_0 = J(S + \sigma)$ is the total energy of the light flash. Equation (4) can be transformed to

$$\frac{1}{E}=\frac{1}{E_0}\cdot\frac{S}{\sigma}\left(\frac{1-\rho_c}{1-\rho_t}\right)+\frac{1}{E_0}. \tag{5}$$

Thus Eq. (5) relates the energy incident on the photosensitive layer to the area ratio $(S/\sigma) = x$. With a proportional relationship between energy absorbed in the scintillator and pulse height at the counter output, we have

$$\frac{1}{V}=\frac{1}{V_0}x\left(\frac{1-\rho_c}{1-\rho_t}\right)+\frac{1}{V_0}, \tag{6}$$

where V is the amplitude of the pulse corresponding to total transfer of scintillation energy to the photolayer (coefficient of light collection k = 1).

As an experimental check of Eq. (6), an FÉU-60 photomultiplier with a photocathode area of 78.5 mm^2 was optically coupled to NaI(Tl) crystals with different exit window areas. S was 78.5 mm^2 for crystal No. 1, 217.8 mm^2 for No. 2, 471 mm^2 for No. 3, and 705 mm^2 for No. 4.

No reflector or diaphragm was used on the portion of the exit window not covered by the photomultiplier. Results of an experiment with a Cs^{137} source are shown in Fig. 1. It is clear that the height of the output pulses decreases significantly and becomes comparable to the intrinsic noise of the photomultiplier when there is a considerable decrease in the diameter of the photocathode and a fixed area for the exit window. Because of this, it is impossible to decrease the photocathode diameter without limit.

To compare the experimental results with the theoretical equation (6), the curve was replotted in Fig. 2 with the coordinates $(1/V) = f(x)$. It is clear from Fig. 2 that the experimental data is in satisfactory agreement with the theoretical relation (6).

The experimental results thus showed that the replacement of a cylindrical scintillator by a spherical one of the type of a photometric sphere is completely proper. It was established that the theoretical relation

(6) satisfactorily describes the behavior of a scintillation counter consisting of optically coupled photomultiplier and crystal of markedly different diameters without diaphragm or reflector on the uncovered portion of the exit window of the crystal.

LITERATURE CITED

1. E.A. Mokhir and Yu.A. Tsirlin, in: Monocrystals, Scintillators, and Organic Luminophors [in Russian], No. 1, Khar'kov (1967), p. 63.
2. Methods of Experimental Physics, Vol. 5, Nuclear Physics, Luke C.L. Yuan and Chien-Shiung Wu (editors), Academic Press, New York (1961) (Vol. 5A); (1963) (Vol. 5B).
3. J. Daniels and Y. Laura Tsui, Canad. J. Phys., 47, 2125 (1969).

ANALYSIS OF γ-RADIATION FIELD IN SOIL FROM RADIOACTIVE FALLOUT

V. V. Pavlov, I. E. Konstantinov, and G. A. Fedorov

UDC 551.578

A knowledge of the γ-radiation dose field is of interest in connection with the problem of the contamination of soil by radioactive matter. In particular, this knowledge is necessary in order to estimate the degree of danger from radioactive contamination to the fruits and roots of plants. The calculation of the dose field and selection of the source model requires the determination of the nature of the distribution of the radioactive matter as a function of depth in the soil. The plane source model, which is often applied to dose calculations, can be of insufficient accuracy since, with the passage of time, the radioactive fallout penetrates the soil.

Spectrometric investigations of the distribution of radioisotopes in samples [1-4] show an exponential law for the distribution of isotopes with depth, in soil of various types. For practical purposes one can consider that all radioactive matter is found within a surface layer of thickness 3 to 6 cm. The dependence on depth of the radioisotope concentration changes with time and is caused by such factors as the age of the radioactive fallout, the type of soil, meteorological conditions, chemical and physical properties of the deposited isotopes, as well as other factors.

Therefore a volume source model, with the distribution of an isotope in the upper layers of the soil being described by some function, is more realistic than the plane source model. We present below the results of an analysis of the γ-radiation field based on a volume source model with a sharply falling off concentration of radioactive matter with depth. These results permit one to make conclusions of practical significance concerning the dependence of the γ-radiation dose field in the soil on the functional form of the distribution of isotopes in the soil. Because the particular isotope chosen has no essential significance, the results of the analysis are presented for Cs^{137}, one of the most long-lived fission products.

We assume, in agreement with the results of [1-4], that the concentration of the isotope as a function of the depth z below the surface may be described in the form

$$q = q_0 e^{-kz}, \tag{1}$$

where q_0 is the concentration in the surface layer; and k is a constant (in cm^{-1}) depending on the type of soil, and other factors.

We shall include multiple scattering in the air and the ground in the calculation for infinite media [5] by the introduction of dose buildup factors into the formula for the dose rate from primary radiation; these buildup factors are for γ-quanta coming from a point isotropic source in an infinite medium and are represented in the form of a sum of exponents [6]. We obtain by this method the following expression for the total exposure dose rate P (in rad/yr) in the soil, for γ-radiation of the given isotope:

$$P = 1.44\sigma \sum_i \gamma_i n_i \varepsilon_i f_i (\varepsilon_i, z, k/\rho). \tag{2}$$

Here $\sigma = q_0/k$ is the surface density of radioactive contamination of the soil, in $\mu Ci/km^2$; γ_i is the linear energy (true) absorption coefficient in air, for γ-radiation of the i-th line, in cm^{-1}; n_i is the yield of quanta of the i-th line per disintegration; ε_i is the energy of the quanta of the i-th line, in MeV; and f_i is the dimensionless function given by

Translated from Atomnaya Énergiya, Vol. 31, No. 6, pp. 639-640, December, 1971. Original article submitted December 10, 1970.

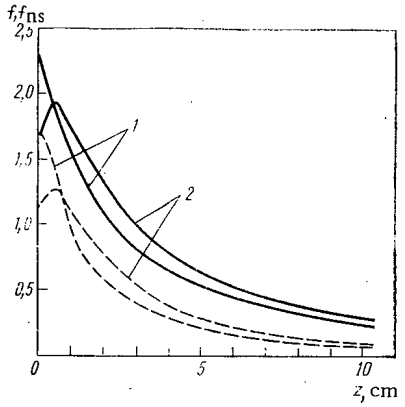

Fig. 1. The total dose rate function f (——) and the primary (due to radiation which is not scattered) dose rate function f_{ns} (– – –) as a function of the depth z of the detecting point for values of k equal to 1 cm^{-1} (curve 2) and 4 cm^{-1} (curve 1). Soil Density 1.7 g/cm^3, γ-quanta from Cs^{137}.

$$f_i(z)=\frac{1}{2}\sum_{j=1}^{2} A_j\left\{E_i(\mu_j z)+e^{-kz}E_i[(k-\mu_j)z]+e^{-kz}\ln\frac{k+\mu_j}{k-\mu_j}\right\}; \tag{3}$$

$$f_i(z=0)=\frac{1}{2}\sum_{j=1}^{2} A_j\ln\left(1+\frac{k}{\mu_j}\right), \tag{4}$$

where $E_i(x)$ is the exponential integral function [7], $E_1(x) = E_i(-x)$, and the coefficient μ_j is related to the linear attenuation coefficient μ_i for γ-radiation of energy ε_i by

$$\mu_j=\mu_i(1+a_j).$$

In the above expression a_j is a parameter in the approximation, in the form of a sum of exponents, of the buildup factor for γ-quanta from a point isotropic source in aluminum,

$$B=\sum_{j=1}^{2} A_j e^{-a_j\mu r}. \tag{5}$$

However, test calculations have shown that such an approximation does not give results close to the solution of the transport equation [8], for sources of γ-quanta with energies 0.661 MeV. Consequently, another approximate buildup factor, based on the results of [9], was proposed:

$$B=1+\mu r+\frac{(\mu r)^2}{4.81}. \tag{6}$$

The values calculated from this formula agree with the data of [8] with an accuracy of not less than 6%, for relaxation lengths μr ranging from 1 to 20.

If one uses Eq. (6) for the buildup factor then the dose function in Eq. (2) takes the form

$$f_i(z)=\frac{1}{2}\left\{E_1(\mu_i z)+e^{-kz}\left[E_i((k-\mu_i)z)+\ln\frac{k+\mu_i}{k-\mu_i}\right]+\frac{k}{k-\mu_i}\left[(e^{-\mu_i z}-e^{-kz})\left(1+\frac{k-2\mu_i}{4.81(k-\mu_i)}\right)+\frac{\mu_i z e^{-\mu_i z}}{4.81}\right]+\frac{ke^{-kz}}{k+\mu_i}\left[1+\frac{k+2\mu_i}{4.81(k+\mu_i)}\right]\right\}; \tag{7}$$

$$f_i(z=0)=\frac{1}{2}\left\{\ln\left(1+\frac{k}{\mu_i}\right)+\frac{k}{k+\mu_i}\left[1+\frac{k+2\mu_i}{4.81(k+\mu_i)}\right]\right\}. \tag{8}$$

Some results of the calculation are given in Fig. 1. It is interesting to note that the maximum dose rate shifts from the soil surface to levels below the surface for low values of the quantity k/ρ. Results of the calculation of the total dose function using Eqs. (3) and (4) agree to within 30% with the results of the more accurate calculations using Eqs. (7) and (8); no less accurate results were obtained in this work. The soil density was taken as $\rho = 1.7$ g/cm^3 in the calculation, and the constant k in the exponent was taken as equal to 1, 2, 3, or 4. The linear radiation attenuation coefficient was taken as the product of the soil density and the mass radiation attenuation coefficient for aluminum:

$$\mu=\mu_{Al}\rho.$$

In our case the magnitude of the penetration depth constant k is significantly greater than the linear attenuation coefficient μ. It follows therefore that some terms in Eq. (7) can be neglected for z greater than 3 to 5 cm, and it is possible to use the dose function formula in a simpler form.

Note that, for detecting points having equal values of ρz, the dose function does not depend on k and ρ separately, but only on their ratio k/ρ.

The results of the calculation show that increasing the constant k/ρ (but keeping k/ρ within a realistic range corresponding to the experimental data of [4], k/ρ between 0.3 and 6 cm^2/g), while keeping the quantity $\sigma = q_0/k$ constant, leads to an increase in the functions f and f_{ns} characterizing the dose field, for points close to the soil surface, and to a decrease for distances (measured by ρz) greater than some 0.8 to 1.7 g/cm^2. However, this rise and fall is quite weak. Thus, for example, an increase in the magnitude of the constant k/ρ by a factor of 4 (from 0.588 to 2.35 cm^2/g) leads to a growth of the dose rate at the soil surface by 43% and a decrease of its magnitude by 17% and 9% for depths equal respectively to 8.5 and 51 g/cm^2. It therefore follows that the use, in the analysis of the dose field, of the exponential function as an approximation to the dependence of the radioisotope concentration on depth, instead of the accurate but more complex function describing the true dependence of concentration on depth, cannot significantly reduce the accuracy to which the characteristics of the dose field are determined.

LITERATURE CITED

1. G. A. Fedorov et al., in: Dosimetry Problems and Radiation Shielding [in Russian], L. R. Kimela (editor), No. 8, Atomizdat, Moscow (1968), p. 125.
2. G. A. Fedorov et al., Nature of the Vertical Distribution of Cs^{137} in Soils in Some Regions of the USSR in 1966-1967 [in Russian], Atomizdat, Moscow (1968).
3. V. F. Brendakov et al., At. Énerg., 25, 331 (1968).
4. Yu. A. Israel' and E. D. Stukin, γ-Radiation from Radioactive Fallout [in Russian], Atomizdat, Moscow (1968).
5. V. V. Pavlov, Dissertation [in Russian], Moscow (1969).
6. H. Goldstein, Fundamental Aspects of Reactor Shielding, Addison–Wesley, Reading, Mass. (1959).
7. Tables of the Exponential Integral Function [in Russian], Izd. AN SSSR (1954).
8. L. R. Kimel' and V. I. Maskovich, Handbook of Shielding against Ionizing Radiation [in Russian], Atomizdat, Moscow (1966).
9. J. Z. Holland, Proc. Int. Conf. on the Peaceful Uses of Atomic Energy, Geneva (1955), Vol. 13, United Nations, New York (1956), p. 110.

INAUGURATION OF THE FRENCH LIQUID-HYDROGEN BUBBLE CHAMBER "MIRABELLE" AT THE INSTITUTE OF HIGH-ENERGY PHYSICS

The assembly and operational tests of the liquid-hydrogen bubble chamber Mirabelle have been completed. This chamber, built by French physicists, was installed in a special building near the world's most powerful proton accelerator at the Institute of High-Energy Physics [IFVÉ] in Serpukhov. The construction of Mirabelle and the joint physical experiments scheduled to be staged with that machine were covered in a Franco–Soviet contract concluded between the USSR State Committee on the Peaceful Uses of Atomic Energy [GKIAÉ] and the French Commissariat de l'Énergie Atomique, in October, 1966.

The ceremony inaugurating the Mirabelle facility was held on October 15, 1971. The crimson ribbon in front of the building entrance was cut by the French minister of industrial and scientific development Francois-Xavier Ortoly, and by the chairman of the USSR State Committee on Peaceful Uses of Atomic Energy A. M. Petros'yants.

After inspecting Mirabelle and the accelerator, the numerous visitors, press representatives, French and Soviet specialists working at IFVÉ, all gathered for a solemn gala meeting at which speeches were delivered by A. M. Petros'yants, Andre Giraud the principal administrator of the Commissariat de l'Énergie Atomique, Academician M. V. Keldysh president of the Academy of Sciences of the USSR, Francois-Xavier Ortoly, and by the vice-chairman of the Council of Ministers of the USSR, the chairman of the State Committee of the Council of Ministers of the USSR on science and industry Academician V. A. Kirillin. The

Fig. 1. Inauguration ceremony. In the foreground Francois-Xavier Ortoly and A. M. Petros'yants.

Translated from Atomnaya Énergiya, Vol. 31, No. 6, pp. 641-642, December, 1971.

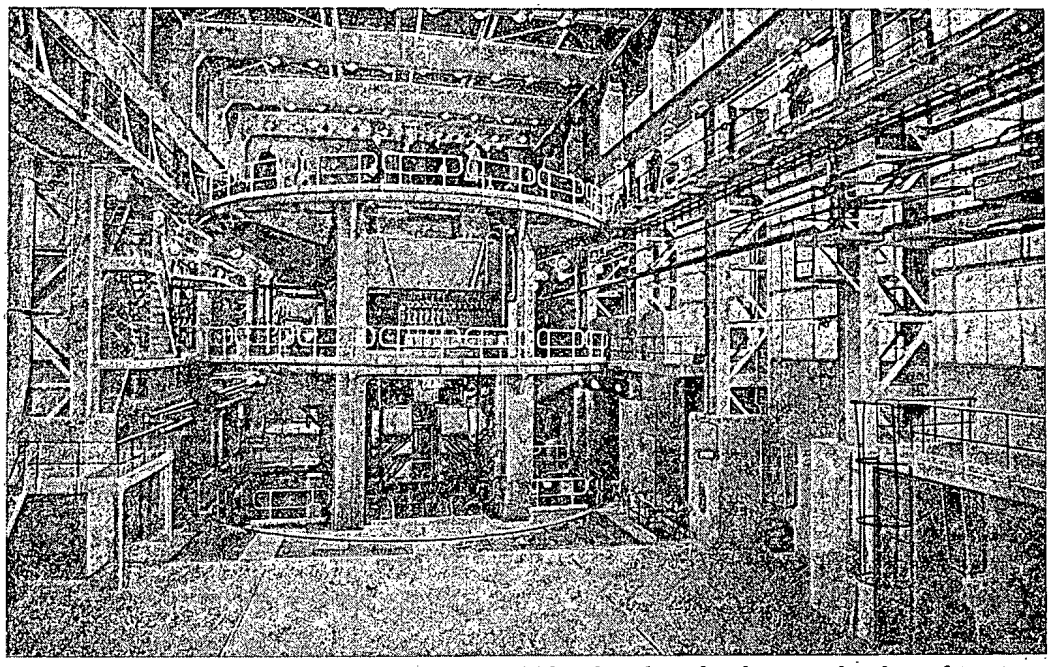

Fig. 2. The Mirabelle liquid-hydrogen bubble chamber facility on the day of its inauguration.

French ambassador to the USSR Roger Seydoux took part in the offficial ceremonies marking the commissioning of the Mirabelle bubble chamber.

A description of the design features and experimental capabilities of the Mirabelle bubble chamber will be presented in one of the coming issues of our periodical.

SOVIET SPECIALISTS VIST BRITAIN

V. V. Orlov

Under the terms of an agreement concluded by the USSR State Committee on the Peaceful Uses of Atomic Energy [GKIAÉ] and the United Kingdom Atomic Energy Authority [UKAEA], a delegation of Soviet specialists made a visit to British nuclear power centers in July, 1971. The delegation was brought up to date on the work being done on fast power reactors at the reactor centers at Risley (near Manchester) and Dounreay (Scotland), and at the Winfrith Heath Research Institute, and also had some concluding talks with British UKAEA specialists in London.

Britain is engaged in an extensive program geared to the building and industrial assimilation of nuclear power stations built around fast reactors. An experimental fast reactor, the 60 MW(th) DFR reactor (cooled by Na–K alloy) had already been in service for twelve years at Dounreay, and has served as a facility for research on fast-reactor fuels and materials to aid in the design of future nuclear power stations using fast reactors. Construction work on a prototype nuclear power station based around the PRF fast reactor, rated at 250 MW(e), is nearing completion at the same site. The startup of this reactor is scheduled for March, and it is to be brought up to full power in early 1973. The distinguishing feature of this reactor startup program is the preliminary "water run-in" of the primary loop, scheduled for the purpose of checking out the operation of the process equipment, checking for generation of vibrations, etc. The PFR reactor, built integrally with the primary loop in a tank 13 m in diameter, will be loaded with fuel in the form of a PuO_2 and UO_2 mixture clad with grade 316 stainless steel. The sodium temperature at the core exit is 562°C, but will be brought up to 580°C later on.

The parameters of the superheated steam upstream of the turbine are 170 atm and 510°C.

The system devised for inspecting core performance is of special interest, particularly measurements of acoustical noise with the aid of a specially developed device which underwent successful tests on the DRF reactor.

The UKAEA is utilizing its experience in the building of the PFR reactor (actually built by the firms TNPG and BNDC under contract with UKAEA) in the development of plans for large commercially competitive nuclear power stations to be built around the CFR fast reactors rated at 1300 MW(e). It is anticipated that an order for the leading nuclear power station of that output rating will be forthcoming sometime in 1972, and that orders will be placed for the fabrication of plant equipment by 1974–1975, while construction work on the CFR fast reactor will be in progress by that time. In all the reactor and power plant projects concerned here, the coolant will be sodium at the same temperatures as in the PFR, the integral construction of the reactor will be retained, with oxide fuel and, possibly, carbide fuel.

The cost estimate outlook for nuclear power development in Britain indicates that getting fast reactors on the line feeding electric power into the national power grid will result in savings of ~500 million pounds sterling (as referred to the current level of expenditures), and will solve the country's fuel problem, which is particularly important for Britain inasmuch as the islands do not provide their own native resources of natural uranium. Further, British specialists do not view stepping up plutonium breeding rates as a major problem in the design of fast reactors, and instead remain contented with doubling times of the order of 15 years. This position is understandable when we take into cognizance the scale of construction of nuclear power stations with thermal reactors (~40 million kW by 1980) covering the plutonium needs for the initial period of fast-reactor development, and the comparatively modest expected rates of growth of nuclear power stations over the next few decades (~150 million kW by 2000). The specific cost of the fast reactors is close, according to British estimates, to the cost of thermal reactors.

Translated from Atomnaya Énergiya, Vol. 31, No. 6, pp. 642-643, December, 1971.

As for nuclear safety problems, British specialists feel that these are solved just as reliably in the case of fast reactors as in the case of thermal reactors. While considering the construction of nuclear stations near large populated centers one of the basic requirements for nuclear power stations in Britain, UKAEA specialists are carrying on an extensive program of work to familiarize power engineers with fast-reactor technology, so as to convince them of the safety inherent in those facilities. Theoretical and experimental investigations of "maximum" damage are being carried out with the object of demonstrating that the external tank and lid of the PFR are capable of sustaining damage equivalent to an explosion of ~100 kg TNT. The PFR design also withstands ~10 atm sodium vapor pressure. The reactors now being built (PFR) and in the design stages (CFR) have no containment shells. The main problem is approached as one of improving the reliability of the equipment, control systems, and shielding, and one of working out an operational system of reactor monitoring and checkout.

An ambitious program of work has been developed on one of the principal current problems in the building of fast reactors: studying swelling of steels bombarded by fast neutrons. Experiments are underway both at DFR and on a special accelerator of variable-energy heavy ions at Harwell. Accelerated C^{2+} ions are being employed in a study of the effects of irradiation on steel and alloys, all the way up to dosages corresponding to 400 displacements of each atom in the lattice (an integrated dose of ~40 displacements per atom, or about 10^{23} neutrons/cm^2, was achieved at DFR, while the dosage in PFR and CFR will be 1.5 to 2 times higher yet). These investigations have uncovered some conclusions of practical importance.

1. Swelling of steels is a threshold type process, commencing at doses of 6 to 10 displacements per atom, while the swelling rate slows down at doses of ~40 displacements/atom, with a tendency to saturation.

2. Swelling tapers off markedly (at <600°C) in 15-20% cold-worked steels. The swelling maximum then shifts from T ≈ 500°C to T ≈ 600°C. It is precisely these steel grades (grade 316 in the case of fuel-element cladding and grade 321 for hexagons) that are selected for use in the PFR reactor now being built at Windscale.

3. Bulk swelling of steels in the PFR steel will not exceed 5% when the burnup of heavy atoms is 7.5%.

4. High-nickel alloys (PE-16 nimonic, 44% Ni, 35.3% Fe, 17% Cr, 3.5% Mo) swell to a much lesser extent than steels (less than 1 vol.% even when the exposure dose ~250 displacements/atom).

Searches are also underway for alternative ways of coping with swelling and its aftereffects (180°C rotation of bundles, slight widening of clearances, cooling of bundle walls below 500°C, etc.). The pronounced effect exerted by radiation-induced creep in steels on the performance of fuel assemblies is also coming under scrutiny.

The Zebra critical facility at Winfrith Heath is being used in studies of fast-reactor physics, and a procedure for fitting the neutron constants with the aid of macroscopic experiments has been developed. Calculations of U^{235} utilization in a fast reactor were also carried out at Winfrith Heath, demonstrating that a reactor of that type can also function as an excellent converter for production and buildup of plutonium.

The members of the delegation presented reports to their British colleagues on fast-reactor developments in the USSR, and on the preparations for the startup of the BN-350 reactor at Shevchenko.

Familiarization with the work being done in Britain on fast reactors provides convincing evidence of the mutual advantages lodged in the development of further contacts between the specialists of the two countries, putting forth vigorous efforts into this promising developmental trend in nuclear power.

INTERNATIONAL GEOCHEMICAL CONGRESS

R. P. Petrov

In late July, 1971, the First International Geochemical Congress, organized under the joint sponsorship of the Academy of Sciences of the USSR and the International Association of Geochemistry and Cosmochemistry, with the participation of UNESCO, was held in Moscow. The congress organizing committee received 400-odd reports submitted from 23 countries for presentation at the congress. Over half of these papers were read and discussed: the contents of the remaining reports found reflection in a compendium of abstracts published by the time the congress commenced.

In conformity with the present level of knowledge, all of the attention of the participants at this congress was focused on the geochemical analysis of the most important natural processes and on examination of problems relating to the source of matter, and ways in which matter becomes transported and deposited. This degree of single-minded motivation and breadth in the formulation of the problems was dictated by the fact that the work load has distributed over four panel sessions as well as at the plenary sessions. The first of these panel sessions encompassed geochemical problems relating to magmatic processes, the second to hydrothermal processes of geochemical interest, the third to metamorphic processes of geochemical interest, the fourth to sedimentation processes of geochemical interest. In addition, the framework of the congress agenda incorporated a geochemical symposium on the problem "Humans and the biosphere," a combined meeting of panels I and III devoted to the problem of the genesis of granites, and a workshop meeting of the hydrogeochemical section of the International Association of Geochemistry and Cosmochemistry.

With the continuing development of space flight, and following the study of the first specimens of lunar rock, the attention of geochemists has become increasingly attracted by problems relevant to the origin of our planet and of the several geospheres. On the basis of regularities evident in the distribution of the elements in iron and stony meteorites, and utilizing the thermodynamic constants of the elements and their compounds, A. P. Vinogradov (USSR) advanced a new hypothesis of the separation of the structural material of planets in response to high-temperature multistage processes traced as far back as in the interior of the plasma protoplanetary cloud, as the primal cause of the familiar zonation in the earth's structure. The author of the hypothesis assigned special significance, in his interpretation of the causes of the zonal distribution of matter in the cosmic protocloud, to polymorphism of iron–nickel alloys, the stabilizing role played by nickel included in the composition of the alloys and determining the composition of impurities, and the subsequent agglomeration of condensed-phase material accompanied by displacement of silicate components from the core portions of the cloud and by concentration of these silicate components in the peripheral shells corresponding to the present mantle. Only subsequent processes in the evolution of matter led to the fusion of the earth's crust by a zone melting mechanism. The possibility of a multiple recurrence of that development in response to radioactive decay of long-lived isotopes and tidal currents in the nonideal elastic layer of the upper mantle was demonstrated by E. A. Lyubimova (USSR) on the basis of a discussion of the earth's thermal history.

Concepts of the chemical mechanisms at work affecting the medium and the physical state of matter in the upper mantle and in the deeper-lying parts of the earth's crust were developed in many of the reports characterizing both the results of experimental research and the net results of geochemical studies of complexes of deep-seated ultrabasic rock and conditions governing the formation of rift valleys on the ocean bottoms.

An experimental assessment of the conditions of partial fusion of the magma and of the evolution of the magmatic composition under pressures and at temperatures corresponding to depths on the order of 60

Translated from Atomnaya Énergiya, Vol. 31, No. 6, pp. 643-646, December, 1971.

to 100 km down from the earth's surface was presented in a report by N. I. Khitarov and colleagues (USSR) and in abstracts submitted by I. Kushiro et al. (Japan). According to data submitted by Soviet investigators, the evolution of the basic tholeiitic magma leads to silica enrichment of the melt and to the isolation of solid residues of the pyroxenite and eclogite types. Japanese scientists demonstrated the petrogenetic value of large quantities of water present in the interior of the earth. Among the other reports in this area, we find of general interest results reported on a geochemical study of eclogites by N. Bakun-Czubarow (Poland), and a review of materials on drillings in the bottom of the Pacific Ocean, presented in a joint report by participants of the expedition on board the Glomer Challenger (A. P. Lisitsyn for the USSR, A. Fisher et al. for the USA).

The participants at the congress devoted close attention to discussions of the cooling conditions of magmatic melts (F. K. Shipulin, USSR) and of the formation of hydrothermal solutions linked to magmatic processes and high-temperature metamorphism. It is important to note, in this context, that, in addition to experimental research data on phase equilibria at high water vapor pressures (V. Marshall, USA; L. N. Kogarko, USSR; D. Hamilton and D. Nolan, et al., Britain), wide use is currently being made of the results of studies of vapor–liquid inclusions in interpretations of the crystallization conditions of the melt and the nature of hydrothermal solutions (V. B. Naumov, N. P. Ermakov, F. P. Mel'nikov, V. A. Kalyuzhnyi, S. D. Malinin, USSR; V. Pomarleanu, Rumania; L. Bauman et al., German Democratic Republic, etc.).

A. I. Tugarinov (USSR), reviewing results of research in the study of gas–liquid inclusions in minerals from 1000 occurrences throughout the world, reported that the density of hydrothermal solutions usually ranges from 0.7 to 1.0 g/cm^3. In all instances where homogenization of inclusions to the vapor phase occurs, this phase is represented by high-density carbon dioxide (0.35 to 0.9 g/cm^3). Hydrothermal mineralization is observed over a wide range of temperatures around 850°C at pressures of hundreds and thousands of bars, which is in most cases well in excess of the loads generated by the rock stratum. Precipitation of minerals from carbon dioxide – water hydrothermal solutions is linked primarily to a decline in the carbon dioxide pressure, which is attributed either to degassing via fissure zones or to carbonatization of the host rock. Enrichment of the solutions with carbon dioxide is favorable, according to the views expounded by A. I. Tugarinov, to the reserve process, viz. leaching of the components out of the host rock.

Some disagreements were voiced in the interpretation of the history of the formation of the oxygen-containing atmosphere determining the entire course of the hypergenic geochemical formations, and the congress participants generated a brief but most interesting discussion when they took the floor on those disputed points. A. V. Sidorenko, together with V. A. Teplyakov et al. (USSR), taking the silica-rich pre-Cambrian rock as metamorphosed formations of weathering of the crust, the graphitic accumulations as transformed material of organic origin, and the extensive manifestation of alkaline metasomatosis as evidence arguing for the existence of saliferous deposits, and also accounting for the isotope ratios of the sulfur in the pre-Cambrian rocks by fractionation similar to coeval fractionation, are of the opinion that the atmosphere of $3 \cdot 10^9$ years age was an oxygen-containing atmosphere. In the opinion of these scientists, all of the geochemical factors in the early pre-Cambrian age were not different in principle from the geochemical factors prevalent in the phanerozoic ages. Counterposed to those views were the concepts developed by A. B. Ronov (USSR) on the basis of a systematic study of noncoeval rocks from the Russian platform, the Canadian shield, and from several other territories, as well as an analysis of some of the geological processes and phenomena of relevance, from which he inferred the existence of some appreciable history of evolution of the composition of the atmosphere and oceans.

The views of A. V. Sidorenko stood in opposition to the opinions advanced by the Canadian geologist R. Folinsby. On the basis of data on precision radiological dating and results of geological observations, this research investigator feels that all of the archaic occurrences (I pre-Cambrian, $3.5 \cdot 10^9$ to $2.6 \cdot 10^9$ years) were formed in an oxygenless atmosphere. The uraniferous conglomerates at Witwatersand and Blind River belonging to the early II pre-Cambrian ($2.6 \cdot 10^9$ to $2.2 \cdot 10^9$ years) and containing diffuse gold, to judge by the enormous quantities of pyrite present, were formed under nonoxidative conditions. The immense quantities of oxygen present in the atmosphere appeared later than $2.2 \cdot 10^9$ years ago, indicating the formation of jaspilite formations containing ferric oxide iron, jasper, and carbonates.

Of greatest immediate interest to the readers of our periodical would be the results of geochemical investigations of processes culminating in the formation of considerable quantities of uraniferous minerals or mineral complexes usually found in conjunction with uraniferous minerals in the same ore zones.

Results of isotope investigations are brought to bear on the interpretation of the nature of sources of ore material in much of current geochemical research. But the possibility of using these results to determine the absolute age of minerals was not discussed in detailed fashion at the congress. The investigators centered the brunt of their attention in their studies of the isotope ratios of oxygen, carbon, sulfur, lead, and other elements on the solution of the basic outstanding problems concerning the origin of minerals and the history of the development of geochemical processes. Experimental research conducted by S. B. Brand, G. S. Plyusnin, and colleagues (USSR) not only confirmed the possibility of fractionation of isotopes of the light petrogenic elements in metasomatosis, but also established the fact that fractionation of lithium isotopes, mostly at low temperatures with tapering off at higher temperatures, can be utilized to construct a veritable lithium geothermometer. Losses of radiogenic argon and strontium isotopes in the thermal metamorphism of ancient rocks due to neogenic intrusion may be quite impressive in scope, as shown by the work of L. L. Shanin, I. B. Ivanov, and co-workers (USSR). These events are responsible for such differences in isotope ratios that the isotopes are trapped in the phlogopite crystal alone, and yield ages, in terms of potassium–argon ratio data of 1750 million years for the central parts and 10 to 20 million years for the peripheral parts. Extremely low He^3/He^4 ratios in uraniferous minerals (10^{-10}) and very high He^3/He^4 ratios in lithium-bearing minerals (10^{-5}) provide, in exactly the same way as the corresponding computed ratios of those isotopes in granites and in various other geological formations, confirmation, in the view of E. K. Gerling et al. (USSR), of the concept of the formation of He^4 predominantly through radioactive decay of uranium and thorium, while He^3 is held to form predominantly as a result of nuclear reactions.

More recently, the oxygen isotope ratio has been invoked to aid in interpretation of the genesis of minerals, on several occasions. Reviews of the literature compiled by A. M. Migdasov et al. (USSR) demonstrated enrichment of juvenile waters and juvenile carbon dioxide by the heavy oxygen isotope, as compared to contemporary sea water. At the same time, if we judge by the isotope composition of the oxygen in ancient carbonate, siliceous, and phosphate rocks, sea water was distinguished in the past by a still lower O^{18} fraction. The conspicuous way in which C^{12} is confined to biogenic formations, and the definite increase in the C^{13} content in transformed hydrocarbons can be used to advantage in solving some specific genetic problems (V. S. Lebedev, USSR). But work in this direction has been of very limited scope to date, unfortunately.

Investigations by E. K. Lazarenko and G. P. Mamchur (USSR) provide evidence of a definite value of data on carbon isotopes for prospecting applications. The originality and novelty of the problem of carbon isotope ratios consists in the fact that unoxidized forms (graphites) differ drastically from all oxidized forms (carbonates, gases) corresponding to biogenic carbon, in their C^{13} content. This has led to the inference (J. Hofs, West Germany) that a primary nonbiogenic origin of the reduced form of carbon is to be sought.

Analysis of regularities in the distribution of sulfur isotopes has been attracting the attention of both Soviet and foreign investigators. The significance of this trend of work has been expressed with greatest clarity in the lines of reasoning presented by V. I. Smirnov (USSR) in his reviews of results of studies done of the ores of pyrite occurrences. From all the occurrences investigated to date, he managed to single out two of genetic type. The first occurrence of this type, a high-temperature occurrence (200-450°C) to judge by decrepitometric data, differs in the persisting sulfur isotope ratio, which is close to the meteoritic standard. This is in harmony with the concepts voiced on the direct accumulation of sulfides of their primary deep-seated sources linked to the basaltic magma. The second such occurrence is a low-temperature occurrence (below 100°C) by broad variations in the isotopes of the sulfide series, which attributed to superficial processes, bacterial processes included, accompanied by appreciable fractionation of the sulfur isotopes. F. V. Chukhrov, in joint work with L. P. Ermilova (USSR), found, on the basis of a study of sulfide and barite concretions in a stratum of sedimentary rock, that the separation of sulfur isotopes is affected by a number of paleogeographic factors. In the views of V. A. Grinenko et al. (USSR), the platform sulfur is heavier than the geosynclinal sulfur. The latter is close to the meteoritic standard.

The isotope composition of the sulfur found in deep-lying zones of the earth's interior cannot be established objectively, since there are no criteria for recognition of the juvenile series (V. I. Vinogradov, USSR). Oceanic basalts accepted as mantle formations are close to lunar rock in their sulfur isotope ratios. The ocean is rich in S^{34}, and S^{32} contents in metamorphosed rock is fairly high. Efflux of S^{34} to the surface is associated with metamorphism. Recent sediments are richer in S^{34} than ancient sediments, on the whole. But no direct time dependence of the sulfur isotope ratio has been established, as G. Nilson (West Germany) pointed out. He nonetheless singled out a certain regular relationship between changes in the sulfur isotope composition and the computed gross production of organic material on the earth.

I. Mincheva-Stefanova and Vl. Amov (Bulgaria), as well D. Richards (Australia), independently arrived at the conclusion that there is no need to view lead as a material of pallial origin. Isotope investigations conducted at occurrences in Bulgaria, New Zealand, and southern Australia provide evidence of the identity of isotope ratios of sulfur in the mineral associations of those occurrences and in certain underlying more ancient petrographic complexes. This state of affairs is viewed as a sufficiently weighty argument in favor of the origin of the lead in those occurrences coming from the underlying rock strata.

Some of the reports took up the problem of the source of the constituents forming rocks and ores. In the opinion of Ya. N. Belevtsev (USSR), thermal solutions borrow iron, copper, thorium, and uranium from sedimentary–vulcanogenic and metamorphic rocks as these recrystallize, dissolve, or remelt under conditions of metamorphism or ultrametamorphism. A. L. Liskovich and Yu. V. Kazitsin (USSR), turning their attention to efflux of iron, magnesium, calcium, and other elements from alkaline metasomatosis zones, inferred that the efflux of radioactive uranium and thorium takes place in response to the formation of orthoclastic metasomatites from granitoids, and amounts to 2.4 – 15 g/m^3. K. D. Subbotin, R. A. Khazov, et al. (USSR) meanwhile draw attention to the presence of not only tin, beryllium, and rare-earth mineral complexes in those species, but also, on the basis of studies of metasomatic rocks in the western framework of the Russian platform, point out the presence of accessory uraniferous and thoriferous minerals.

Results of work done by colleagues of the Institute of Experimental Mineralogy of the Academy of Sciences of the USSR are of special interest in attempts to interpret the conditions governing the extraction, displacement, and deposition of the constituents by hydrothermal solutions. Simulation of metasomatic zonation (V. A. Zharikov, G. P. Zaraiskii, F. M. Stoyanovskaya) developed on the contact between carbonate and aluminosilicate rocks, in the presence of sodium chloride solution at temperatures of 600°C and pressures of 1000 kg/cm^2, showed that the diffusion coefficient of silicon is greater than that of calcium or magnesium. A certain degree of asymmetry in the zonation is responsible for this. Wollastonite is developed from pure silica, and the diopside and monticellite zones are developed from mixtures of the oxides CaO and MgO. After the substitution of the pure calcium and magnesium compounds by natural carbonates, and substitution of the silica by granitoids, the overall directivity of the process remains unaffected. With the introduction of $FeCl_2$ in the composition of neomineralizations into the solution, magnetite began to occupy a certain place in the column. Experimental data not only confirmed the concepts put forth by D. S. Korzhinskii (USSR), but also opened up broad avenues for improved knowledge about the physicochemical conditions relating to mineralization. In an experimental study of filtration of solutions of electrolytes ($NiCl_2$, $CuCl_2$, etc.), through thin platelets of rock, carried out by V. A. Zharikov and Yu. V. Alekhin (USSR), a constant cation deficit in the salt dissolved in the filtrate was detected. The nonequivalence of the cation and anion concentrations in the dissolved salt that was brought to light, changes in the acidity of the solutions in the course of the filtration, combine to provide experimental confirmation of the hypothesis of acidic–basic hydrothermal differentiation put forth by D. S. Korzhinskii and demonstrate that the scales of this hydrothermal differentiation depend on the density, composition, and concentration of the solution and the nature of buffer reactions with the host rock. It was established, in the course of investigations of one of the most widely occurring systems $Al_2O_3–SiO_2–KCl + H_2O$ (I. P. Ivanov and O. N. Belyaevskaya, USSR), disclosed that the transition of potassium from the solution to the solid phases, under conditions of formation of high-temperature metasomatic rock in a granitoid formation, such as are characteristic of many ore occurrences, is accompanied either by the release of free water or by absorption of that free water from the solution. A rise in the temperature displaces the equilibrium of the reaction involving liberation of water into the region of lower pH values and lower K^+ activities.

The most interesting of the reports characterizing geochemical factors active in the formation of minerals were those reports directly relevant to the conditions governing deposition of ore minerals, radioactive minerals included. By relying upon radiography of specimens irradiated by thermal neutrons in nuclear reactors, I. G. Berzina and S. M. Kravchenko (USSR) showed that uranium is an excellent indicator of crystallization differentiation of the magma. The residual fractions, the bulk of the porphyraceous basalts (anamesite porphyry), become enriched with uranium. The concentration of uranium in anamesite porphyry is much higher than in phenocrysts and alloliths of magnetite, apatite, and sphene.

The crystallization conditions of ore constituents in low-temperature hydrothermal processes may differ substantially, as demonstrated by B. I. Omel'yanenko (USSR), from the conditions prevailing in the formation of metasomatites near the ore vein. Different metasomatic columns combine with ore mineralization of like type. A direct relationship between the method of pitchblende deposition and the properties of pitchblende has been established (V. P. Rogova, A. A. Nikitin, and G. B. Naumov, USSR). The metasomatic generations differ in the smaller crystal lattice constants (5.38 Å to 5.40 Å) and in the larger oxygen

coefficients (2.49 to 2.59). In the spherulitic pitchblendes formed in open cavities, the respective constants have values 5.40 to 5.43 Å and 2.43 to 2.32.

By way of interpretation of the conditions governing the concentration of constituents, processes involving interaction of solutions with ion exchange minerals are being resorted to more and more frequently, and these minerals are the best sorbents under low-temperature conditions, according to available experimental data (N. F. Chelishchev, USSR). Of the organic materials acting as concentrators of germanium, gallium, uranium, and vanadium (S. M. Maiskaya, L. A. Kodina, and V. N. Generalova, USSR), a special place is reserved for lignin, which is capable of facilitating the migration of those constituents in depolymerization and of storing them in a secondary concentration. Meanwhile, the uraniferous thermal springs transform graphite and, judging by a report submitted by Z. M. Motorinz, N. T. Sokolova, and M. A. Kremneva (USSR), graphite loses the orderedness of its crystal lattice in the vicinity of pitchblende, and its grain size becomes diminished.

Processes involving concentration of radioactive materials in sedimentary complexes are related to the hydrogeochemical setting and environment: the distribution pattern of the uranium, radium, and deuterium in turn serves as a basis for the delineation of horizons with isolated waters of a sedimentation nature in artesian oil- and gas-bearing basins, and for determining the position of zones of intrusion of noncoeval infiltration waters (F. A. Alekseev, USSR). A. K. Lisitsyn (USSR) has linked the clearcut and pronounced variations in the ratios of ferric and ferrous iron, in the values of the Eh and pH parameters, and in the concentrations of selenium, uranium, and molybdenum in the rocks of aquiferous horizons, to the range of propagation and migration of those waters. The halogenetic processes eventuating in the concentration of constituents in evaporitic liquid and solid formations (M. G. Valyashko, USSR) also lead, in some cases according to a report by M. Dallaglio (Italy), to uranium accumulations in brines.

The applied significance of geochemical investigations, alluded to in many of the papers submitted, becomes perfectly evident from the direct relationship between the abundance of the elements in the earth's crust and the scales of accumulation of the elements in ore occurrences (L. N. Ovchinnikov, USSR). The study of the regularities of the zonal distribution of the elements in the vicinity of hydrothermal ore bodies (S. V. Grigoryan, USSR) is of interest in the development of geochemically validated directions in prospecting and exploration work.

The international congress comprised a highly representative forum of specialists and geochemists. It contributed to a correct illumination of the major achievements of Soviet geochemistry, to a valuable exchange of scientific knowledge, and unquestionably has furnished an excellent basis for further joint work involving combined efforts of scientists in the Soviet Union and other countries.

CONFERENCE ON NEUTRON PHYSICS

S. I. Sukhoruchkin

The Conference on Neutron Physics, organized by the Main Committee of the Institute of Atomic Energy together with the Academy of Sciences of the USSR and the Institute of Nuclear Research of the Academy of Sciences of the Ukrainian SSR, was held from May 25-28, 1971 in Kiev. Nearly 200 scholars from the Soviet Union and socialist countries participated. Scientific questions of neutron physics as well as various applications of nuclear data were discussed at the eight sessions. The conference was opened by the chairman of the organizational committee, Academician M. V. Pasechnik. In his opening words A. K. Kruglov (Main Committee of the Institute of Atomic Energy) emphasized the importance of coordination of experiments within the country and among member countries of the CMEA for the resolution of actual scientific and practical problems.

Problems of nuclear data requirements for reactor calculations on fast neutrons (M. F. Troyanov et al.), for a determination of the operating periods of the heavy water reactor (P. P. Blagovolin), for calculations of the properties of reactor shielding (A. A. Abagyan), for the resolution of the problems of guarantees (G. B. Yan'kov), and for calculations of thermonuclear apparatus (Yu. F. Chernilin) were examined at the first session. At the second session general questions of the interaction of neutrons with nuclei were discussed. Possibilities of a theory of the nucleus for the prediction of neutron cross sections were examined in a report by P. E. Nemirovskii. In papers by V. S. Stavinskii, V. M. Kolomiits, and A. V. Ignatyuk competitive models were examined, which were the most extensively applicable to the calculation of cross sections: the statistical method, the entrance states model, and the direct process mechanism. Three papers from the Joint Institute for Nuclear Research described results of experiments with utracold neutrons (A. V. Strelkov), further investigation of the neutron–electron interaction by the neutron diffraction method (Yu. A. Aleksandrov), and perspectives for experimental investigations with polarized neutrons and nuclei (V. P. Alfimenkov). Problems of the study of the structure of highly excited states by neutron spectroscopy were discussed in an interesting paper by V. G. Solov'ev.

Experimental results of investigations of neutron cross sections of nonfissionable and fissionable nuclei were communicated in 13 reports at the third and fourth sessions. These reports were devoted to problems of determining the quantum characteristics of neutron resonances (G. V. Muradyan), to the study of reactions with charged particle emission (Yu. P. Popov), to a determination of the level density of deformed nuclei with a mechanical selector by the time of flight method with the VVR-M* reactor of the Institute of Nuclear Research, Academy of Sciences of the Ukrainian SSR (B. P. Vertebnyi), to deviations from statistical distributions, and to a determination of neutron levels and γ-lines (S. I. Sukhoruchkin). Problems in the study of elastic and inelastic scattering and of spectra of secondary neutrons (and γ-quanta) were elucidated in papers by O. A. Sal'nikov, M. S. Fedorov, M. V. Savin, and V. A. Tolstikov.

The interest of those present was stimulated by papers of scholars from socialist countries: D. Zeliger and his colleagues (German Democratic Republic), "An Investigation of the Mechanism of Inelastic Scattering of 14 MeV Neutrons in Light and Intermediate Nuclei," and the survey of the experiments by I. Chikai and his colleagues (Hungarian People's Republic) on the (n, 2n) reaction at 14 MeV. Papers by V. N. Kononov, "Techniques and Results of Measurements of the Value of α for U^{235} and Pu^{239}," and by S. I. Sukhoruchkin, "Analysis and Evaluation of Experimental Data for the Value of α," examined both new results for these constants and problems associated with the comparison of data from different types of experiments (for example, data received by the filtered neutron and time of flight methods). A summary of the

*VVR-M = water-cooled reactor, type M. – Trans.

Translated from Atomnaya Énergiya, Vol. 31, No. 6, pp. 647-648, December, 1971.

results of measurements of the U^{238} radiative capture cross section performed at the FÉI and the Joint Institute of Nuclear Research was given by V. A. Tolstikov.

Finally, the problems of the energy dependence of the number of secondary neutrons (Yu. A. Khokhlov), of the measurement of fission cross sections (V. A. Shigin), and of the multileveled parametrization of this cross section and the influence of the Doppler effect (A. A. Luk'yanov) were examined.

A separate session was devoted to the physics of nuclear fission. This session was opened with an interesting review paper by V. M. Strutinskii on the new fission theory results which he has developed. Reports discussed experimental data on the spectra and the angular distributions of neutron fission (V. N. Nefedov), the possible influence of the effects of pairing on the process of fission (P. E. Vorotnikov), problems in the calculation and measurement of fission barriers (A. N. Protopopov), an analysis of data on the distribution of masses and the kinetic energies of fission fragments (B. D. Kuz'minov), and on the radiative processes accompanying fission (G. A. Petrov). The original reports of A. A. Vorob'ev et al., "The Formation of Light Nuclei in the Fission of Uranium Isotopes with Thermal Neutrons," and B. N. Maksyutenko, "The Possibilities of a New Method of Interpreting the Decay Curves of Delayed Neutrons," were also heard.

Problems concerned with the collection and evaluation of nuclear data occupied a large place in the work of the conference and were discussed in eight papers, which were presented mainly by the co-workers of the FÉI: A. I. Abramov, V. G. Zolotukhin, and M. N. Nikolaev, "An Evaluation of Nuclear Data," L. N. Usachev, "The Use of Integral Experiments for the Correction of Systems of Constants," A. I. Abramov, "The Evaluation of Radiative Capture Cross Sections," L. N. Yurova, "Integral Experiments," V. I. Popov, "On the Activity of the Center for Nuclear Data in Obninsk and Plans for the Near Future." In addition, reports were heard on the role of standard cross sections for the measurement of neutron flux density (R. D. Vasil'ev) and on the influence of neutron cross sections on a number of integral characteristics (N. I. Laletin, G. Ya. Trukhanov).

Methodological problems, mainly concerning new sources of neutrons for the purposes of spectroscopy by time of flight, were examined at a special session. G. A. Petrov presented a paper on the Gatchina neutron spectrometer, "GNEIS," which is under construction, on the base of a 1 GeV synchrophasotron, and V. V. Kolotyi presented one on some features of a time of flight neutron spectrometer on the base of the U-240 cyclotron at the Institute of Nuclear Research, Academy of Sciences, Ukrainian SSR. The possibilities of using plasma apparatus, including apparatus of the "plasma focus" type for neutron spectrometry, were discussed in a paper by N. V. Filippov and T. I. Filippova, and G. V. Muradyan reported on the application of the pseudo-random impulse method on pulsed sources for the measurement of neutron cross sections. The paper by a group of co-workers of the Joint Institute of Nuclear Research, "IBR-30 and IBR-2* as Sources of Neutrons for Spectrometric Studies," generated much interest. E. Ya. Doil'nitsyn (FÉI) told of a new detector which he developed for neutron spectrometric investigations.

The concluding session was devoted to a discussion of actual problems in nuclear physics. Review papers by Academician A. S. Davydov on certain problems in nuclear theory, by V. M. Strutinskii on nucleon shells and density fluctuations in nuclei, and by A. G. Sitenko on nuclear diffraction processes were heard. The participants in the conference emphasized the ever-expanding role of neutron physics in the study of the structure of nuclei and the mechanism of nuclear reactions. The conference affirmed that neutron physics is intimately related to the practical problems of reactor building and the problem of guarantees, protection, and so on. In conjunction with the new demands for increased precision in nuclear data, problems of understanding the interaction mechanism of neutrons with the nucleus and the technique of precision measurements of nuclear constants begin to compose two sides of the same problem. For the resolution of this problem the extensive development of neutron physics, and especially the further improvement of its methodological capabilities, in essential. Since the coordination of all experiments is an important condition of the rapid attainment of these established practical objectives, the participants of the conference arrived at the opinion that the periodic conducting of similar conferences or meetings (with invitations to scholars from other countries) is advisable. The success of the conference was made possible through the efforts of the co-workers of the Institute of Nuclear Research, Academy of Sciences, Ukrainian SSR. The proceedings of the conference, containing all original and review papers, will be published in a separate collection in the beginning of 1972.

* IBR = Fast-neutron pulsed reactor – Trans.

SECOND INTERNATIONAL WORKING SYMPOSIUM ON THE TECHNOLOGY OF THERMONUCLEAR REACTORS

V. S. Strelkov

The Second International Symposium on the Technology of Thermonuclear Reactors was held in Oak Ridge (USA) from June 28 to July 2, 1971. More that 150 specialists took part in its work. The objectives of the symposium were to examine the technological and engineering problems of thermonuclear reactors, to discuss the capabilities of modern techniques in the creation of a reactor, to outline the essential developments and experiments in the area of the creation of magnetic systems, sources of power supply, walls of the reactor, the blanket, etc., and to estimate the economic capabilities and influence on the surrounding environment of thermonuclear power engineering.

The work of the symposium was of an informal nature, and the speeches concerned both particular and general problems; the time of speeches varied from 5 to 50 minutes; and from 15 to 25 people were usually present at a session. Short resumes, and not papers, will be published.

Closed systems, open traps, and θ-pinches were accepted as the most probable systems for a reactor. Of the closed systems, the tokamak and the stellarator were examined. The Livermore group of American physicists examined the open trap with direct energy conversion, and from Los Alamos the toroidal θ-pinch, Super-Scyllac, project was described, in which, according to the authors' opinion, fulfillment of the Lawson criterion is possible. Both these projects were discussed at the Fourth International Plasma Physics Conference in Madison (USA).

The papers of the sections "Engineering Problems in Blanket Design" and "Neutron Physics" were essentially devoted to the problems of the "blanket." This question was investigated most thoroughly in a study by J. Mitchell (Culham, Great Britain). The blanket consists of three parts: lithium for the production of tritium, graphite, and a shield for the coils from the magnetic field. Each part has a radial thickness of 64, 36, and 60 cm, respectively, i.e., the overall thickness of the blanket is 1.6 m. The blanket covers the longitudinal magnetic field coils, which are enclosed in a common ribbed shell. Borated water with iron instead of the usual lead is used to protect the coils from neutrons. The speaker affirmed that this exchange is completely effective. Liquid sodium is used for heat removal, and a great amount of attention was devoted to problems of its transfer in a strong magnetic field.

In the section "The Heating of Plasma and the Ignition of the Reaction" various methods of heating plasma were discussed: ohmic heating, turbulent heating, high-frequency heating, adiabatic compression and shock waves, heating using a laser, an electron beam, and a method of creating plasma using beams of fast atoms.

A paper by R. G. Mills (Princeton, USA) discussed the possibilities of plasma heating with Joule heat in the tokamak in the presence only of bremsstrahlung energy losses from the plasma. In order to increase the effectiveness of the heating, the use of adiabatic compression after preparatory current heating is proposed, due to the displacement of the plasma column by a transverse magnetic field in the region of a stronger longitudinal magnetic field.

The report of G. N. Popkov and V. S. Strelkov (Institute of Atomic Energy, USSR) examined the tokamak as a reactor, taking into account bremsstrahlung and cyclotron losses, and also the thermal conductivity of the plasma. Both theoretical data (neoclassical) and the results of the extrapolation of experimental results in the region of thermonuclear parameters were used to evaluate the thermal conductivity.

Translated from Atomnaya Énergiya, Vol. 31, No. 6, pp. 648-650, December, 1971.

Sweetman and Thompson (Culham, Great Britain) discussed the questions of the use of beams of neutral particles for injection into a straight trap and also the possibility of recuperation of the energy of the particles in such a system.

Post (Livermore, USA) described a new corkscrew trap "Baseball II" using superconducting materials for the magnetic system and beams of neutral particles for the creation of plasma. The system for heating the plasma in the closed trap Ormak through the injection of a beam of neutral particles is described in a report by Morgan (Oak Ridge, USA).

A paper by Rebut (France) was devoted to the heating of plasma to thermonuclear temperatures using a laser.

Ribe (Los Alamos, USA) dealt with questions of the shock heating of plasma in the Super-Scyllac installation.

A report by Christensen (USA) examined problems of high-frequency heating of plasma to thermonuclear temperatures at hybrid frequencies. Basic attention was devoted to the possibility of the placement of high-frequency loops within the blanket, to the choice of a material for these loops, and to their construction.

Sixteen persons attended the session on "Surface Phenomena." The papers were devoted to phenomena on the first wall of the thermonuclear reactor, which arise from roentgen and neutron radiation and also from the bombarding of charged and neutral particles. The processes which occur on the wall will lead to its erosion and to the contamination of the plasma. An analysis of the dependence of the various processes on the energy of the incident particles shows that for a reactor physical sputtering is important. The life time of a 1 cm thick niobium wall is about 5.5 years with a neutron flux intensity of $4 \cdot 10^{15}$ neutron/cm^2 $\cdot$sec. At the same time a flux of impurities of $2 \cdot 10^{11}$ particles/cm$^2 \cdot$sec will enter into the plasma.

A paper by Phillips (Los Alamos, USA) was devoted to an analysis of the processes which occur on the wall of the discharge chamber in experiments with dense plasma. The processes of heating the surface layer, of heat transfer, and of generated thermal deformations were investigated. The construction of a discharge chamber, made from a bank of aluminum disks insulated by Al_2O_3, is proposed. The disk is enclosed in a tube of glassTextolite from the outside. A study was made of the failures of the usual porcelain and of the new chamber.

In conclusion, the chairman of the section, Kaminsky (USA), demonstrated that detailed calculations of the erosion of the wall in the reactor require a knowledge of the absolute values for the particles and quanta fluxes incident on the wall. Physicists studying plasma should provide this information, and scholars studying surface phenomena must develop recommendations for the choice of materials and for the decontamination of the walls in plasma apparatus.

At the section "Engineering Studies of Magnetic Systems" 24 papers were heard. In a review paper on superconducting magnetic systems M. S. Lubell (Oak Ridge, USA) cited parameters of new superconducting materials and of the largest superconducting magnets for various physical studies. The Nb_3Sn and V_3Ga superconductors being manufactured at present have a large critical magnetic field intensity (225 and 210 kOe) with a rather high critical temperature (18.3 and 14.5°K).

In the near future, utilization of new superconducting materials is anticipated (for example, Nb_3Al and $Nb_{3,76}(Al_{0,73}Ge_{0,27})$) with still larger parameters (H_{cr} = 300-400 kOe at 20°K).

The paper presented the basic data on magnets which are either in operation or which are being started in the next months, in which NbTi, Nb_3Sn, and V_3Ga are used as superconducting wires. A field is obtained of up to 150 kOe in a small volume (the diameter of the inner aperture of the magnet is several centimeters). In large volumes (magnets with a diameter of nearly 5 m for the CERN and the Argonne Laboratory bubble chambers) fields of nearly 50 kOe are expected. Moreover, many special superconducting magnet systems are prepared for plasma studies (Multipole, Baseball II, and others) which create in large volumes magnetic fields with an intensity of tens of kilooersteds.

A paper by Hancox (Culham, Great Britain) was devoted to the technique of stabilizing superconducting solenoids. Dynamic and adiabatic stabilization allows an order of magnitude increase (up to $0.5 \cdot 10^5$ A/cm^2) in the critical current density. The problem of the optimal composition of wire or bus bar for superconducting magnets is discussed in the study. On the basis of these investigations the second part of the paper examined the superconducting magnet system of a stellarator reactor with the following parameters: major

radius of the torus, R = 10 m, minor, r = 1.75 m, H_0 = 50 kOe, H_{max} = 160 kOe, the thickness of the blanket is 1.5 m, the size of the helical winding pole is 1.25 × 1.25 m. The superconducting magnet system weighs 5000 ton (50 ton of which is the superconductor), with 1/5 of this quantity going into the creation of the helical winding.

After the review papers for this section experiments were discussed that dealt with magnet systems for physical studies: magnets for bubble chambers (see above) and for the apparatuses Baseball, IMP, Bumpy Torus, W-7, and others. All these and a number of other American installations (several tokamaks, etc.) have gone into construction or will go into construction in the near future.

A paper by Murphy (USA) detailed the results of the outlined development of a vacuum jacket for a tokamak reactor magnet system. The vacuum chamber is a structure with a height of about 30 m and a diameter of more than 50 m. The speaker related the basic difficulties in creating such a system and spoke of possible ways to eliminate them.

A number of papers were devoted to the specific problems of creating magnet systems. Thus, Phyle (Princeton) paused on the problem of the influence of the form of the toroidal magnet on the character of the distribution of mechanical stress under the influence of ponderomotive forces. It was demonstrated that in a toroidal magnet consisting of individual coils of roughly oval form, buckling stress is practically nonexistent. It should be noted that an analogous idea was expressed in the Soviet Union in 1960.

Five papers were also heard on the power supplies for pulsed magnet systems and pulsed superconducting magnets. James (Culham, Great Britain) constructed a graph of the energy increase of power supplies by years, from which it is evident that if by 1970 the average value for the energy of a power supply was equal to 15 MJ, then by 1980 it will grow to 100 MJ.

Lacure (Los Alamos, USA) told of a project for a superconducting storage device for the Super-Scyllac.

A paper by McInturff (Brookhaven, USA) was devoted to pulsed superconducting magnets. The study presented theoretical estimates and experimental data on the losses which arise with the achievement of pulse fields with growth rates of the magnetic field up to 5 kOe/sec. It is shown that with metallic and intermetallic insulation (AgSn, SnCu) of superconducting fibers the losses are comparable to those arising with organic insulation.

In conclusion, the magnet systems of toroidal reactors were examined.

Ota (Japan) related a calculation of the optimal parameters of the tokamak reactor, taking into consideration the various physical and technological limitations. The construction of a reactor having maximal yield at the specified major radius of the torus was considered optimal. An example was presented of an optimized tokamak reactor with the parameters: P = 5000 MW, P_{wor} = 20 keV, τ = 0.6 sec, R = 5.2 m, r = 1.1 m, H_0 = 80 kOe.

In the paper by Phyle (Princeton) mentioned above, a design is presented for a magnet system of superconducting materials for a tokamak reactor, which operates both on a mixture of deuterium and tritium and on pure deuterium. The dimensions of the magnet system for this are: major radius of the torus, 5 m for the DT and 10 m for the DD reactor; minor radius, 1.7 m and 4 m; and the magnetic field intensity in both cases, 160 kOe.

A report by Long (Oak Ridge, USA) was also devoted to a design for a magnet sytem for a tokamak reactor, with a radius of 10.5 m. It is affirmed that a system with a common vacuum is technically and economically more suitable than separate cryostats for each coil. The values of the thermal fluxes in the system were determined, and questions of the cost of superconducting materials and refrigeration equipment were also examined.

The construction of windings from superconducting materials for the stellarator W-7 was described in a paper by Wipf (Germany). The major radius of the system is 2 m, the inner radius of the coils is 40 cm, and the outer radius is 70 cm. The windings are in the preparatory stage.

The last two papers of this section were devoted to an investigation of magnet systems for the thermonuclear stellarator reactor.

Papers by Georgievskii (Kharkov Physicotechnical Institute, USSR) and Hubert (France) demonstrated that the use on reactor magnet systems of helical windings of the torsatron type with modulation according

to a special spiraling angle law permits a substantial simplification of the magnet system of a stellarator reactor. As a result, the economic indices of the stellarator and tokamak reactors seem to be similar. Moreover, such a stellarator has a number of advantages: it permits operation in a stationary mode; a diverter can be applied which does not destroy the configuration of the magnetic field; it substantially lessens the ponderomotive forces which act on the windings, etc.

CONCLUSIONS

1. The symposium demonstrated that the problem of the creation of a thermonuclear reactor is not restricted to tasks of thermal insulation and the heating of plasma. There exists a wide range of tasks associated with the development of large magnet systems and heavy-duty power supplies, with phenomena on the wall of the reactor, with the radiation resistance of materials, and with the necessity of protecting superconducting materials, of producing tritium, and of removing heat from the reactor. For the resolution of these problems 5-10 years are needed.

2. Abroad (especially in the USA, but also in Germany and Great Britain) an extensive program of investigation is being conducted. The large number of participants is witness to this fact (there were more than 120 persons from the USA, representing 11 universities, 10 experimental centers, and 8 firms).

3. At the symposium the results of a previously outlined study of various aspects of the toroidal reactor (tokamak and stellarator) were discussed and of reactors based on the toroidal θ-pinch and the open trap.

4. The thermonuclear reactor seemed to the participants of the symposium to be optimal in the sense of its influence on the surrounding environment and to be an economically acceptable alternative to the resolution of the problems of power engineering in the future.

ENGINEERING ASPECTS OF RADIATION EMBRITTLEMENT OF REACTOR PRESSURE VESSEL MATERIALS

A. D. Amaev

A conference of experts belonging to an IAEA team was held in Vienna, May 10-13, 1971, to hear reports and discussion on effects of irradiation and other factors responsible for embrittlement of pressure vessel steels under service conditions; proposals were heard from representatives of IAEA members on best ways of conducting standard investigations of the "standard" grade of steel within the framework of national developmental programs, with the object of comparing results and estimating the radiation strength of various grades of steels. The basic trends in materials science research being carried on to improve the operational reliability of reactor pressure vessels throughout the entire operating history of nuclear power stations came under discussion.

The conference, under the chairmanship of the renowned specialist on reactor materials R. Nichols (Engineering and Materials Science Laboratory at Risley, Britain), attracted 17 scientists from Britain, Belgium, Euratom, Italy, the USSR, the USA, France, Sweden, Czechoslovakia, Switzerland, and Japan.

In line with the decisions taken at preceding conferences held by this team of experts, it was recommended that a "Standard minimum program of investigations on a 'standard' grade of steel" be prepared for materialization within the framework of national developmental programs. Proposals on this type of program were forwarded by representatives of West Germany, Japan, Czechoslovakia, and the USSR. The proposals of USSR and Czechoslovsk experts, which were accepted as a basis for this work, take as their point of departure the need to carry out a certain minimum of research while relying on procedures already worked out. The standard minimum program envisages investigations of the steel grade A533 (0.25% C, 1-1.5% Mn, 0.7 to 1% Ni, 0.5% Mo) delivered by the USA to all nations participating in IAEA free of charge, by agreement with IAEA. Parameters stipulated are: the site of selection of coupons from the steel block; the neutron dose and irradiation temperature to which the coupons are to be subjected; the types of specimens or coupons to be tested, and the properties to be determined, and finally a reasonable time within which the investigations should be completed.

With reference to reactor pressure vessel materials, there are some general problems whose solutions are of close interest to countries engaged in the building and operation of pressure vessel type reactors. In the opinion of the experts, these problems include:

1. Radiation-induced embrittlement and factors which affect it (structure and composition of the steel, methods for inspecting embrittlement, practical and theoretical aspects of removing radiation damage by heat treatment).

2. Effect of the combined effects of operating conditions on the properties of pressure vessel materials (strain ageing and thermal ageing combined with radiation effects, behavior of high-strength steels, and problems relating to the use of high-strength steels as materials for reactor pressure vessels, fatigue strength under cyclically alternating loads, hydrogen embrittlement with reference to service conditions of high-strength steels).

3. Analysis of failure conditions and safety design problems (use of thick-walled welded structures, particularly in the radiation exposure zone, loss of ductility and analysis of this phenomenon in its relevance to the operational reliability of pressure vessels, the use of data culled from the mechanics of failure in the

Translated from Atomnaya Énergiya, Vol. 31, No. 6, pp. 650-651, December, 1971.

design of reactor pressure vessels, phenomena accompanying fatigue growth of cracks, a program of study of test coupons for forecasting changes in the properties of the steel, establishment of limiting permissible conditions for safe pressure vessel service, simulation and programming for electronic computer analysis of the effect of various factors on the properties of materials, dealing with the effect of the neutron spectrum in evaluating data of investigations on test coupons, etc.).

At the present time, the experts are united in their views on approaches to operational safety of reactor pressure vessels. Monitoring the operating temperature of the pressure vessel is seen as a guarantee eliminating brittle failure. The operating temperature of the loaded pressure vessel must always be higher than the ductile-to-brittle transition temperature.

Reports submitted by L. Stiel (USA), G. Sievers (West Germany), and T. Fujimura (Japan) demonstrated enhanced brittleness in A302 and A533 steels resulting from protracted temperature effects. These effects, combined with strain ageing, make a significant contribution to the rise in the critical ductile-to-brittle transition temperature of irradiated steel.

At the present time, the mechanics of failure of materials is being studied intensively in many countries, and this includes research on irradiated samples.

A thorough-going report by L. Stiel noted that the presence of copper impurity (over 0.1 wt.%) in steel is undesirable, since enhanced proclivity to embrittlement may occur under radiation exposure conditions. Sulfur and phosphorus also exert a harmful effect. Investigation of the behavior of the metal of the weld and of the heat-affected zone under irradiation conditions is particularly timely in the light of the inhomogeneous structure and composition of the steel in the metal of welded joints. The experts are therefore of the opinion that operational safety problems for reactor pressure vessels must be approached with primary attention given to the welded joints.

At the present time, our state of knowledge on the combined effects of the host of service factors affecting the properties of materials and the state of pressure vessel designs is such that there is still need for periodic inspection of pressure vessels on the basis of specially worked-out programs.

The discussion of the engineering aspects of radiation embrittlement held by the IAEA work team was both fruitful and helpful. The activities of the IAEA work team as an organizing center are most deserving of approval.

INTERNATIONAL SYMPOSIUM ON FAST METHODS IN MONITORING ENVIRONMENTAL RADIOACTIVITY

L. V. Artemenkova

An international symposium organized under joint auspices of the government of the Federated German Republic and IAEA was held at the Radiation and Environmental Research Institute near Munich, July 5-9, 1971. The symposium attracted participation by 217 specialists from 30 countries, with about 80 reports presented. Rapid methods for analyzing pollution of the environment by radioactivity can be of great importance, on the one hand, in dealing with accidents at nuclear facilities, and on the other hand for monitoring the normal operation of nuclear facilities, thereby rendering monitoring more efficient and more extensive, above all from the standpoint of protecting the environment. The reports heard and discussed covered a broad range of problems, demonstrated a wide variety of approaches to solving those problems, and reflected the present state of the art in the advanced countries throughout the world at both scientific and engineering levels.

The reports were grouped in the following topical categories (corresponding to panels): general problems or basic problems, chemical laboratory techniques, field methods, conventional dosimetric work and health physics, emergency monitoring, data processing, and future developments.

In the discussion of general problems or basic problems, reports by K. Morgan and D. Harley (USA) devoted much attention to dosimetry and protection of the environment and dealing with radioactive contamination, in response to the continuing growth of nuclear power and the extensive program of construction of nuclear power stations anticipated in some countries. Special attention was given to the need for serious formulation of dosimetric and ecological research, and carrying out that research. Morgan expressed the view, however, that the extent of radiation exposure suffered by the nearby population on account of nuclear industry is many times less than the radiation exposure suffered by the same population as a result of radiation therapy and radiation diagnostics, and that nuclear power plants are much safer than power plants burning fossil fuels, which are in fact a source of one of the most prominent and most dangerous pollutants, sulfur dioxide. Nevertheless, Harley emphasized the point that the USA public is calling for keeping the level of radioactive contamination of the external environment and the exposure dose experienced by the population to a minimum.

Estimates of pollution hazard to the environment through serious accidents, organization of monitoring services, description of the volume of radiometric measurements, and methods of measurements received due attention in other reports presented at the first panel listed.

The largest number of reports presented at any one panel was at the chemical panel. A review report was delivered by the Polish scientist D. Minczewski. Other reports deal with specific techniques for determinations of α-active, β-active, and γ-active isotopes in various objects in the external environment and in foodstuffs, with preparation of samples using wet ashing and dry ashing, and methods and equipment designed to speed up those processes, especially the wet ashing process (B. Borrel, West Germany). Some attention was given to rapid methods for radiochemical isolation of fission products, and specifically iodine isotopes. Isolation and identification of isotopes of fission products with $T_{1/2}$ of several seconds were achieved by automating the separation process (G. Hermann, West Germany).

Widespread use is made of extraction, chromatography, and tissue sorbent methods (É. Krisyuk et al., USSR) for separation of isotopes in aqueous solutions. Methods of analyzing highly saline solutions of sea water described by N. Ikeda et al. (Japan) are of practical interest. A highly novel technique for rapid determinations of trace quantities of α-emitters and β-emitters in biological materials, by "wet" ashing

Translated from Atomnaya Énergiya, Vol. 31, No. 6, pp. 651-652, December, 1971.

using hydrogen peroxide with iron added as catalyst, was proposed by B. Sansoni and W. Kracke (West Germany).

Methods for sampling, separation, and radiometry of inert β-active gases were also discussed at the chemical panel. Rapid monitoring of the composition of a mixture of radioactive gases was achieved through chromatographic separation, using radiation detectors (several types were studied as promising examples for the application) and automatic data processing. Different variants of this method are probed in detail in papers by M. Dupuis et al. (France) and by L. A. Artemenkova et al. (USSR).

Fairly simple methods for sampling air in measurements of low concentrations of radioactive inert gases in the atmospheric air (Kr^{85}, Xe^{133}) were discussed in papers submitted by American scientists. One cubic meter of air was bled from a pressure cylinder containing several dozen liters, to supply a portable compressor, and then the radioactive gas was secured by cryogenic techniques and a charcoal trap for subsequent measurements. This method is useful in determining the concentration of Kr^{85}, say, to fairly high accuracy (at the level of $\sim 14 \cdot 10^{-9}$ Ci/m^3).

Widespread current use of spectrometry in laboratory measurements for identification of isotopes of samples of the environmental medium is testified to by the numerous papers presented at the panel on physical laboratory methods. The large volume of measurements is being handled rapidly thanks to the use of multichannel analyzers and digital computers.

NaI(Tl) scintillation crystals and Ge(Li)-semiconductor large-area detectors are being used as radiation detectors. Several variants of this equipment and results of measurements of a particular group of isotopes in samples of the environmental medium were described in papers presented by scientists from Britain, the USA, West Germany, Japan, Czechoslovakia. Another group of reports devoted to physical laboratory techniques and conventional dosimetric monitoring discussed the possible use of a scintillation counter incorporating liquid scintillator for measuring certain isotopes, and more specifically the low-energy β-emitters T and C^{14}. Methods for taking tritium samples from the atmosphere were described at the same time. It is interesting to note that the sampling method and sampling equipment are exceedingly simple. For example, J. Gorand et al. designed a sampler in the form of two cylindrical vessels of different height, one nested in the other. The higher cylinder, of lesser diameter, is filled with dry ice and is placed inside the other cylinder, in which the tritium sample taken from a water vapor stream is collected. The sensitivity of the method is approximately $1.4 \cdot 10^{-9}$ Ci/liter water, with the measuring time of the specimen on a liquid-scintillator type counter 30 min.

Solid scintillators, anthracene or a plastic with a developed surface, are recommended for tritium activity measurements, but G. Tzerbib et al. (France) have pointed out that reliance on a liquid scintillator yields better results.

Several trends can be singled out in the discussion of field methods for environmental radioactivity monitoring: the development of comparatively simple methods and devices for rapid measurements under field conditions; the use of specially equipped transportation vehicles (airplanes, truck vans, etc.), the use of a variety of methods (ionization chambers and luminescence dosimeters) for continuous monitoring and for compiling collation maps of the environmental γ-ray dosage in the neighborhood of nuclear facilities; development of special analyzers for field measurements.

Two approaches to rapid methods for environmental radioactivity monitoring are available. For example a paper by H. Beck et al. (USA) presented experience accumulated in the design of a truck-mounted field laboratory utilizing almost all available modern equipment for measuring activity in environmental samples (semiconductor detectors cooled by liquid nitrogen; 4000-channel analyzer; digital computer, etc.). At the same time, several other papers emphasized the need for field laboratory equipment based on simple and reliable instrumentation, the use of simple monitoring techniques, and precise organization of the work, especially when dealing with emergencies. Attention is directed to the fact the simplest radiochemical operations can be adhered to in field measurements in many cases, e.g., measuring the total β-activity and γ-radiation doses in the environment.

There was keen interest in a report by H. Winter (West Germany) on utilization of luminescent dosimetry techniques for environmental monitoring of radioactivity. The paper reports investigations of the properties of various types of detectors and cites comparative experimental data. Solid-state dosimetry techniques ensure easy and inexpensive large-area monitoring.

In the discussion of conventional dosimetric and emergency monitoring, as well as processing of results, attention is focused on the organization of monitoring activities on the scale of entire plants or on a governmental level. In view of the fairly extensive volume of work done on dosimetric and radiometric environmental monitoring, the need for automatic processing of measurement results is stressed.

Reports presented at subsequent panels stressed the feasibility of centralized computerized data processing, and also the acceptable environmental monitoring costs in that case. Discussions also revolved around emergency monitoring conducted by special services which are responsible for the use of simple experimental techniques and equipment that may be more efficient than centralized processing of samples.

Special attention was given to forecasting and assessment of damage and to monitoring of the most dangerous isotopes from the standpoint of radiation hazard (I^{131} and Pu^{239}) at the sessions on emergency monitoring. Several novel and unique express methods for monitoring these isotopes were put forward for consideration. An express method for monitoring I^{131} and several other fission-product isotopes, suggested in a report by A. N. Nikitin et al., met with a certain degree of interest.

The symposium was well organized and provided a source of abundant information. The symposium participants stressed the need for regular publication of collections of articles on environmental monitoring techniques, as a definite contribution to the further development and implementation of those techniques.

BRIEF COMMUNICATIONS

A return visit to Poland was made by representatives of the periodical Atomnaya Énergiya on October 4-9, 1971. During this trip our staff colleagues met and talked with the editor in chief of the Polish counterpart, the periodical Nukleonika, Sz. Szenewski, with editorial staff members K. Przewlocki and L. Gurski, and with the editorial secretary W. Zelazny, to discuss cooperation between the two editorial staffs in the area of improving information on the state of nuclear science and nuclear engineering in Poland and in the USSR. The meetings were most cordial, and revealed complete unanimity of views on the problems discussed, so that a concrete program of collaboration for the immediate period ahead was readily drawn up and agreed upon.

Our colleagues were afforded the opportunity to visit the Krakow Institute of Nuclear Physics, the Warsaw Institute of Physics of the Polish Academy of Sciences, and to become familiarized in detailed fashion with the various scientific-research laboratories of the Nuclear Research Institute at Swierk and the Institute of Nuclear Engineering of the Mining and Metallurgical Academy in Krakow.

A seminar and concurrent exhibition on the topic "Radioactive isotopes, radioisotope engineering, and engineering cost effectiveness of the use of radioisotopes in the national economy" was held at Kursk, June 17-18, 1971, with the participation of representatives of industrial plants in the Kursk region. Simulators of isotopes, of nuclear radiation sources, and of preparations for medicinal purposes were on display at the exhibition, along with exhibits of process control instruments and dosimetric instruments.

A school constituting a forum for exchange of experience on applications of relay type radioisotope instruments in the AUS RRP [integrated unitized (modularized) system of radioisotope relay devices] system for contactless process control in various branches of industry was held at the "Atomic energy" pavilion of the Exposition of Achievements of the National Economy of the USSR on June 14-17, 1971. Representatives from 27 plants and agencies took part in the school.

The ASU RRP integrated unitized system was developed by the Riga scientific-research institute for radioisotope instrumentation [NIIRP]. This system incorporates units for general-purpose industrial applications and for special applications, e.g., explosion-proofed devices for use in the cool mining and processing industries and spark-proof devices for use in the chemical processing industry.

Under the terms of a working plan of collaboration for 1971 drawn up between the USSR State Committee on the Peaceful Uses of Atomic Energy [GKIAE] and the Czechoslovsk Atomic Energy Commission, a Czechoslovak delegation visited the Soviet Union in June, 1971 to be brought up to date on experience in the design and development of nuclear instruments using integrated circuitry. The delegation was hosted by the All-Union Scientific-Research Institute for Radioisotope Instrumentation, were the design of analyzers and integrated-circuitry components was discussed. Czechoslovak specialists examined prototypes of the equipment being developed in the USSR, and gave an account of the use of integrated circuits in nuclear physics equipment being developed and fabricated in Czechoslovakia.

Translated from Atomnaya Énergiya, Vol. 31, No. 6, p. 653, December, 1971.

BOOK REVIEWS

M. L. Gol'din

MONITORING AND AUTOMATION OF ORE FRAGMENTATION AND COMMINUTION PROCESSES

(SECOND EDITION, REVISED AND ENLARGED)*

Reviewed by A. Pugachev

Gol'din the author of this book, has been working in the field of design and applications of radioisotope devices for automatic process control of fragmentation, size reduction, and beneficiation of iron ores for quite some time. He is well versed in the techniques and technology of these processes, and has a lot of experience behind him in the publication of scientific work.

Ore size reduction and comminution processes take up a lot of space in any treatment of the production of either ferrous or nonferrous metals. For that reason, although Gol'din's contribution is centered around examples of iron ore processing, all of the process monitoring and automatic control techniques are equally applicable to size reduction and comminution processes in the treatment of nonferrous metals, and in some cases even to size reduction processes involving nonore materials.

The publication of this book is most timely, since it answers to one of the major problems on the agenda of the current five-year plan: automation of production and implementation of the achievements of nuclear physics in the national economy of the country at all levels. The book compensates to some degree for the dearth of literature on applications of radioisotope equipment in the monitoring and automation of production processes.

When we look back at the first edition of this book, we note that the material and text have undergone at least a partial revision. Some additional data drawn from the field of monitoring of ore processing and from the field of instrument design have been included in the text.

Five years or more have elapsed since the first edition appeared in print. During that time, quite a lot of work has been done in the field of nuclear instrumentation and applications of radii radioisotope devices to monitoring and automation of technological processes. It is most unfortunate that the author failed to take the changes occurring in the period elapsed into account in his revision. For example, in the discussion of reliability, activity calculations, and some other topics, the examples used for illustration are the GR-1 line of instruments, manufacture of which was terminated as far back as 1966. At the present time industry is making use of a much broader array of devices, such as the GR-6, GR-7, the UAS RRP system, etc. But the author remains silent about the reliability of these devices and systems, as well as on practical applications of the γ-relay devices now available. Examples of practical applications of radioisotope devices in the book are accorded at most about thirty pages, and that only in the form of a cursory review. Nothing is said about how radioisotope devices are employed, or what problems they are best capable of solving. No automation flowsheets or arrangements are cited. Material on practical applications of neutron methods in moisture gaging is scanty and inadequate. Only work done in other countries on moisture measurements is mentioned, and examples of the utilization of such devices as the Neitron-3 in the USSR are not cited at all, whether for moisture gaging and monitoring or for technological process control. At the same time, "some aspects of theory and experiment" are treated in excessive detail, and this applies particularly to the VSTE electronic weight-measuring device. Even the amplitude-frequency and phase-frequency characteristics of the VSTE, and the operators for some of its components, are cited. And yet, as any reader is well aware, radioisotope instrumentation is now being adopted quite extensively and intensively by industry for automatic process control, including applications in the size reduction and crushing of ores of ferrous and nonferrous metals.

*Atomizdat, Moscow (1971), 385 pp.

Translated from Atomnaya Énergiya, Vol. 31, No. 6, pp. 653-654, December, 1971.

The book would gain considerably if topics pertaining to practical utilization of radioisotopes in this sphere of production had been treated more adequately. It is to be hoped that the author will take these points into account in any future edition.

Despite certain flaws, the book authored by Gol'din will be useful to those involved in automation of ore crushing and size reduction processes, and also to those persons interested in applications of radioisotope devices in industry.

The textual presentation and the format of the book are praiseworthy.

V. I. Karpukhin and V. A. Nikolaenko

TEMPERATURE MEASUREMENTS USING IRRADIATED DIAMOND*

Reviewed by V. I. Klimenkov

This book publicizes a new method of temperature measurements, one in which the working fluid of the temperature-recording device is diamond irradiated in a nuclear reactor. The authors are members of a team of inventors who devised this novel method. While engaged for several years in investigations of radiation damage in materials, they discovered a new approach to measurement of temperature, utilizing the properties and regularities in the behavior of radiation-induced defects in the crystal lattice of solids. The method was first applied in practice in our country, and is now gaining increasingly wider acceptance, so that this brochure will be of interest to a broad range of workers in science and industry.

The first chapter contains a highly detailed, though concise, treatment of information on radiation damage, as the underlying basis for the operating principles of the diamond heat indicator. The second chapter cites examples of successful applications of the heat indicator to measurements of working temperatures in installations that are remote or hard to get at, such as gas-turbine rotors, piston rings in internal-combustion engines, nuclear reactor fuel elements, etc. What makes such measurements feasible is that only a minute amount of pile-irradiated diamond placed at the site of measurement is needed to effect the measurement, and no wiring or leads are required. The third chapter goes into fabrication techniques and use of diamond heat indicators, and advantages of their use in terms of technique and cost in some applications. The fourth chapter discusses temperature measurements in a nuclear reactor, and the outlook for the use of unirradiated diamond in that application. When irradiated in a reactor together with an object whose temperature is to be measured, the diamond stores information not only on the temperature but also on the exposure dose. But the use of diamond as a standard indicator of irradiation conditions is still held back by difficulties associated with some unsolved problems in the area of exposure dose units, as is duly noted in the brochure.

The book can be used to great advantage not only as a source of information on the method, its scientific groundwork, and examples of applications, but also as a practical handbook, which is one of its salient advantages. But on that level some questionable details in the treatment of viewpoints on the nature of radiation-induced defects are to be viewed as excessive. Many of the points considered in this context, particularly the mathematical formalism, are entirely unnecessary for the subsequent presentation. It would seem preferable to present the alternatives and offer more generalized physical concepts.

Despite its small volume, the book is packed with information. It gets across to the reader the enthusiasm the authors feel for their creation. The style of presentation is lively, and renders the job of becoming familiar with the new method described, an offspring of nuclear engineering and now imparted to the national economy, a pleasure.

*Atomizdat, Moscow (1971), 72 pp.

INDEX

SOVIET ATOMIC ENERGY

Volumes 30-31, 1971

Declassified and Approved For Release 2013/02/26 : CIA-RDP10-02196R000300090004-9

SOVIET ATOMIC ENERGY

Volumes 30-31, 1971

(A translation of Atomnaya Énergiya)

C

D

E

F

G

L

M

R

S

T

U

V

Y

Z

SOVIET ATOMIC ENERGY
Volumes 30-31, 1971
(A translation of Atomnaya Énergiya)

Volume 30, Number 1 January, 1971

Volume 30, Number 2 February, 1971

Volume 30, Number 3 March, 1971

Volume 30, Number 4 April, 1971

Volume 30, Number 5 May, 1971

Volume 30, Number 6 June, 1971

Volume 31, Number 1 July, 1971

ABSTRACTS

LETTERS TO THE EDITOR

Volume 31, Number 2 August, 1971

Volume 31, Number 3 September, 1971

Volume 31, Number 4 October, 1971

Volume 31, Number 5 November, 1971

ABSTRACTS

LETTERS TO THE EDITOR

Volume 31, Number 6 December, 1971

Declassified and Approved For Release 2013/02/26 : CIA-RDP10-02196R000300090004-9

Declassified and Approved For Release 2013/02/26 : CIA-RDP10-02196R000300090004-9

Declassified and Approved For Release 2013/02/26 : CIA-RDP10-02196R000300090004-9

COMPUTER APPLICATIONS IN THE EARTH SCIENCES

An International Symposium

Proceedings of a conference on the state of the art, held at The University of Kansas, Lawrence, June 1969

Edited by **Daniel F. Merriam**
Chief of Geologic Research, Kansas Geological Survey
The University of Kansas, Lawrence, Kansas

Internationally renowned authorities systematically review the state of the art of computer applications in the earth sciences, including past developments, current uses, and future possibilities. The application of computers to the earth sciences and the current computer methods developed are presented in relation to innovations in problem solving and data processing. Subjects covered include geochemistry, geophysics, hydrology, mining geology, oceanography, paleoecology, paleontology, petroleum engineering, petroleum geology, petrology, sedimentology, stratigraphy, and structural geology. Uniquely coordinating various disciplines, this volume provides an invaluable information framework for geologists, mathematicians, computer scientists, and engineers.

Approx. 282 pages PP 1969 **$12.50**

PLENUM PUBLISHING CORPORATION
Plenum Press • Consultants Bureau • IFI/Plenum Data Corporation
227 WEST 17th STREET, NEW YORK, N. Y. 10011

In United Kingdom: Plenum Publishing Co. Ltd., Donington House, 30 Norfolk Street, London, W.C. 2.

THE MANY-BODY PROBLEM

Mallorca International School of Physics, August 1969

Director: **L. M. Garrido**
Professor of Theoretical Physics, University of Barcelona, Spain

Edited by **A. Cruz**
University of Zaragoza

and **T. W. Preist**
University of Exeter

Examines numerous aspects of the many-body problem, a subject of vital importance for advanced research in modern physics, including nuclear, plasma, and solid state physics, and statistical mechanics. The volume attempts to encourage new fields of research in physics and to consolidate those in which progress is already evident. Eminent physicists from Western Europe and the United States contributed to this valuable work. They include:

L. J. Boya
E. R. C. Caianiello
C. B. Dover
C. P. Enz
I. Fujiwara
L. van Hove
N. J. Horing
P. C. Martin
W. Thirring
E. J. Verboven

333 pages PP 1969 **$15.00** (444)
LCC No. 77-94344

PLENUM PUBLISHING CORPORATION
Plenum Press • Consultants Bureau • IFI/Plenum Data Corporation
227 WEST 17th STREET, NEW YORK, N. Y. 10011

In United Kingdom: Plenum Publishing Co. Ltd., Donington House, 30 Norfolk Street, London, W.C. 2.

Declassified and Approved For Release 2013/02/26 : CIA-RDP10-02196R000300090004-9